

NBS
PUBLICATIONS

A11100 989628

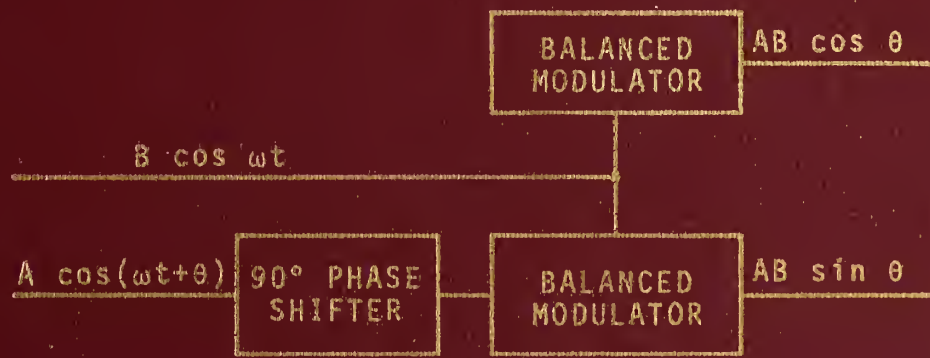


NAT'L INST OF STANDARDS & TECH R.I.C.
A11100989628
Beatty, Robert Willis/Automatic measureme
QC100 .U556 V151,1976 C.1 NBS-PUB-C 1976

NBS MONOGRAPH 151

U.S. DEPARTMENT OF COMMERCE / National Bureau of Standards

Automatic Measurement of Network Parameters— A Survey



QC
100
.U556
No.151
c.2
1976

763070

National Bureau of Standards

Automatic Measurement of Network Parameters—A Survey

NOV 10 1976

OCT 1976

0-100
.4583
NO. 151
1976
C. 2

R. W. Beatty

Electromagnetics Division
Institute for Basic Standards
National Bureau of Standards
Boulder, Colorado 80302



U.S. DEPARTMENT OF COMMERCE, Elliot L. Richardson, *Secretary*

James A. Baker, III, *Under Secretary*

Dr. Betsy Ancker-Johnson, *Assistant Secretary for Science and Technology*

NATIONAL BUREAU OF STANDARDS, Ernest Ambler, *Acting Director*

Issued June 1976

Library of Congress Cataloging in Publication Data

Beatty, Robert William, 1917-

Automatic measurement of network parameters.

(NBS monograph; 151)

Includes bibliographical references.

Supt. of Docs. No.: C 13.44:151

1. Electric network analyzes. 2. Electric measurements. 3. Microwave measurements. I. Title. II. Series: United States. National Bureau of Standards. Monograph; 151.

QC100.U556 no. 151 [TK3001] 602'.1s [621.319'2] 76-12432

National Bureau of Standards Monograph 151

Nat. Bur. Stand. (U.S.), Monogr. 151, 113 pages (June 1976)

CODEN: NBSMA6

U.S. GOVERNMENT PRINTING OFFICE
WASHINGTON: 1976

For sale by the Superintendent of Documents, U.S. Government Printing Office
Washington, D.C. 20402 - Price \$4.50
Stock No. 003-003-01621-7

	Page
Acknowledgments	vii
1. Introduction	1
1.1. General	1
1.2. Definitions of Network Parameters	1
1.3. Classification of Methods	4
1.4. Relative Importance and Accuracy	6
1.5. Relative Range and Resolution	6
2. Description of Developments	8
2.1. Standing Wave Samplers; Moving Probe	8
a. Slotted Lines	8
(1) Reciprocating Probe Motion	8
b. Slotted Line Recorder	8
c. Circular Slotted Lines	9
d. Sweep-frequency Techniques	10
e. Nodal Shift Techniques to Determine $ S_{11} $	11
(1) Semi-automatic Method	11
(2) Automatic Method Using Magic T	12
(3) Offset Probe Coupled to Sliding Short	13
2.2. Moving Standing Wave; Fixed Probe	13
a. Single Frequency	13
b. Long Line-sweep Frequency Method	16
c. At Various Discrete Frequencies	17
2.3. Coupling to Auxiliary Waveguides	18
a. Coupling from Rectangular to Circular Waveguide	18
b. Coupling from Rectangular to Rectangular Waveguide	20
(1) Rotating Slot Coupler	20
(2) Variable Phase Shifter	23
c. Coupling Coaxial Tees to Circular Waveguide	24
2.4. VSWR, L_R , $ \Gamma $, $ S_{mm} $, or $ S_{nn} $ only	25
a. Magic T	25
b. Non-directional Couplers	27
(1) Ratio of Detected Voltages	27
(2) Difference of Detected Voltages	28
(3) Heterodyne Detection	29

	Page
c. Rectangular Waveguide Directional Couplers	30
(1) High-directivity Rectangular Waveguide Coupler	30
(2) Compensated Directional Coupler	31
(3) Semi-automatic Tuning	32
(4) High Resolution Reflectometer	32
d. Lumped Resistance Bridge	34
2.5. $ S_{11} $ and $ S_{21} $ Versus Frequency	35
a. Rectangular Waveguide	35
b. Coaxial	39
2.6. Gain or Loss Versus Frequency	41
2.7. Display of Complex Z or Γ	41
a. Multiple Probes	41
(1) Four Fixed Probes	42
(2) Three (or five) Fixed Probes	43
b. Directional Couplers and Hybrids	46
(1) Semi-automatic Diagraph	46
(2) Servo Control	46
(3) Balanced Modulator	49
(4) Hybrid Tees	52
c. Long Line, Variable Frequency	52
(1) Swept Frequency	52
(2) Stepped Frequency	53
d. Rotating Slot Coupler	56
e. Z at 1592 Hz	56
2.8. Phase Shift	57
a. Single Sideband, Suppressed Carrier, Quadrature Method	57
b. Modulated Sub-carrier System	57
c. Balance-modulated Sub-carrier, Quadrature and Ratio Technique	58
d. Two-probe Phase Detector on Slotted Line	60
e. Pulsed Signal Technique	60
2.9. Complex S_{21}	61
a. Fourier Techniques	61
(1) Square Wave Testing	61
(2) Pulse Testing	64
b. Other Applications	64
(1) I-F Substitution	64
(2) Balanced Modulator Circuits	65

Contents (Continued)

	Page
2.10. Envelope Delay	68
a. Carrier Phase Shift Versus Frequency	68
b. Phase Shift of Envelope	70
c. Two-tone Method	71
d. Frequency Modulation Technique	72
e. Differentiating Phase Shift with Sawtooth Frequency Sweep	73
2.11. Complex Reflection and/or Transmission Coefficients	73
a. Using Balanced Modulator	73
(1) Hybrid Circuit Operating at r. f.	73
(2) I-F Input to Display Unit	74
b. Complex V and I	75
c. I-F Substitution Without Computer Control	75
d. Frequency Translation by Sampling	80
(1) Swept Frequency	80
(2) Computer Controlled	81
e. I-F Substitution with Computer Control	83
3. Trends	85
3.1. Introduction	85
3.2. Status Through 1972	85
a. I-F Substitution, Comparison by Rapid Switching	85
b. Frequency Translation by Sampling	86
c. Time Domain to Frequency Domain Transformation	86
d. Six-port Coupler	86
e. Ratio Measurements Without Standards	87
f. Calibration of Automatic Network Analyzers	88
g. Interface Systems	88
3.3. Recent Developments	89
a. I-F Substitution, Comparison of Rapid Switching	89
b. Frequency Translation by Sampling	90
c. Time Domain to Frequency Domain Transformation	90
d. Six-port Coupler	93
e. Ratio Measurements Without Standards	93
f. Calibration of Automatic Network Analyzers	93
g. Interface Systems	95
h. Computer Operated Bridges	96
i. Slotted Lines	96

Contents (Continued)

	Page
3.4. Future Options	96
a. Introduction	96
b. Interface Developments	96
c. Automatic Tuning	97
d. Performance Degradation Diagnosis	97
e. Automatic Calibration	97
f. Extended Range of Operation	98
g. Reduction of Size and Cost	98
h. Improved Resolution and Accuracy	98
i. Unforeseen Developments	98
4. References	99
a. Chronological List	99

Acknowledgments

The personnel and facilities of the Electromagnetics Division's Metrology Information Center were helpful in collecting pertinent references. The author is grateful for the assistance of Mr. Wilbur J. Anson, Mr. Ira S. Berry, and Mrs. Anne Y. Rumpfelt of that center. Reviewers included Mr. Fred R. Clague, Mr. W. E. Little, Mr. C. M. Allred, and Dr. R. A. Kamper of the National Bureau of Standards, Dr. Gerald D. Haynie of the Bell Telephone Laboratories, Mr. George R. Kirkpatrick of the Hewlett-Packard Company, and Mr. Thomas E. MacKenzie of the General Radio Company.

As indicated in the text, various journals granted permission to reproduce certain figures from published papers. Mrs. F. M. Indorf typed the manuscript and put it into proper form for publication.

AUTOMATIC MEASUREMENT OF NETWORK PARAMETERS - A SURVEY*

R. W. Beatty**

National Bureau of Standards

Boulder, Colorado

A survey is made of principles, methods, and systems developed for semi-automatic and automatic measurement of network parameters such as the complex scattering coefficients, impedance, VSWR, return loss, attenuation, and group delay time. The period covered is from 1922 to 1975 and developments range from simple ideas such as a motor driven probe for a slotted line, to computer-controlled transmission and reflection measurement systems.

The essential ideas and features of each development are briefly described and both similarities and differences between various schemes are pointed out. Trends in modern developments are noted and some of the options open for future work are mentioned. A bibliography of 151 references is included.

Key words: Automatic network analyzers; computer-controlled measurement; magic tee; microwave measurement methods; multiple probe devices; reflectometers; rotating probe devices; slotted lines; survey of automatic techniques; swept frequency measurements; Wheatstone Bridge.

1. Introduction

1.1. General

This paper is concerned with the development of automatic methods of measuring basically the magnitudes and phase difference, or the complex ratio of two sinusoidal voltages; and applications of this capability to determining complex reflection coefficients and transmission coefficients and group delay times of electrical networks.

1.2. Definitions of Network Parameters

Networks can be characterized by scattering coefficients of the form S_{mn} where S_{mn} is the complex ratio of the amplitude "b" of a wave emerging from port m to the amplitude "a" of a wave incident upon port n, where there is no interreflection of waves at the ports due to port terminations or sources that might produce reflected waves.

The waves might be voltage or power waves, for example, so more than one type of scattering coefficient might be designated as S_{mn} . Unless stated otherwise, only voltage waves using the scheme illustrated in figure 1-1 are used in this paper. There are many relationships between different sets of parameters characterizing networks [80].

*A condensed version of this Monograph was published in the Microwave Journal, Vol. 17, No. 4, (April 1974), pp. 45-49, and 63.

** Dr. R. W. Beatty retired from the National Bureau of Standards July 1974, and is now a Consulting Electronics Engineer at 2110 - 4th Street, Boulder, Colorado 80302.

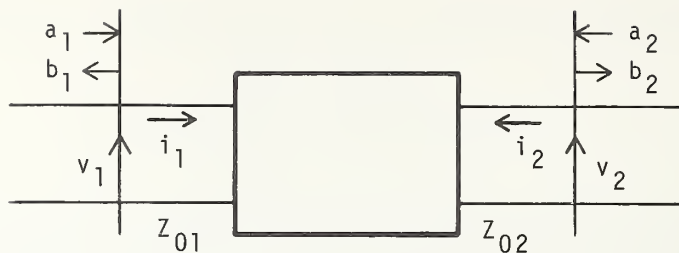


Figure 1-1. Diagram of a 2-port network showing two schemes for characterization.

$$\begin{cases} v_1 = a_1 + b_1 \\ Z_{01} i_1 = a_1 - b_1 \end{cases}$$

$$\begin{cases} v_2 = a_2 + b_2 \\ Z_{02} i_2 = a_2 - b_2 \end{cases}$$

$$\begin{cases} v_1 = Z_{11} i_1 + Z_{12} i_2 \\ v_2 = Z_{21} i_1 + Z_{22} i_2 \end{cases}$$

$$\begin{cases} b_1 = S_{11} a_1 + S_{12} a_2 \\ b_2 = S_{21} a_1 + S_{22} a_2 \end{cases}$$

$$Z_1 = \frac{v_1}{i_1}$$

$$S_{11} = \left(\frac{b_1}{a_1} \right)_{a_2 = 0}$$

$$S_{12} = \left(\frac{b_1}{a_2} \right)_{a_1 = 0}$$

$$\Gamma_1 = \frac{b_1}{a_1}$$

$$S_{21} = \left(\frac{b_2}{a_1} \right)_{a_2 = 0}$$

$$S_{22} = \left(\frac{b_2}{a_2} \right)_{a_1 = 0}$$

$$L_{R1} = 20 \log_{10} \frac{1}{|\Gamma_1|}$$

$$A_{21} = L_{21} = 20 \log_{10} \frac{1}{|S_{21}|}$$

$$(\text{VSWR})_1 = \frac{1 + |\Gamma_1|}{1 - |\Gamma_1|}$$

$$\psi_{21} = \text{Arg. (argument of)} S_{21}$$

For example, if we consider scattering coefficients relating voltage wave amplitudes a_m and b_m where a_m denotes a wave incident upon port m and b_m denotes a wave emerging from port m , then the voltage reflection coefficient Γ_m "looking into" port m is

$$\Gamma_m = \frac{b_m}{a_m}, \quad (1)$$

The corresponding normalized (actual impedance divided by Z_0) impedance Z_m is

$$Z_m = \frac{1 + \Gamma_m}{1 - \Gamma_m}, \quad (2)$$

where Z_0 is the "characteristic impedance" associated with a waveguide mode at port m or simply a normalizing impedance (especially convenient if no waveguides are involved).

If the network has waveguide (or transmission line) ports, the voltage standing wave ratio (VSWR) is

$$\text{VSWR} = \frac{1 + |\Gamma|}{1 - |\Gamma|}, \quad (3)$$

The corresponding return loss L_R is

$$L_R = 20 \log_{10} \frac{1}{|\Gamma|}, \quad (4)$$

In the case of transmission of energy from port m to port n , one can measure the transmission coefficient S_{nm} . The corresponding attenuation A_{nm} or characteristic insertion loss $L_{n,m}$ is

$$A_{nm} = L_{nm} = 20 \log_{10} \frac{1}{|S_{nm}|}. \quad (5)$$

The characteristic phase shift $\psi_{n,m}$ is the phase of S_{nm} .

The group delay time τ_{nm} is

$$\tau_{nm} = - \frac{d\psi_{nm}}{d\omega}, \quad (6)$$

where ω is the angular frequency. For a lossless transmission line of length ℓ ,

$$\psi_{21} = -\beta\ell = -\frac{2\pi}{\lambda} \ell = -\frac{2\pi f}{v} \ell = -\frac{\omega\ell}{v},$$

and

$$\tau = - \frac{d\psi_{21}}{d\omega} = \frac{\ell}{v},$$

where v = the velocity of propagation.

If v is independent of frequency, then the delay time τ is independent of frequency in this case, and one can see that there will be no delay distortion of the envelope. In order to determine whether there will be delay distortion produced by a given component or system, one is interested in the portion of the delay time that is frequency-dependent. Sometimes the portion of the delay time that is "flat" with frequency is called the absolute group delay and the portion that varies with frequency (the source of delay distortion of the modulation envelope) is called relative group delay.

1.3 Classification of Methods

In addition to the above network parameters, various others have been defined and used. They can usually be expressed in terms of the above parameters and the relationships are given in various texts and articles.

The measurement of each or all of the above network parameters have been automated to some degree. The various developments leading to fully automated systems which measure all of the above parameters will be classified according to what is measured.

The scheme for classifying methods for automatically measuring network parameters is as follows. This scheme was arbitrarily chosen.

- (1) Standing-wave samplers (slotted lines, etc.)
- (2) VSWR, $|\Gamma|$, L_R , $|S_{m,m}|$ or $|S_{n,n}|$. (Reflectometers, etc.)
- (3) $|S_{mm}|$ or $|S_{nn}|$ and $|S_{m,n}|$ or $|S_{n,m}|$.
(Return Loss and Attenuation or Characteristic Insertion Loss.)
- (4) $|S_{mn}|$ or $|S_{nm}|$, Attenuation or Characteristic Insertion Loss.
- (5) $\Gamma = |\Gamma|e^{j\psi}$, $S_{mm} = |S_{mm}|e^{j\psi_{m,m}}$, $S_{nn} = |S_{nn}|e^{j\psi_{nn}}$.
- (6) $\psi_{m,n}$ or $\psi_{n,m}$ (Characteristic Insertion Phase Shift).
- (7) $S_{12} = |S_{12}|e^{j\psi_{12}}$ or $S_{21} = |S_{21}|e^{j\psi_{21}}$.
- (8) τ_{nm} (Group or Envelope Delay).
- (9) Γ , S_{mm} , S_{mn} , S_{nm} , S_{nn} , τ .

Other schemes of ordering these developments are also used. For historical interest, the references are listed in chronological order, and some highlights are shown in figure 1-2.

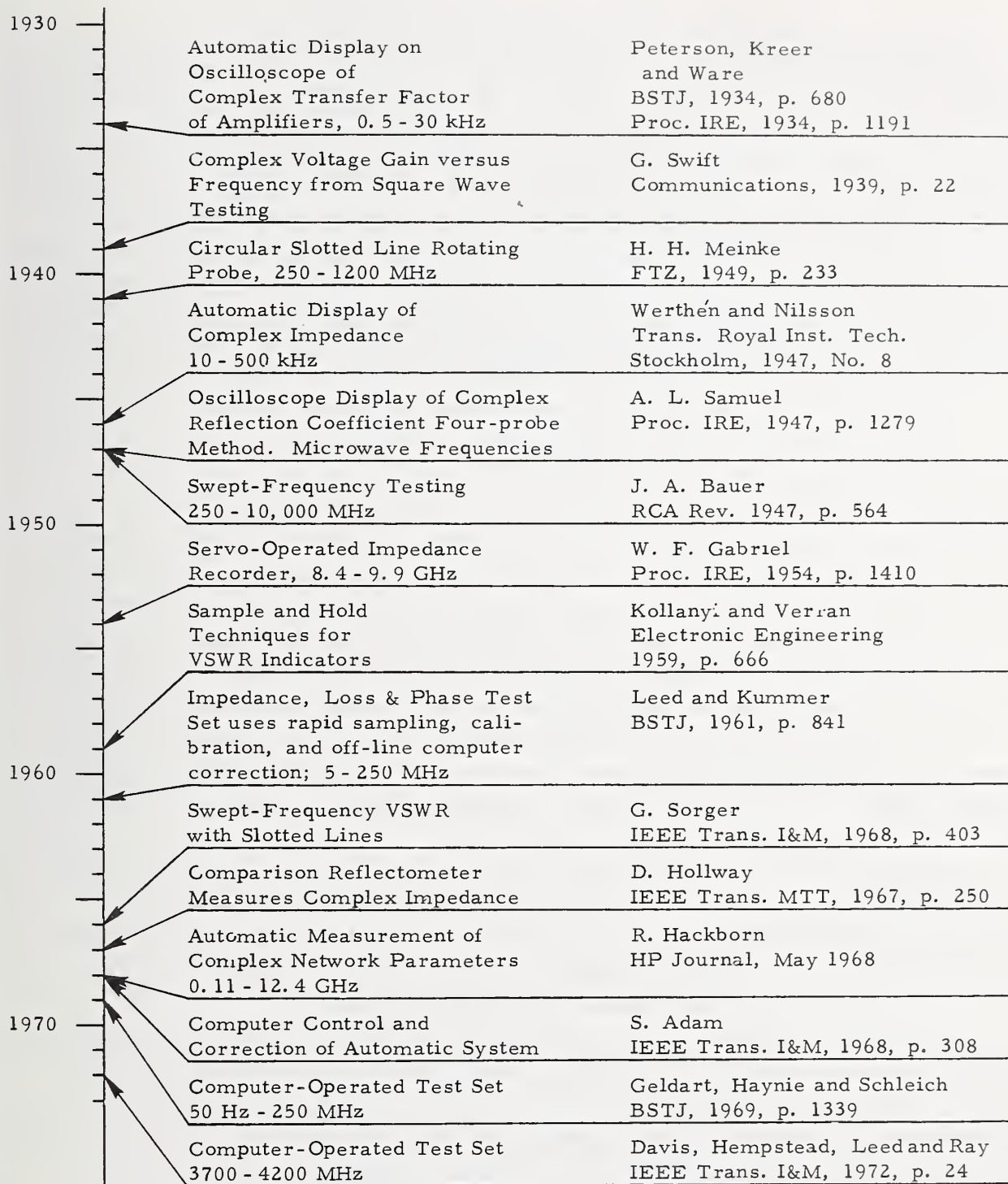


Figure 1-2. A few highlights in the development of automatic measurement of network parameters.

1.4. Relative Importance and Accuracy

In reviewing a large number of developments which took place over a period of more than 40 years in various countries, there tends to be a lack of continuity. It may be difficult for the reader to assess the relative importance and accuracy of the various methods. It is hoped that the classification scheme used will be helpful as well as the chronological arrangement of references. Usually the later developments are built upon experience gained in earlier developments and thus are more significant. However, there are likely to be further developments along different lines. For example, instead of automatically correcting for imperfections of components by a calibration procedure, one might consider the approach of automatically tuning, adjusting, or trimming components until their performance closely approaches the ideal. Whatever direction is taken, it is expected that a broad knowledge of principles previously used in making automatic measurements will be helpful.

The assessment of the relative accuracy of different methods is particularly difficult. It is generally possible to refine any basic method or modify it in such a way as to improve the accuracy. In many cases, the development of a particular method is halted when a commercially competitive instrument or system is obtained, even though the technology exists to make it more accurate. One should not conclude that a particular method is necessarily or inherently inaccurate, because it is possible that later improvements of components and techniques may greatly increase the accuracy obtainable. For example, early versions of automatic impedance measurements using slotted lines were limited in accuracy due to probe loading effects, mechanical imperfections, and other factors. Many of these problems were largely overcome within the last 10 years or so, and more developments are in progress.

In cases where the developer of a particular method carefully investigated and stated accuracies, some information is available. But in many cases, methods have been described without a study of errors, and one cannot tell without further study what accuracy is obtainable.

A simple statement of percentage accuracy may be of little value since both systematic and random errors are present. The factors of resolution, stability, and repeatability are limiting ones and may not be necessarily characteristic of a method so much as how it is instrumented. There is always operator error, even with automatic systems.

1.5. Relative Range and Resolution

It is generally possible to increase the range and resolution of measurement obtainable with any basic measurement method or system by making appropriate refinements and modifications. However, the developer usually reaches a point beyond which he is not willing or able to go for reasons of economy or expediency. The range and resolution are often limited by capabilities of sources and their power supplies and stabilization circuits, and by the capabilities of detectors, for example. Thus, one expects greater dynamic range (at least 60 dB) when using superheterodyne detection than when using bolometer or crystal detection of audio modulation envelopes (30-40 dB). One expects greater resolution when using frequency synthesizers or phase-locked sources and regulated power supplies than when using

uncontrolled sources operating with simple and inexpensive power supplies. The objectives of great dynamic range, good stability, repeatability, resolution and accuracy have led to the development of more complicated systems. However, one cannot conclude in general that excellence is proportional to the complexity of the system, even though there is a tendency to achieve better system performance, if not reliability, by adding more components, more procedural stems and more software to automatic measurement systems.

In trying to evaluate the capabilities of the various methods described in this survey, one must be guided by the above and other considerations, and must exercise individual judgment based upon experience. The point at which the development of any method stops is usually the result of compromises and tradeoffs. As our technology continues to improve, it will become practical to extend the development of some methods beyond the point at which they previously stopped.

2. Description of Developments

2.1. Standing Wave Samplers; Moving Probe

a. Slotted Lines

(1) Reciprocating Probe Motion

Automatic display of a voltage standing wave was accomplished [13] by a motor drive which gave the slotted line's traveling probe a reciprocating motion as shown in figure 2-1.

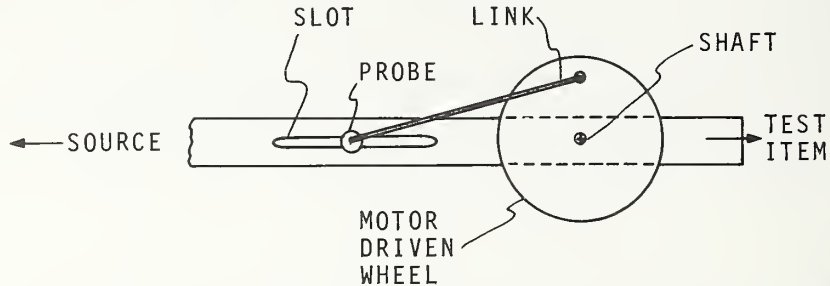


Figure 2-1. Reciprocating motion of probe in slotted line.

The rectified probe output was fed to the vertical plates of a cathode ray oscilloscope (CRO) and the sawtooth sweep on the horizontal plates was synchronized with the probe motion. A long persistence screen on the oscilloscope permitted simultaneous observation of a calibration curve using a short-circuit termination and the standing wave caused by the test item. The complex reflection coefficient was calculated in the usual way from the VSWR and displacement of the voltage minimum as read from the screen of the oscilloscope.

b. Slotted Line Recorder

Instead of rapidly moving the probe back and forth, it may be driven slowly by the same motor that drives a recorder chart in order to store the probe output variation versus position [66]. This has the advantage that repeatable deviations from the ideal response due to irregularities in probe penetration, for example, can be subtracted out when the difference between two measurement conditions is of interest. Multiple plots upon the same chart make comparison of probe outputs easy. It is also easy to subtract a constant voltage from the probe output and record the difference, obtaining a greatly expanded VSWR scale. Figure 2-2 shows a sketch of such a system. The substitution technique consists of measuring the test item first with a $\lambda/4$ section of air line inserted between it and the slotted line, then repeating the measurement with the air line removed. Comparison of the two curves takes advantage of the storage feature of the recording process and makes possible a more accurate measurement. This technique is strictly for single frequency operation and employs limited automation not for speeding up data taking, but for increasing accuracy of measurement.

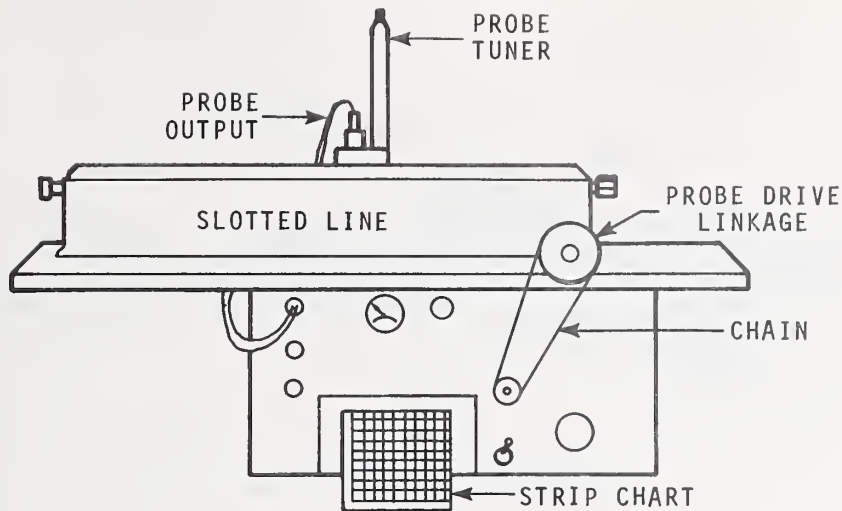


Figure 2-2. Sketch of slotted line recorder system.

c. Circular Slotted Lines

Slotted lines of coaxial or rectangular cross-section formed in a circular arc were constructed as early as 1941.

These circular slotted lines were constructed [10, 16, 21, 40] as shown in figure 2-3 so that a motor driven rotating probe could rapidly sample the voltage standing wave. The rectified output of the probe was displayed on a CRO whose sweep was synchronized with the probe rotation. Various refinements were made, such as using a standard piston attenuator to measure relative voltage levels.

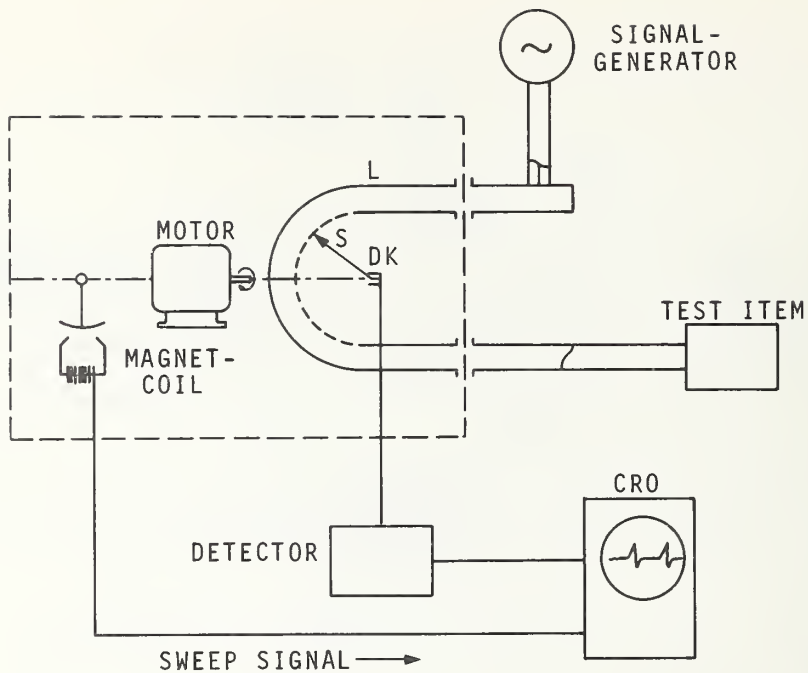


Figure 2-3. Apparatus for measuring impedance with a circular slotted line and rotating probe.

d. Sweep-frequency Techniques

A semi-automatic method was devised to display on a CRO or X-Y recorder curves of slotted line probe output versus frequency as the frequency was swept [73, 87]. After each sweep, the probe was moved a small amount, say 0.1 wavelength and a new curve recorded. After a total movement of a least half wavelength, a time exposure of the oscilloscope or a stored pattern on the recorder looked like figure 2-4. One could then read at any particular frequency the ratio of maximum to minimum from the envelope of the pattern.

One can see that this procedure gives the same result as though one had set the frequency to a number of discrete values across the band and moved the probe to give maximum and minimum output at each frequency. If maximum and minimum values were then connected by a smooth curve, the same pattern envelope would be obtained.

Of course it is easier to obtain this curve by sweeping the frequency continuously and moving the probe in discrete steps.

If one were to combine this technique with one in which the probe is moved automatically, the data could be obtained more rapidly.

The method gives only VSWR versus frequency and one cannot obtain any information about the phase of the voltage reflection coefficient. The VSWR is not read out directly but must be determined from the plotted pattern's envelope.

It is necessary to level the output of the swept source and to pay attention to reduction of reflections. Some improvement in accuracy can be obtained using a coupled sliding load technique.

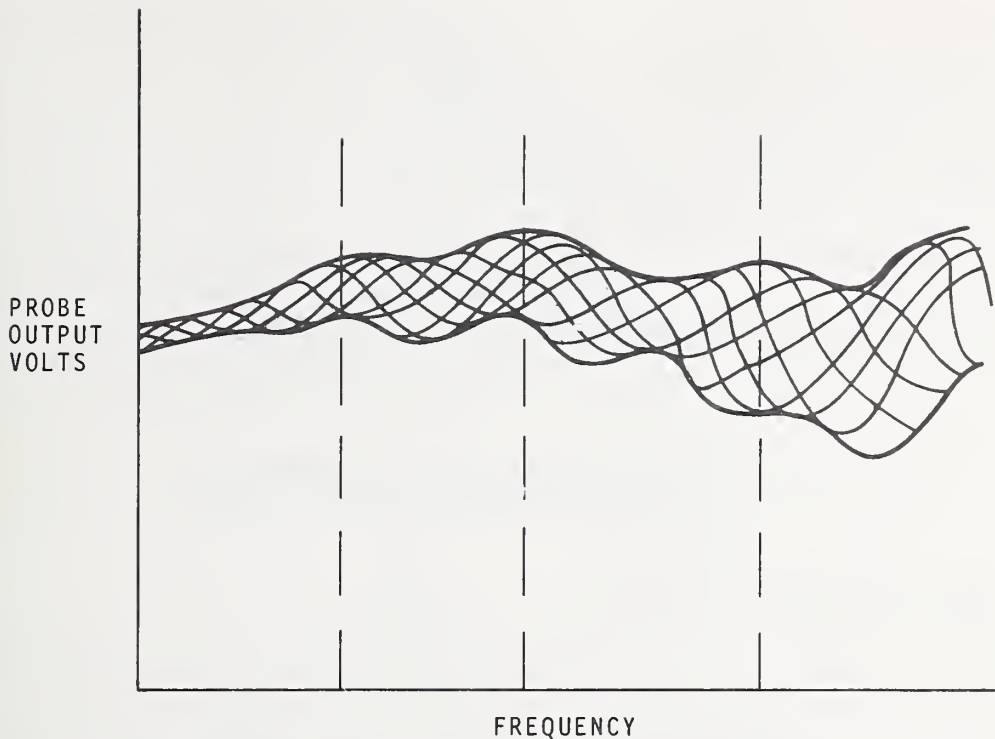


Figure 2-4. Multiple traces made by sweeping the source frequency for various positions of the probe.

Further work has been done to automate the system [140]. The frequency is stepped through 256 increments throughout the range 2-18 GHz, while the slotted line carriage is moved slowly over a distance of half wavelength at the lowest frequency. The dc output is digitized and the maximum and minimum values stored in a memory. The ratio of maximum to minimum is determined internally and converted to a linear analog voltage which is displayed on an oscilloscope or an X-Y recorder. A direct readout of VSWR versus frequency is thus provided.

e. Nodal Shift Techniques to Determine $|S_{11}|$

Several ideas have been used to reduce the tedium of determining the residual VSWR of a lossless 2-port by the nodal shift technique.

(1) Semi-automatic Method

Figure 2-5 shows how a vibrating probe can display on a CRO the probe voltage near a voltage node in a slotted line produced by a short-circuit which terminates the lossless 2-port under investigation. The probe is mechanically coupled to the short-circuit so that only the nodal shift is measured as the short-circuit is manually slid in the waveguide. The scale of the CRO is arranged so that one can read the residual VSWR directly [40].

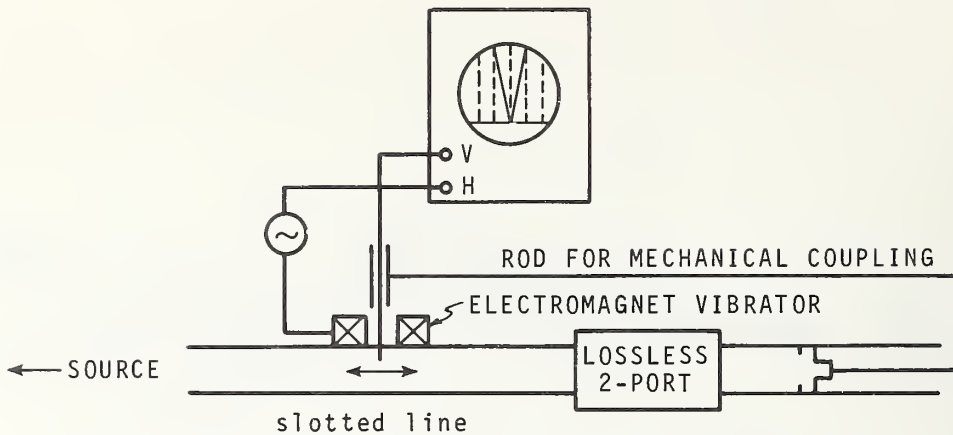


Figure 2-5. Vibrating probe coupled to sliding short-circuit automatically shows nodal shift on CRO.

(2) Automatic Method Using Magic T

Figure 2-6 shows a basic idea used to automatically plot nodal shift versus position of a sliding short-circuit terminating the lossless 2-port under investigation [56]. The node-tracking short-circuit connected to the magic T is maintained at a position to give a detector minimum or reference level by one of two possible methods. The difference between the positions of the two short-circuits is then converted to an electrical signal by a differential servo arrangement and recorded.

One method to control the position of the node-tracking short-circuit compares the rectified detector output with a dc reference voltage to obtain an error signal used to drive the node-tracking short-circuit.

Another method phase modulates the signal reflected by the node-tracking short-circuit by means of a ferrite phase modulator. A phase sensitive detector then produces an error signal to drive the node-tracking short-circuit.

Instead of using a magic T, it was suggested that a rotary standing wave indicator might provide a suitable alternative, but this was not tried [56].

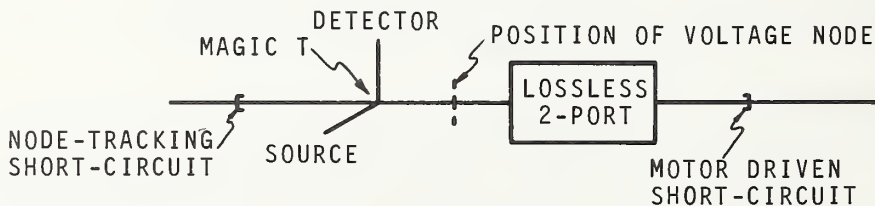


Figure 2-6. Simplified arrangement for recording nodal shift data using magic tee.

(3) Offset Probe Coupled to Sliding Short

Figure 2-7 shows a particularly simple method for automatically recording nodal shift data. The probe in the slotted line is slightly displaced from the nodal position and mechanically coupled to a motor-driven short-circuit which terminates the lossless 2-port under investigation. The node position shifts relative to the probe as the short-circuit is driven in synchronism with the recorder chart. The probe output accurately indicates the amount of nodal shift and may be calibrated by a run in which the coupling rod is disconnected and the probe remains in one position. The source is made effectively non-reflecting by setting the coupled probe on a maximum position and adjusting the tuner to eliminate cyclical variations in probe output [99].

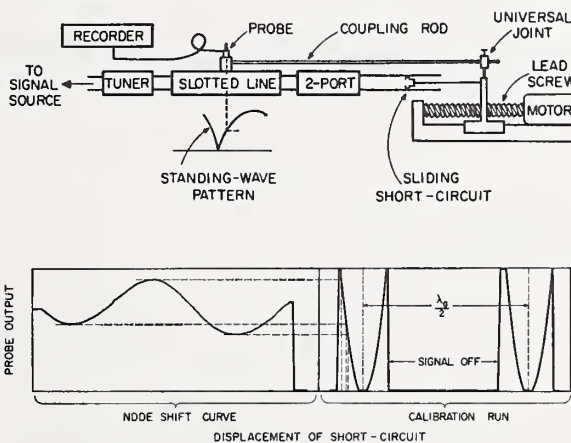


Figure 2-7. Offset probe coupled to motor-driven short circuit.

2.2. Moving Standing Wave; Fixed Probe

a. Single Frequency

Instead of moving a probe in a slotted line to sample a standing wave, methods have been devised to move the standing wave past a fixed probe. One can automatically display the standing wave on an oscilloscope or recorder. It is only necessary to synchronize the sweep with the motion of the standing wave. The standing wave is moved by placing a rapidly varying phase shifter between the probe and the test item. The variable phase shifter may take a number of forms such as a rapidly vibrating long squeeze section (figure 2-8) [10, 24] or a rotating dielectric disc (figure 2-9) which dips into a rectangular waveguide through a slot [10]. A ferrite phase shifter (figure 2-10) permits electrical, rather than mechanical rapid variation of phase shift [52]. Figure 2-11 shows a varying phase shifter using a trombone line stretcher.

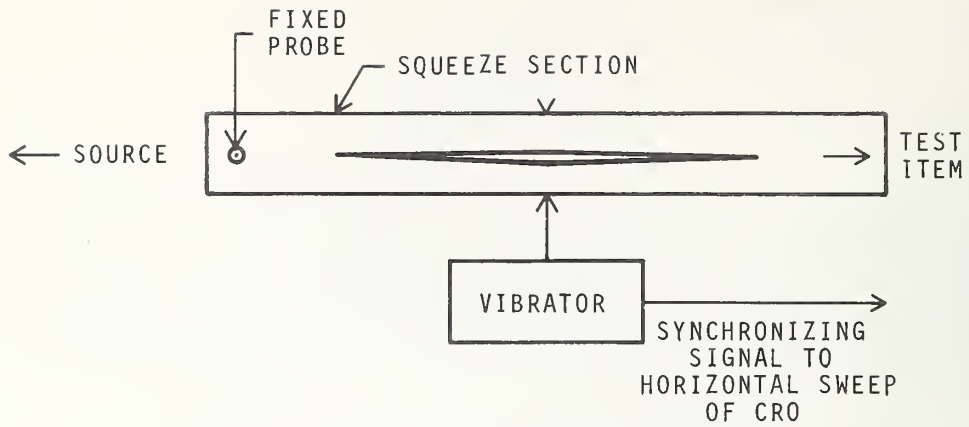


Figure 2-8. Rapidly vibrating squeeze section.

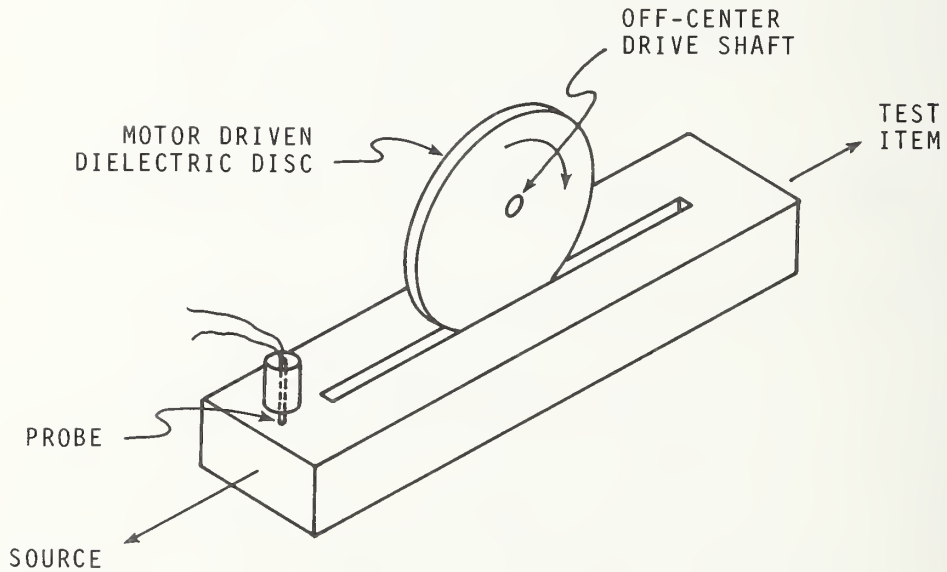


Figure 2-9. Rotating dielectric disc dipping into waveguide through a slot.

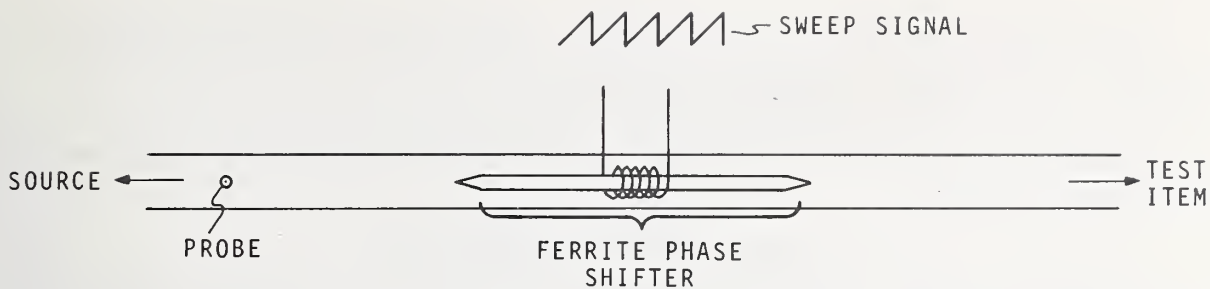


Figure 2-10. Ferrite phase shifter.

In coaxial line, a rapidly moving trombone type line stretcher (figure 2-11) may be used.

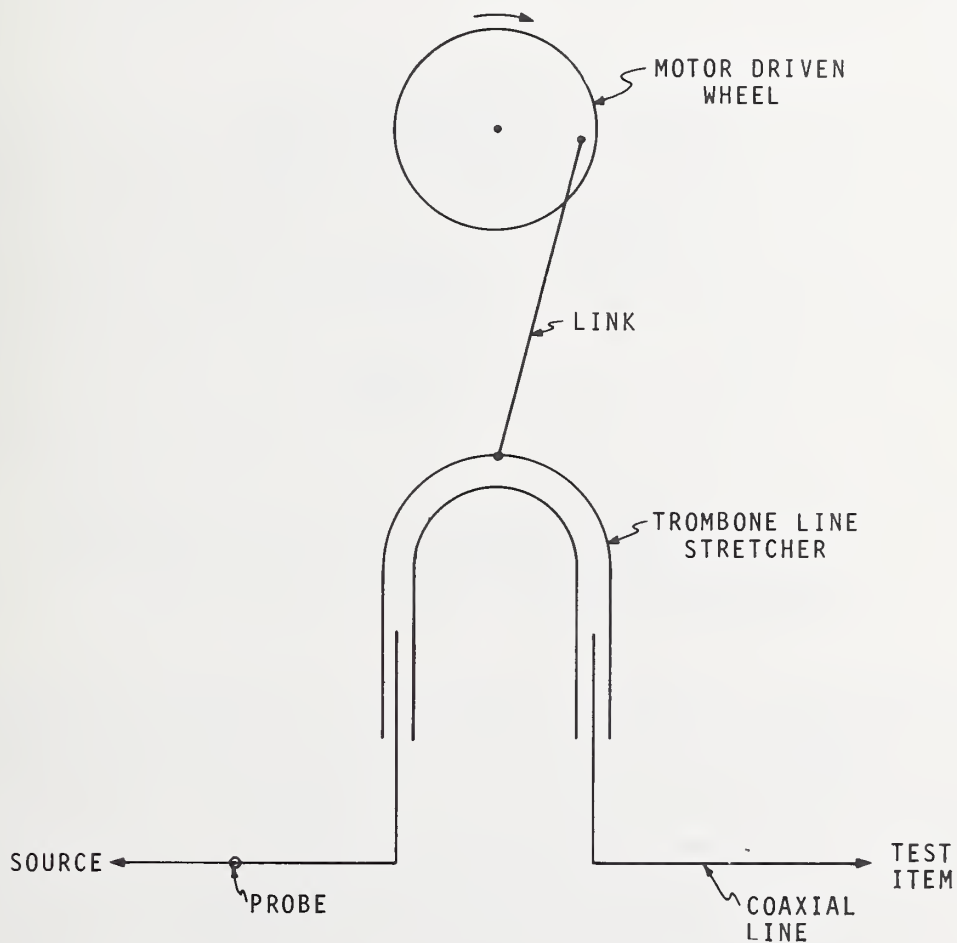


Figure 2-11. Rapidly moving trombone line stretcher.

In case that the load to be measured can be rapidly slid back and forth inside the waveguide, a phase changer is unnecessary, but this situation is not often encountered.

In these techniques, it is important that the variable phase shifter does not introduce significant reflections, that the source reflections are negligible, and that the probe loading is small.

b. Long Line-sweep Frequency Method

Instead of sliding a load inside a waveguide or using line stretchers or phase shifters to move the standing wave past a fixed detector, one may sweep the frequency to change the phase of the reflected wave. If a long line is used as shown in figure 2-12 then a complete cycle of phase shift may be obtained with a reasonably small change of frequency. It is then more likely that the magnitude of the voltage reflection coefficient will remain reasonably constant over this small frequency change. The accuracy of this technique depends strongly on the uniformity of the long line and the accuracy with which its characteristic impedance is known.

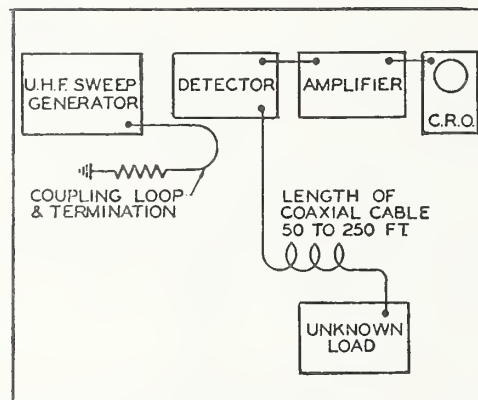


Figure 2-12. Block diagram of equipment for radio-frequency impedance measuring method. (Reprinted by permission: J. A. Bauer, "Special Applications of Ultra-High-Frequency Wide-band Sweep Generators", RCA Rev. 8, no. 3, Sept. 1947.)

An instrument called a panoramic indicator, using this principle, was built to cover the television channels, operating from 40 to 220 MHz [9]. The interference patterns were displayed on a CRO and the vertical scale was calibrated using a short-circuit termination. The attenuation of the long line was also indicated automatically.

Further investigation of this basic idea [9] led to its use at higher frequencies up to 1 GHz to measure not only magnitudes of reflection coefficients, but also their phases. The arrangement of apparatus is shown in figure 2-13. Phase is determined by comparing the frequencies at which voltage minima occur when the test item is replaced by a short-circuit [32].

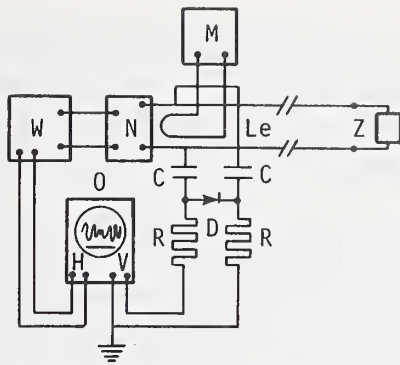


Figure 2-13. Circuit employed to determine the reflection coefficient of an unknown impedance (Z) terminating the line Le ($Z_0 = 300$ ohms). W wobbulator (sweep generator), N matching network, D detector, O oscilloscope (horizontal deflection synchronized with the frequency variation of the wobbulator, vertical deflection proportional to the A.C. output voltage of the detector), M marker, C isolating capacitors (100 pF), R resistors (10,000 ohms), to prevent H.F. voltage from entering the oscilloscope.

c. At Various Discrete Frequencies

The basic idea of moving the standing wave past a fixed probe was considerably refined in a method requiring insertion of various lengths of precision waveguide or transmission line (figure 2-14) between a fixed probe and the test item [94]. As each section of waveguide is inserted, the source frequency is stepped rapidly through many discrete values in the desired frequency range. The probe output is automatically measured using a digital voltmeter and the output data is manually punched on cards for computer processing. Calculated curves are fit to the measured data and the impedances of the source and of the probe are taken into account when calculating the magnitude and phase of the reflection coefficient of the test item.

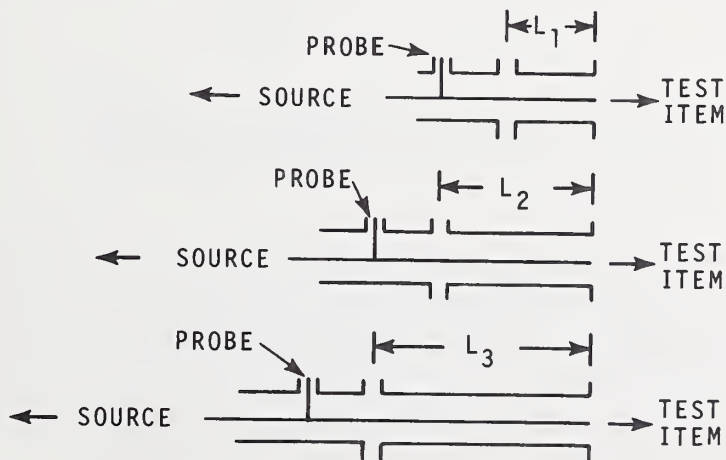


Figure 2-14. Insertion of various lengths of line between probe and test item.

Although this method has been considerably refined, it is not yet fully automated in that one must manually insert various lengths of line both in the determination of the impedances of source and probe as well as in measuring the test item. Also the computer processing of the data is done at some later time and requires manual feeding of the data to the computer.

The accuracy obtained (using 14 mm standard air lines) with this technique is very good, but depends strongly upon the excellence of the connectors one must use to insert various lengths of line. As the diameter of the air lines and the size of the connector decreases, one must degrade the accuracy correspondingly.

2.3. Coupling to Auxiliary Waveguides

a. Coupling from Rectangular to Circular Waveguide

The measurement of impedance in a rectangular waveguide by moving a probe along a slot either by reciprocating or circular motion requires careful mechanical construction. A considerable simplification in construction is accomplished by coupling to a circular waveguide in such a way that the rotation of a probe gives the same output versus angle characteristic as probe output versus distance in the conventional slotted line. This can be accomplished as shown in figure 2-15 by coupling at a position off-axis in the rectangular waveguide where

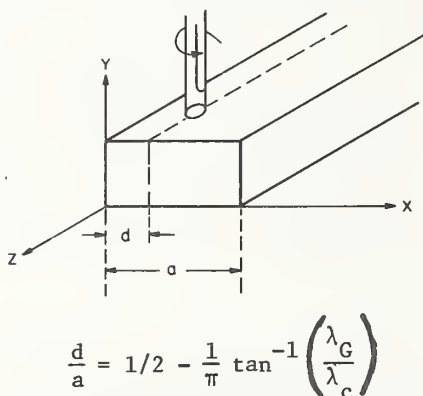
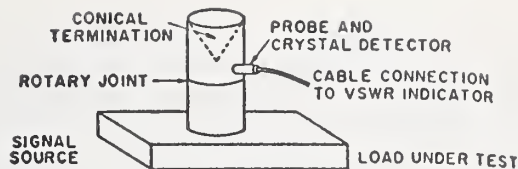
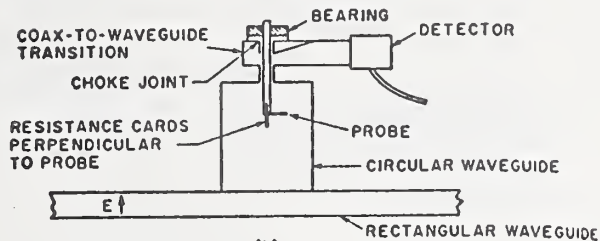


Figure 2-15. Rotating probe coupling to magnetic fields in a rectangular waveguide.

the magnetic fields of a progressive wave in the $TE_{1,0}$ mode are circularly polarized. (The axial and transverse components of magnetic field are perpendicular and 90° out of phase for a progressive wave.) A reflected wave then produces an ellipticity in the polarization of the electric fields in the $TE_{1,1}$ mode in the circular waveguide. By means of a rotating electric field probe, the VSWR and relative angular position of the voltage minimum in the main waveguide may be determined. Two possible designs for the rotating coupler are shown in figure 2-16. This principle is used in non-automatic systems [29, 40, 42] and is also used in automatic systems.



(a)



(b)

Figure 2-16. (a) and (b) Two circular-coupler designs for impedance measurement. (Reprinted by permission: S. B. Cohn, "Impedance Measurement by Means of a Broadband Circular-polarization Coupler", Proc. IRE, 42, no. 10, October 1954, pp. 1554-1558.)

One automatic system uses a three-slot off-axis coupler [28] from rectangular to circular waveguide and displays the complex Γ on a CRO [39]. Instead of rotating a magnetic field probe in the circular waveguide, a circular to rectangular transition feeds a section of rectangular waveguide containing an electric probe. Rotation of this latter section gives a response depending upon the ellipticity of polarization of the wave in the circular waveguide. Square-wave modulation of the source at 3 KHz and 50 Hz rotation of the probe unit produces a detected 3 KHz square wave with a 100 Hz modulation envelope. The mean level of the detector output is proportional to $V_I^2 (1 + |\Gamma|^2)$ and is used to level the source voltage V_I . The 100 Hz signal goes to a 90° phase splitter and produces a circle on the CRO with a radius proportional to $|\Gamma|/(1 + |\Gamma|^2)$. (The error due to this not being $|\Gamma|$ is less than 6.25% for $|\Gamma| < 0.25$.) A magnetic pickup head produces a signal corresponding to a certain angular position of the rotating probe. This signal is used to create a brightness modulation pulse which results in a spot on the CRO. The correct spot position is determined by calibrating it against a short-circuit termination. This system operated over a 10% frequency range at X-band with a total uncertainty in VSWR within $\pm 3.5\%$ at 1.7 VSWR.

Another variation on the basic idea is to use a fixed magnetic probe and rotate the polarization of the field by means of a ferrite Faraday polarization rotator [44]. The latter technique shown in figure 2-17 avoided mechanical problems with rotating probes, but did not yield the phase of Γ . Such a system operated over a frequency range of 8,550 to 10,000 MHz with errors in VSWR within $\pm 4\%$ for VSWR's up to 2.00.

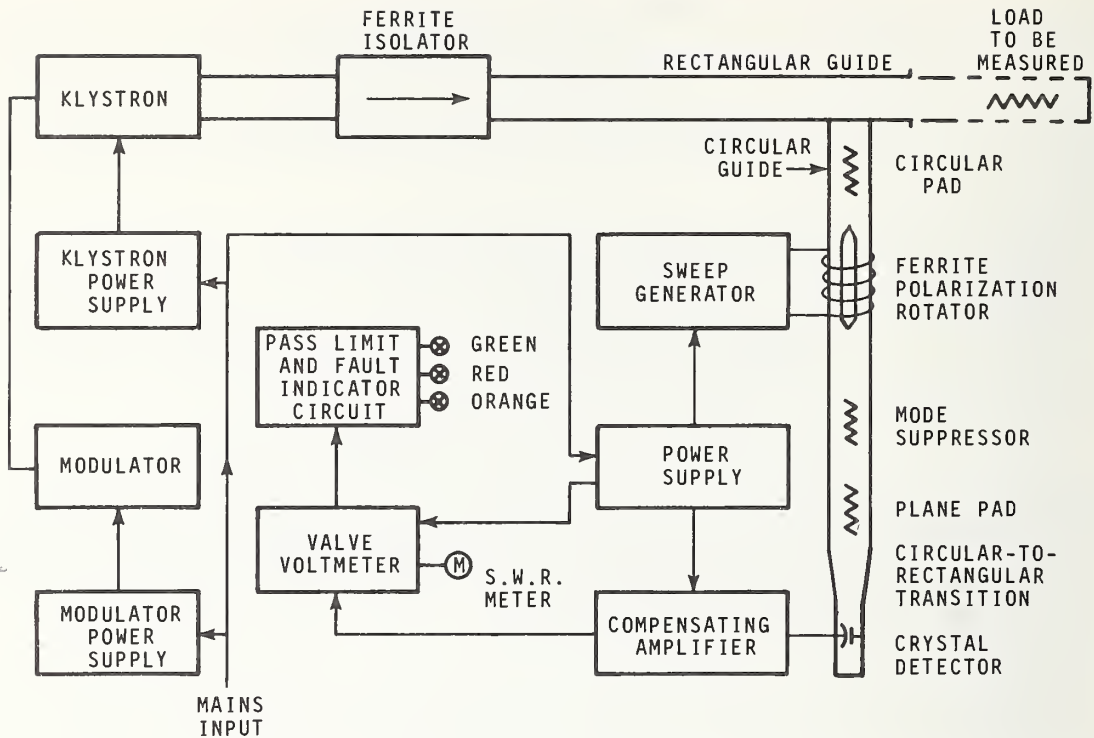


Figure 2-17. Block diagram of the automatic standing-wave indicator using a ferrite polarization rotator. (Valve voltmeter = vacuum tube voltmeter.)

Other arrangements which were suggested [28] include a rotating coupling loop in the auxiliary circular waveguide or a 4-probe system analogous to that previously developed [11], with probes placed at 45-degree intervals around the circumference of the auxiliary circular waveguide.

b. Coupling from Rectangular to Rectangular Waveguide

(1) Rotating Slot Coupler [63]

If one couples from one rectangular waveguide to an auxiliary rectangular waveguide at the same off-axis position as in figure 2-15, by means of a rotating dumbbell shaped slot (figure 2-18), the phase of the coupled reflected wave depends upon the angular orientation of the slot, but the phase of the coupled incident wave is practically independent of the slot angle. Thus, as one rotates the slot, the phase of the coupled reflected wave varies with respect to the phase of the coupled incident wave. For one rotation of the slot, the phase of the coupled wave goes through two complete cycles.

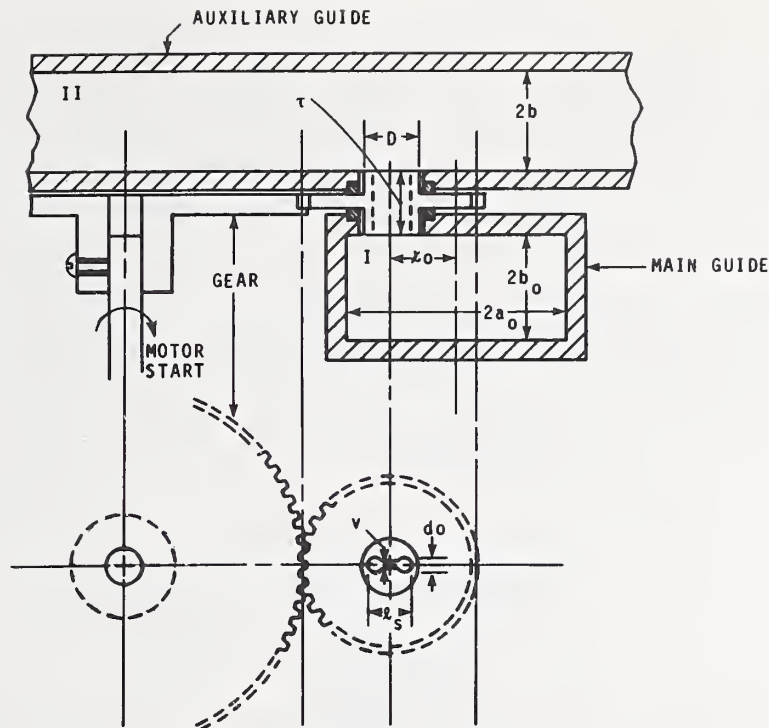


Figure 2-18. The construction of the rotating slot of the coupler. (Reprinted by permission: S. Tsuchiya, "A Smith-diagram Display Unit of Small Reflection Coefficients using the Vibrating-dummy Method", Proc. IEEE, 51, no. 11, Nov. 1963, pp. 1444-1454.)

The interference of the incident and reflected waves at the fixed probe in the auxiliary waveguide produces an output which follows the standing wave pattern in the main waveguide [63].

The detected a-c voltage from the probe at twice the frequency of the rotating slot is proportional to $|\Gamma| \cos \psi$, where $|\Gamma|$ and ψ are respectively the magnitude and phase of the measured voltage reflection coefficient. This output is divided and the portions are fed to the horizontal and vertical plates of a CRO after shifting the phase of one portion by 90° (so that it is proportional to $|\Gamma| \sin \psi$). The circle which appears on the screen has a radius proportional to $|\Gamma|$ and the phase is marked by a brightening pulse which is synchronized with the slot rotation. The measurement system is illustrated in figure 2-19.

Another feature accompanying this technique is the elimination of reflections from a load which is given a reciprocating motion inside the waveguide. The reciprocating motion produces a phase modulation of the reflected wave. If one adjusts the amount of this modulation, one can make the carrier disappear. Then by filtering out the sidebands, one has eliminated the reflection at the carrier frequency. Thus, one has simulated a non-reflecting load which is needed to calibrate the system. The arrangement is shown in figure 2-20.

Although this method is highly original and interesting, it has not been widely used. Methods not requiring mechanical motion and not bandwidth-limited have been subsequently developed.

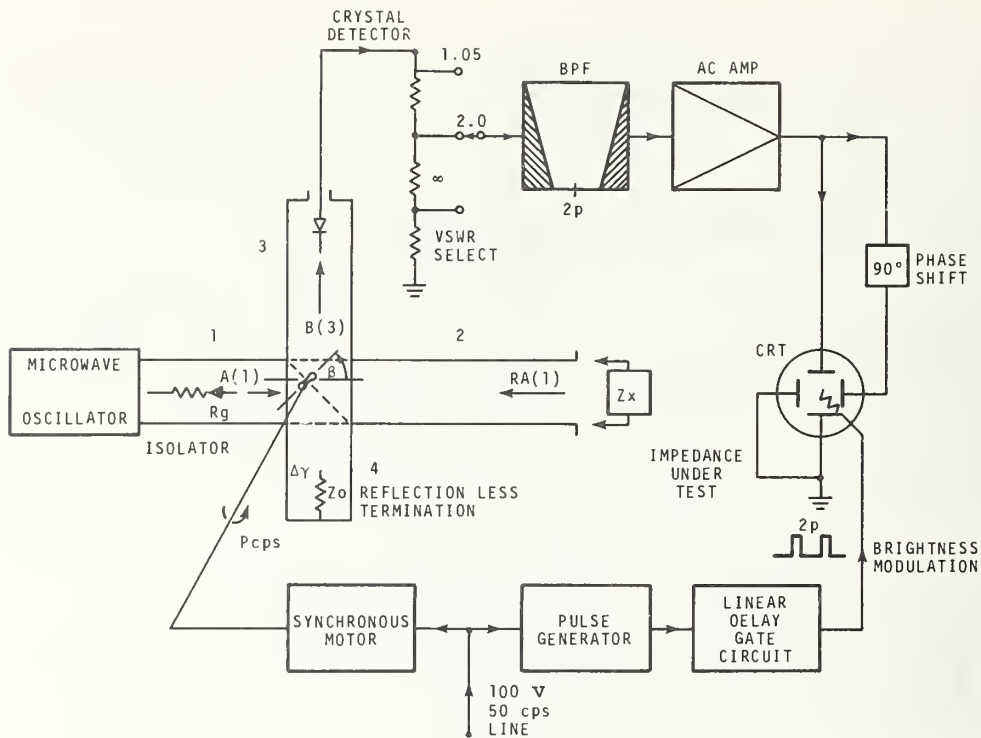


Figure 2-19. The arrangement of the impedance display unit. (Reprinted by permission: S. Tsuchiya, "A Smith-diagram Display Unit of Small Reflection Coefficients using the Vibrating-dummy Method", Proc. IEEE, 51, no. 11, Nov. 1963, pp. 1444-1454.)

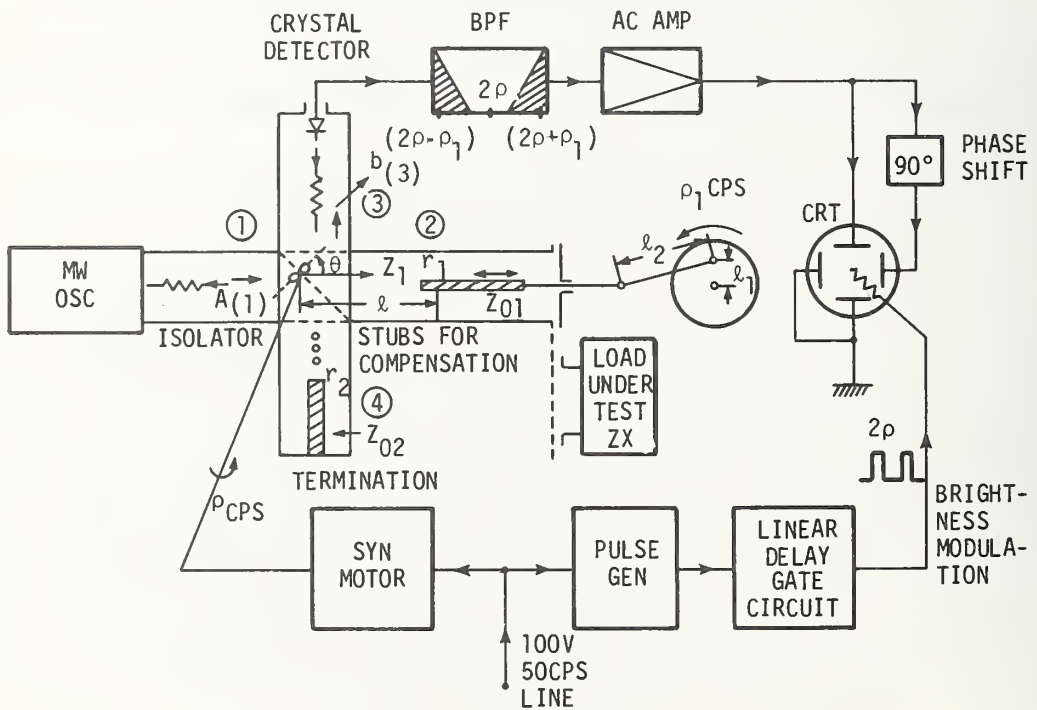


Figure 2-20. Arrangement for giving a sliding load a reciprocating motion to phase modulate reflection. (BPF = band pass filter.) (Reprinted by permission: S. Tsuchiya, "A Smith-diagram Display Unit of Small Reflection Coefficients using the Vibrating-dummy Method", Proc. IEEE, 51, no. 11, Nov. 1963, pp. 1444-1454.)

(2) Variable Phase Shifter

A logical extension of these ideas that has occurred to the author is shown in figure 2-21. In a cross-guide coupler, it is known (but apparently not so well-known [130]) that one can reproduce the usual slotted line response of a traveling probe in the main line by locating a fixed probe in the auxiliary waveguide on one side of the coupling hole and a sliding short-circuit on the other side [17, 43, 81]. The thought naturally occurs that one could achieve an automatic display of the standing wave (or of Γ) by imparting a reciprocating motion to the short-circuit or by inserting a variable (rotating or ferrite) phase shifter between a fixed short-circuit and the coupling hole. (It is not known whether this same idea has been previously proposed by others, although a similar idea has been reported which uses a motor driven phasable reflecting disc instead of a phasable short-circuit [98].)

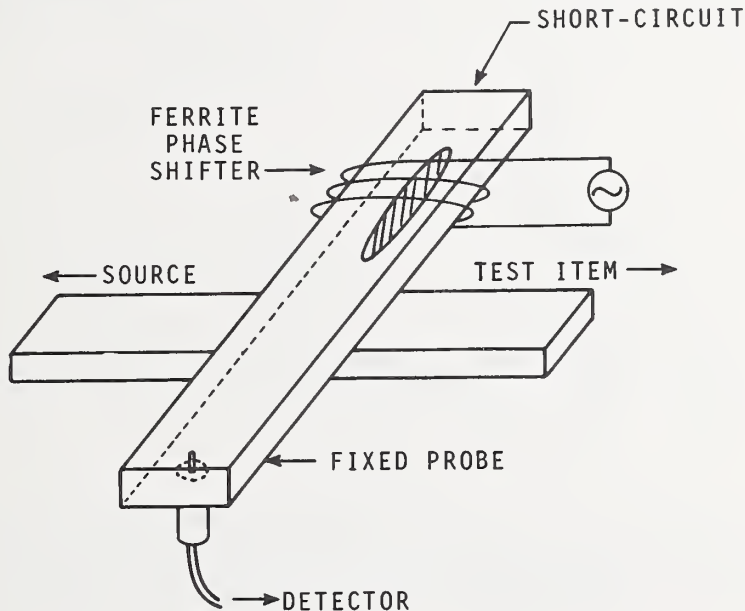


Figure 2-21. Proposed arrangement for automatic display of standing wave.

The usefulness of this method has not been explored, but appears to offer the basis for a broad band technique for applications at frequencies above 40 GHz, where there are presently few automatic systems available.

c. Coupling Coaxial Tees to Circular Waveguide

The above ideas which use off-axis coupling from a rectangular to circular waveguide have not been used in coaxial line because in the TEM mode, the magnetic field is completely transverse to the axis. However, it is possible to couple a circular waveguide to a T-junction of coaxial lines in such a way that a similar situation exists.

As shown in figure 2-22, the currents in the center conductors of the coaxial lines at the T-junction produce magnetic fields equal in magnitude, at right angles in space, and 90° apart in phase. This is the condition for circular polarization and holds when the test item is non-reflecting. When it reflects, then elliptical polarization is produced.

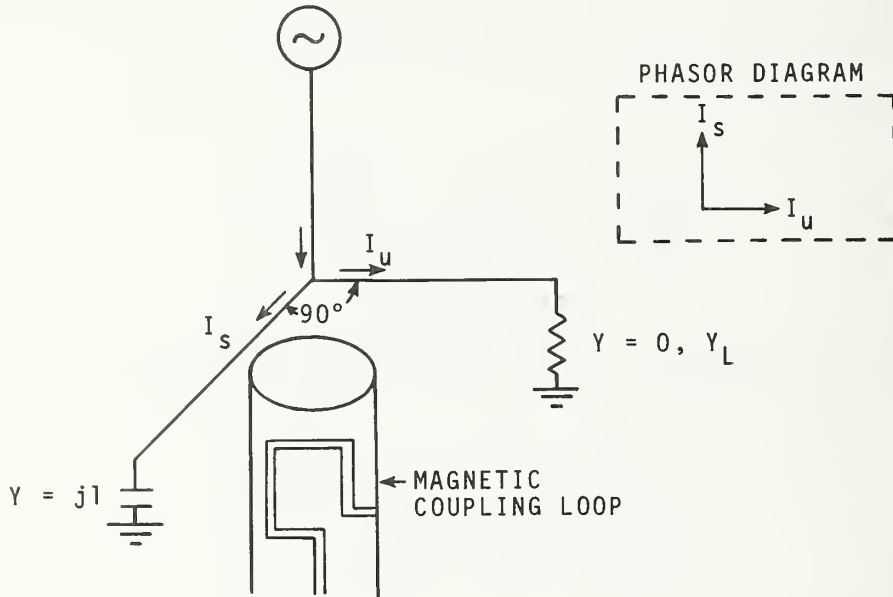


Figure 2-22. Coaxial Tee Junction for impedance measurement (20-300 MHz).

The amount and direction associated with the ellipticity correspond to the magnitude and phase of the reflected wave. An automatic display of the standing-wave pattern may then be produced on a CRO by rotating the probe and synchronizing the sweep with the probe rotation while feeding the rectified probe output to the vertical deflecting circuit [33].

A similar idea is shown in figure 2-23, where again, a circularly polarized magnetic field exists at the probe due to the current I_G being 90° out of phase with the current $(I_s - I_u)$, which is at right angles in space. The same potential exists for producing an automatic display of the standing-wave pattern [41].

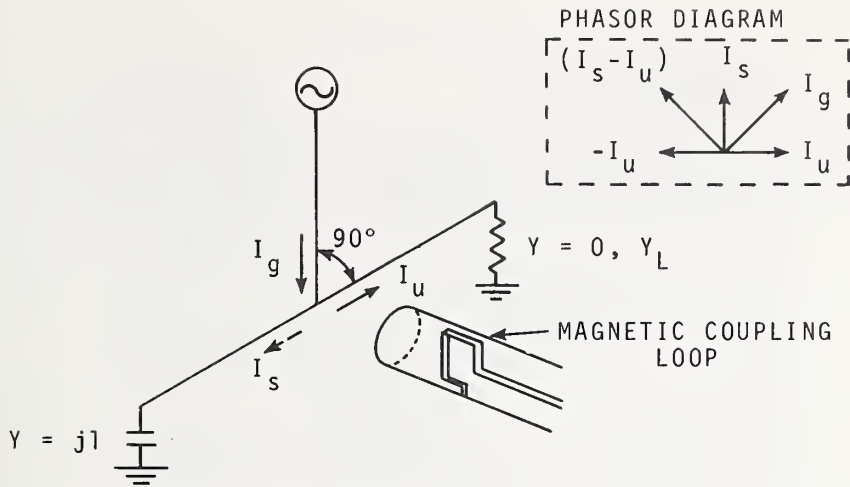


Figure 2-23. Coaxial Tee Junction for standing-wave indicator (50-1000 MHz).

2.4. VSWR, L_R , $|\Gamma|$, $|S_{mm}|$, or $|S_{nn}|$ only.

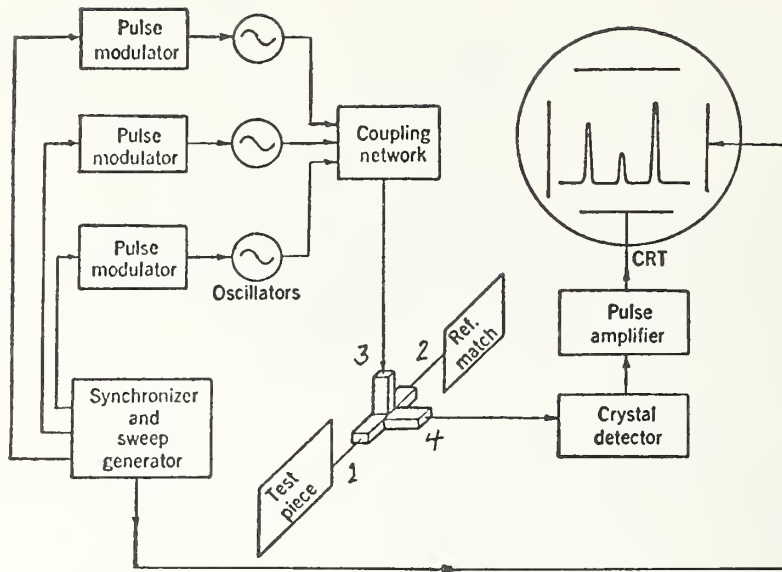
In the following, a direct display of VSWR or $|\Gamma|$ versus frequency on a CRO is obtained automatically.

a. Magic T

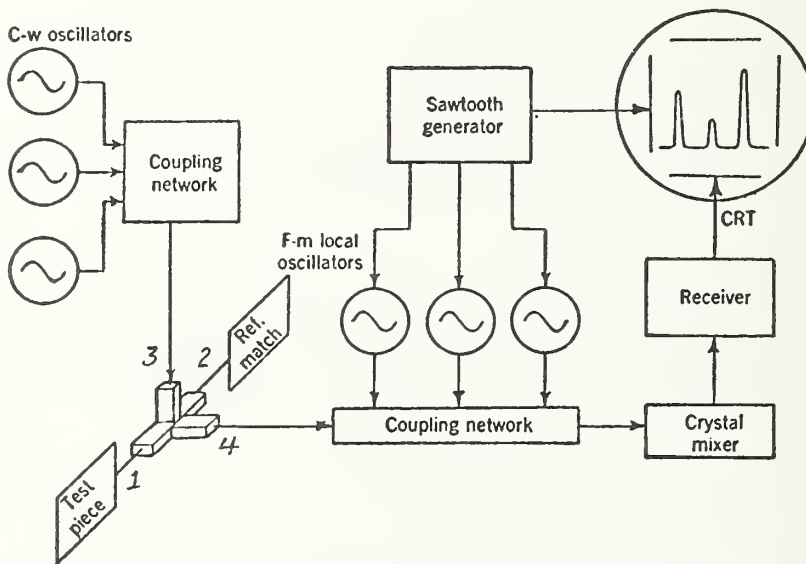
A multi-frequency bridge was developed for production testing and impedance matching. Two versions are shown in figure 2-24. The bridges operate on the principle that the ratio of power, P_D , delivered to the detector on arm 4 to the power P_3 delivered to arm 3 of an ideal magic T is

$$\frac{P_D}{P_3} = \frac{1}{4} |\Gamma_L|^2, \quad (7)$$

where Γ_L is the voltage reflection coefficient of the test item on arm 1, and a non-reflecting termination is on arm 2. After calibration and adjustment, the VSWR's of the test item at 3 frequencies can be simultaneously read from the screen of the CRO [10]. This bridge is not as accurate as a single frequency bridge because presently available magic tees do not maintain ideal properties over a large bandwidth.



a) Multifrequency bridge that employs pulse modulation.



b) Multifrequency bridge that utilizes a panoramic receiver.

Figure 2-24. Multi-frequency bridges using a Magic T. (Reprinted by permission: E. M. Purcell, "Measurement of Standing Waves", Chap. 8, pp. 511-512, and L. B. Young, "Impedance Bridges", Chap. 9, pp. 537-560, Massachusetts Institute of Technology. Techniques of Microwave Measurements, Copyright 1947, McGraw-Hill Book Company, New York.)

b. Non-directional Couplers

(1) Ratio of Detected Voltages

A swept frequency impedance indicator which operated over a bandwidth of 6% at around 10 GHz used a wave sampler consisting of 2 cross-guide couplers located at the same coupling plane in the waveguide [14].

The outputs of the wave sampler are proportional to

$$|v|^2 = A^2 + B^2 + 2 AB \cos \phi \propto |1 + \Gamma|^2 \quad (8)$$

and

$$|Z_o i|^2 = A^2 + B^2 - 2 AB \cos \phi \propto |1 - \Gamma|^2. \quad (9)$$

The ratio of these two voltages is displayed on a CRO. The maximum values correspond to

$$|Z|^2 = \left| \frac{1 + \Gamma}{1 - \Gamma} \right|^2. \quad (10)$$

The wave sampler is shown in figure 2-25 and a schematic of the system is shown in figure 2-26. Although the phase of the impedance is not displayed, it is possible to determine it by calculation after measuring the frequencies at which maximum and minimum values occurred on the CRO. This is facilitated by calibrating the apparatus against a short-circuit termination.

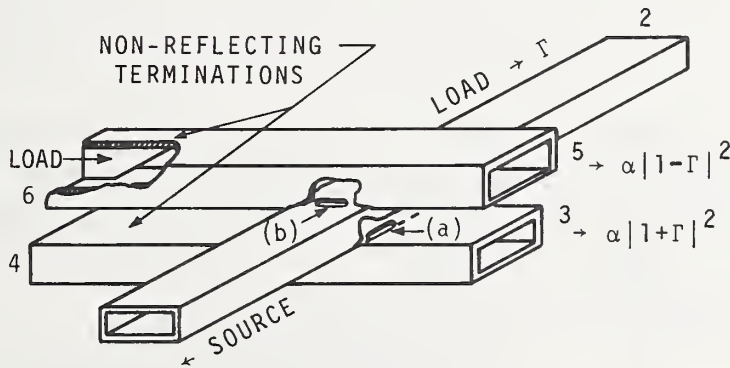


Figure 2-25. Wave sampler. (Reprinted by permission: H. J. Riblet, "A Swept-frequency 3-centimeter Impedance Indicator", Proc. IRE, 36, no. 12, Dec. 1948, pp. 1493-1499.)

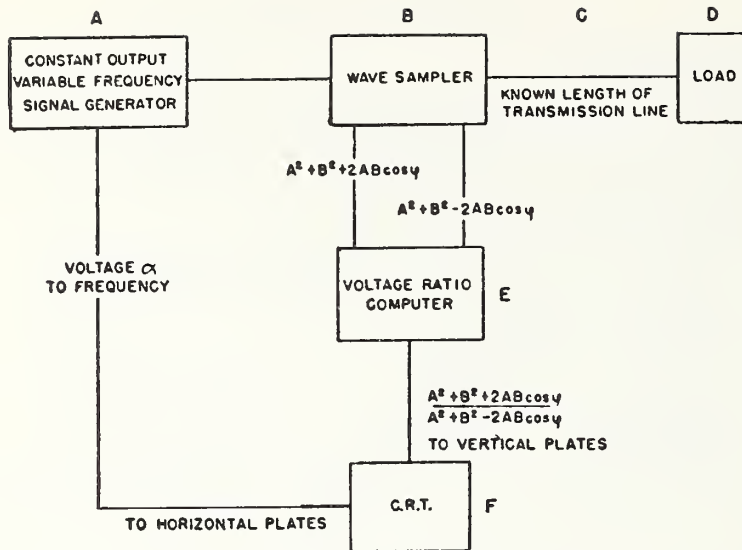


Figure 2-26. Schematic of system. (Reprinted by permission: H. J. Riblet, "A swept-frequency 3-centimeter impedance indicator", Proc. IRE, 36, no. 12, Dec. 1948, pp. 1493-1499.)

(2) Difference of Detected Voltages

The wave sampler previously described [14] was stated to be equivalent to a waveguide having two identical short probes $\lambda_G/4$ apart. Later [68], a broadband reflectometer was developed which featured two identical broadband probes $\lambda_G/4$ apart as shown in figure 2-27.

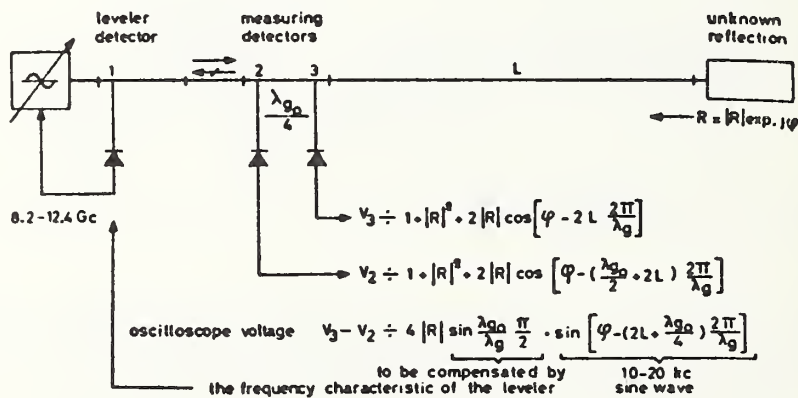


Figure 2-27. Principle of the reflecto"meter". (Reprinted by permission: F. C. deRonde, "A Precise and Sensitive X-band Reflectometer Providing Automatic Full-band Display of Reflection Coefficient", IEEE Trans. on MTT, 13, no. 4, July 1965, pp. 435-440.)

It is interesting to compare these two schemes, which have very similar circuit arrangements, but treat the probe outputs differently. The wave sampler square law detected outputs were fed to a ratio computer whose output was an audio voltage having maximum values ideally proportional to $|Z|^2$. The phase of Z (or Γ) was not displayed but could be calculated from the known lengths of waveguide and the frequencies at which the maxima and zeros occurred [14].

The broadband reflectometer [68] also displays (only the upper half) an audio voltage on the CRO, but it is derived from the difference, rather than the ratio, of the square law detected probe voltages. The $1 + |\Gamma|^2$ terms are eliminated and one observes an audio frequency voltage whose envelope is ideally proportional to $|\Gamma|$. The phase of Γ is not displayed and is ignored in this reflectometer, although it would be possible to determine phase by calculation if one knew the lengths of waveguide involved. This reflectometer operates over an entire waveguide band without serious deterioration of accuracy in contrast with the earlier technique using a wave sampler, which was limited to approximately a 12% frequency range.

A special leveling detector, employing lossy material in the leveling detector circuit compensates for frequency dependence of the two-probe difference output magnitude. This frequency dependence is given by

$$\sin\left(\frac{\pi}{2} \cdot \frac{\lambda_{G0}}{\lambda_G}\right),$$

where λ_{G0} is the guide wavelength at about mid-frequency or 10.2 GHz.

(3) Heterodyne Detection

A sweep-frequency, long line type of meter for displaying $|\Gamma|$ versus frequency was developed in 1948 [12] and operated from 30 - 250 MHz. The frequency was swept with a saw-tooth generator and the signal travelled at least 66 feet before being reflected. Consequently the oscillator frequency changed by the time the reflected signal was received back at the detector. An audio frequency beat note resulting from mixing these two signals was amplified and displayed on a CRO. The peaks of the audio signal were proportional to $|\Gamma|$. The phase angle of Γ was not displayed, but could be obtained by comparing the phase of the beat notes produced at any frequency when the load was replaced by a short-circuit. A block diagram of the system is shown in figure 2-28.

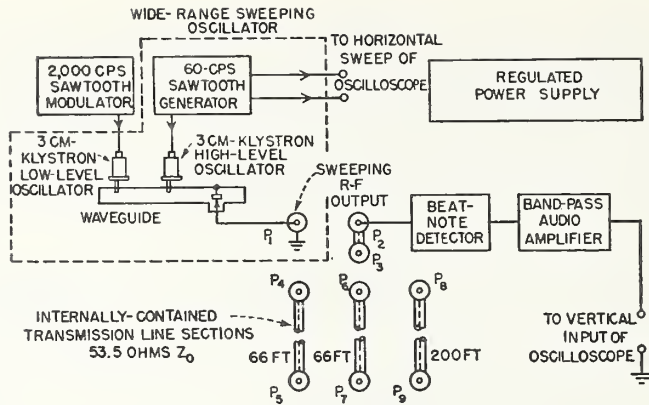


Figure 2-28. Block diagram of the frequency-scanning impedance meter showing lengths of transmission line available within the instrument. (Reprinted by permission: L. L. Libby, "Frequency-Scanning VHF Impedance Meter", *Electronics*, 21, no. 6, June 1948, Copyright McGraw-Hill, Inc., 1948.)

c. Rectangular Waveguide Directional Couplers

(1) High-directivity Rectangular Waveguide Coupler

A swept-frequency reflectometer which displayed $|\Gamma|$ versus frequency over a range of 4250 to 6000 MHz incorporated several basic ideas [20]. It was reasoned in a straightforward manner that an ideal swept frequency reflectometer would incorporate the following 4 perfect components:

1. Power leveler
2. Square-law detector
3. Square-root recorder
4. Hybrid junction.

The swept signal was pulse modulated and the width of the pulse was automatically regulated to keep the incident power constant. As shown in figure 2-29, a barretter detector

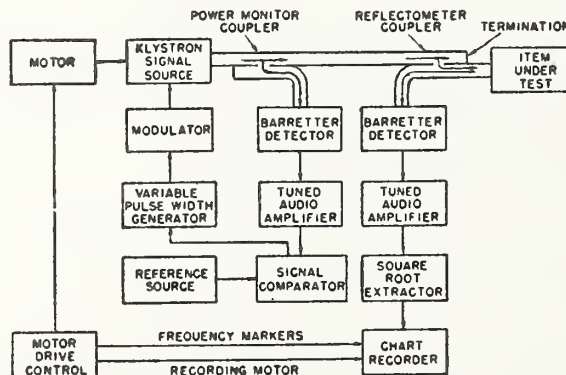


Figure 2-29. Block diagram of automatic broadband reflectometer. (Reprinted by permission: A. L. Witten and R. E. Henning, "A Recording Broadband Waveguide Reflectometer", *National Electronics Conference Proceedings*, 7, Nov. 1951, pp. 173-180.)

was used to achieve accurate square-law detection. The square root of the detected voltage was taken with a servo-controlled squaring circuit which used a vacuum tube harmonic generator. Instead of a hybrid or magic tee, a directional coupler having a directivity in excess of 40 dB was used.

(2) Compensated Directional Coupler

A different $|\Gamma|$ versus frequency display equipment is shown in figure 2-30 [58]. The display is on a CRO and its scale is calibrated by means of a rotary vane attenuator. A 50 MHz bandwidth is swept at 35 GHz. The klystron output was not levelled, but, instead, a compensating signal was applied to control gain of the 12 kHz amplifier following the

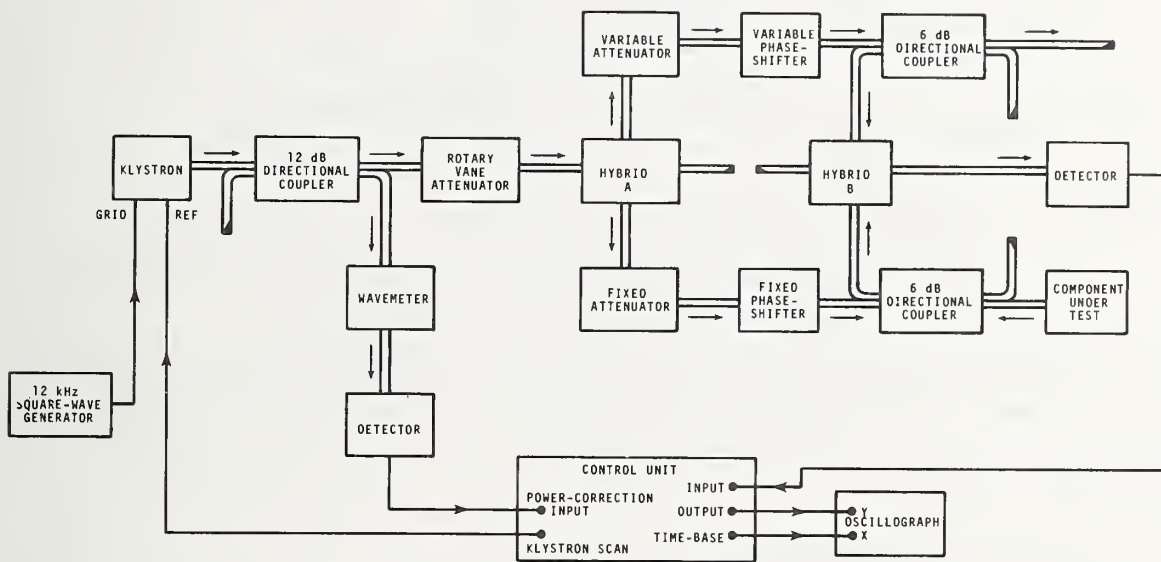


Figure 2-30. Display of $|\Gamma|$ versus frequency using a compensated directional coupler.

detector. A complicated scheme was used to compensate for the imperfect directivity of a directional coupler over a 50 MHz band. This was done by using an identical directional coupler terminated in a non-reflecting load. The signal due to its imperfect directivity was then subtracted from the corresponding signal from the first directional coupler, by means of hybrid "B" as shown in figure 2-30. It was claimed that the effective directivity exceeded 52 dB over at least a 50 MHz bandwidth.

A known $|\Gamma|$ of 0.2 was obtained by terminating a 7 dB attenuator in a short-circuit adjusted to a mean position between minimum and maximum reflected signals. This device is used to calibrate the reflectometer [58].

(3) Semi-automatic Tuning

The tedious adjustment of tuners in accurate fixed-frequency reflectometers was made semi-automatic by the arrangement shown in figure 2-31 [69]. A motor drive gives sliding

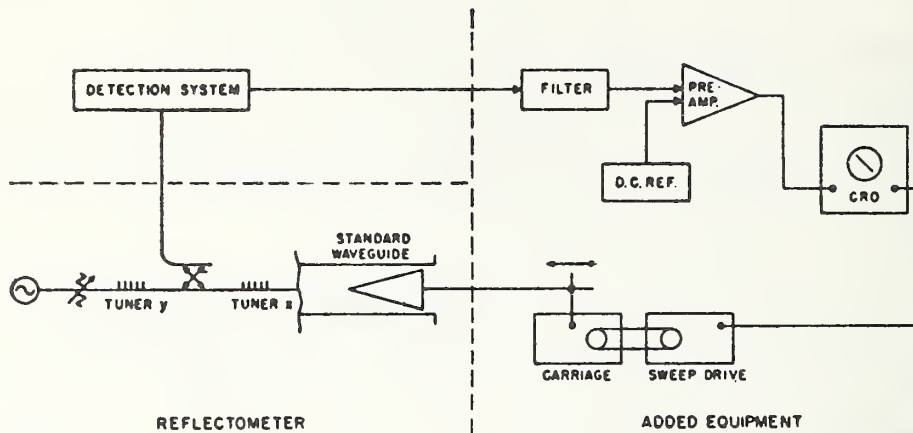


Figure 2-31. Block diagram of the reflectometer system using the semi-automatic technique. (Reprinted by permission: M. H. Zanboorie, "A Semi-automatic Technique for Tuning a Reflectometer", IEEE Trans. on MTT, 13, no. 5, Sept. 1965, pp. 709-710.)

loads in the output waveguide of the reflectometer a reciprocating motion and also feeds a synchronous sweep signal to a CRO. The reflectometer output is displayed on the CRO, where one can instantly see the effect of varying the tuners. The tuning time can thus be substantially reduced.

(4) High Resolution Reflectometer

A technique for measuring small reflections or for adjusting a waveguide termination for non-reflection was developed in 1969 [90]. It is related to the comparison reflectometer [77] and operates on a simple principle. As shown in figure 2-32, the test termination having a voltage reflection coefficient Γ_u is placed at the end of a long (2 meters) section of uniform waveguide. At the input to this waveguide is a taper to a step in the waveguide height which has a frequency-insensitive, calculable voltage reflection coefficient Γ_r . As the frequency is swept the two reflections go rapidly in and out of phase. A reflectometer measuring only the magnitude $|\Gamma|$ of the resulting voltage reflection coefficient has a response shown in figure 2-33. The maxima and minima of this response are approximately proportional to $|\Gamma_r| + |\Gamma_u|$ and to $|\Gamma_r| - |\Gamma_u|$, respectively. It is especially noteworthy that the sinusoidal variations caused by the interference of reflections vanish when the reflection from the termination vanishes. This effect is useful in tuning loads for no reflection and is valid even with imperfect reflectometers. As shown in figure 2-33, one can calibrate the instrument by substituting a standard reflection for the test item so as to obtain a sinusoid of known amplitude. One can then easily read $|\Gamma|$ versus frequency by noting the amplitude versus frequency of the sinusoid produced when the test item is connected.

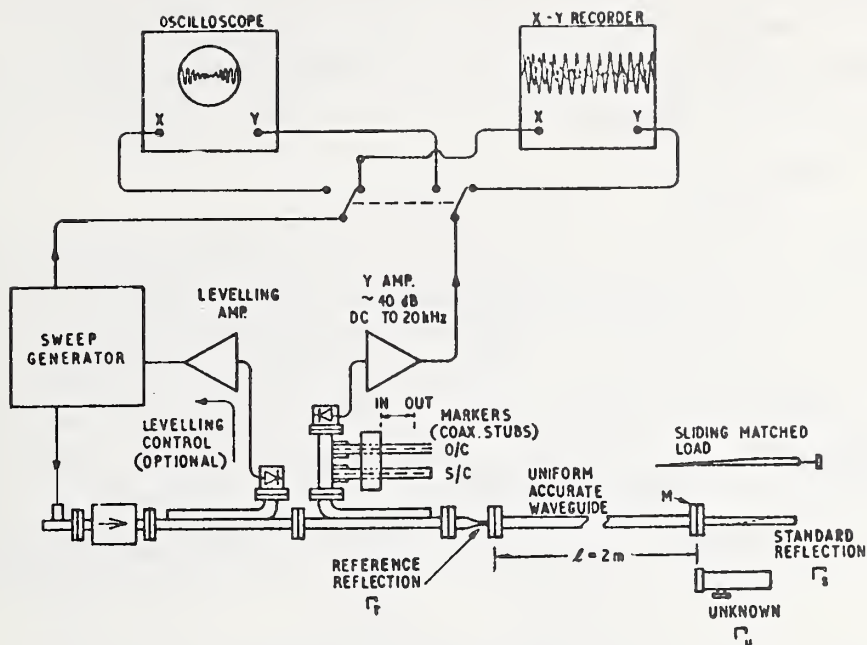


Figure 2-32. The high-resolution reflectometer. (Reprinted by permission: D. L. Hollway and P. I. Somlo, "A High-resolution Swept-frequency Reflectometer", IEEE Trans. on MTT, 17, no. 4, April 1969, pp. 185-188.)

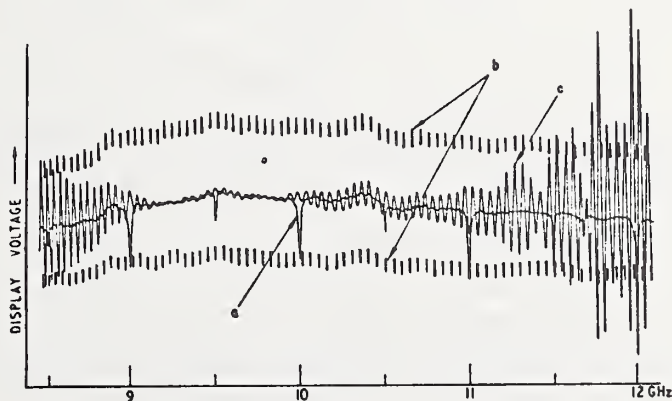


Figure 2-33. A typical broadband display. The amplitude of the sinusoid is proportional to the reflection at the output flange of the "long" waveguide. (a) A well-matched load, shown with frequency markers. (b) A standard reflection $|\Gamma_s| = 0.05$, used for calibration. (c) The input port of an isolator fitted with a broadband matching device. (Reprinted by permission: D. L. Hollway and P. I. Somlo, "A High-resolution Swept-frequency Reflectometer", IEEE Trans. on MTT, 17, no. 4, April 1969, pp. 185-188.)

d. Lumped Resistance Bridge

It is interesting that the magic T and the Wheatstone bridge shown in figure 2-34 have similar properties regarding the measurement of voltage reflection coefficient Γ . In each case the detector response is proportional to Γ_x . Normally, the performance of lumped

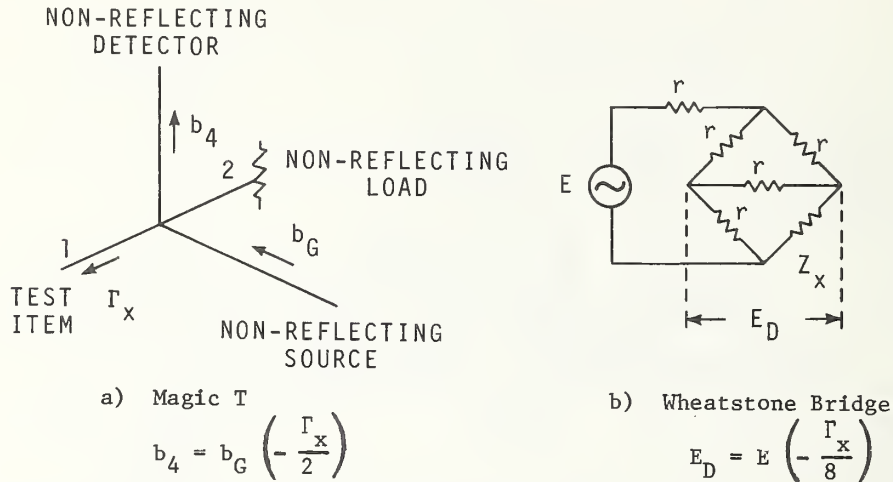


Figure 2-34. Schematic diagrams and detector response equations for Magic T and Wheatstone bridge.

element bridge circuits at low frequencies does not extend to high frequencies because the effect of residual impedances such as lead inductance and stray capacitance modifies the circuit. However, by careful attention to the design of a small bridge circuit, it has been possible to extend normal bridge performance up through frequencies as high as 12.4 GHz [120].

A swept frequency system for displaying $|\Gamma_x|$ versus frequency has been developed [120, 122]. The small bridge circuit includes a detector whose d-c output is fed to the d-c amplifier of an oscilloscope. The VSWR scales are calibrated by inserting standard attenuators between the source and the bridge when the test item is an open circuit. At the lower frequencies, (up to 100 MHz) an external standard resistor and length of line can be used to obtain a ripple response useful for measuring small $|\Gamma_x|$ or high return loss [122].

Although the detector voltage E_D carries phase information concerning Γ_x , this has not been exploited, and is lost when rectification to dc occurs. However, it is conceivable that techniques might be developed in the future to make phase information available.

With the present system, a swept frequency source must be well-leveled and have a low internal reflection coefficient. The bridge directivity is stated to be in excess of 43 dB up through 3 GHz. The detector law should be known or calibrated. With these precautions, the accuracy obtainable is comparable to that of other good swept frequency systems.

2.5. $|S_{11}|$ and $|S_{21}|$ Versus Frequency

In some applications, particularly when one wishes to instantly see the effect of circuit adjustments upon performance, a simultaneous display of both reflection and transmission data is very useful.

a. Rectangular Waveguide

An automatic "simultaneous" display on a CRO of both reflection and transmission characteristics of 2-port devices was produced in 1954 on a swept frequency basis over the range 8.5 to 9.6 GHz [25]. The purpose was to enable broadband TR (Transmit-Receive) tubes to be tuned. The investigation of parasitic resonances was also facilitated.

A klystron oscillator was grid-modulated at 262 kHz while its frequency was swept at 12 Hz. Directional couplers and crystal detectors were used in a straight forward manner to monitor reflected and transmitted power associated with a 2-port. On alternate half-cycles of the frequency sweep, reflection was displayed above baseline on the CRO and transmission was displayed below the baseline as shown in figure 2-35.

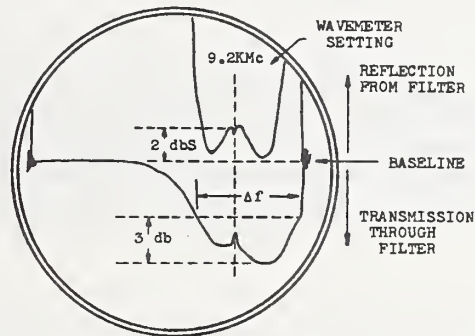


Figure 2-35. CRT display of the characteristics of a filter. (Reprinted by permission: H. H. Rickert and D. Dettinger, "An X-band Rapid-sweep Oscillator", IRE Con. Record, 2, Part 10, 1954, pp. 7-13.)

A different setup for simultaneously recording the magnitudes of reflection and transmission characteristics of a network was described in 1960 [49]. The principle of first recording calibrated grid lines was introduced. Figure 2-36 shows a setup for making swept frequency recordings of $|\Gamma|$ versus frequency and typical results are shown in figure 2-37. Figure 2-38 shows a setup for making swept frequency recordings of attenuation versus frequency and typical results are shown in figure 2-39. Simultaneous separate recordings of $|\Gamma|$ and attenuation are made with the setup shown in figure 2-40. The use of separate recordings permits one to pre-record calibration grid lines separately for $|\Gamma|$ and attenuation recordings, so as not to get too many lines on the same chart.

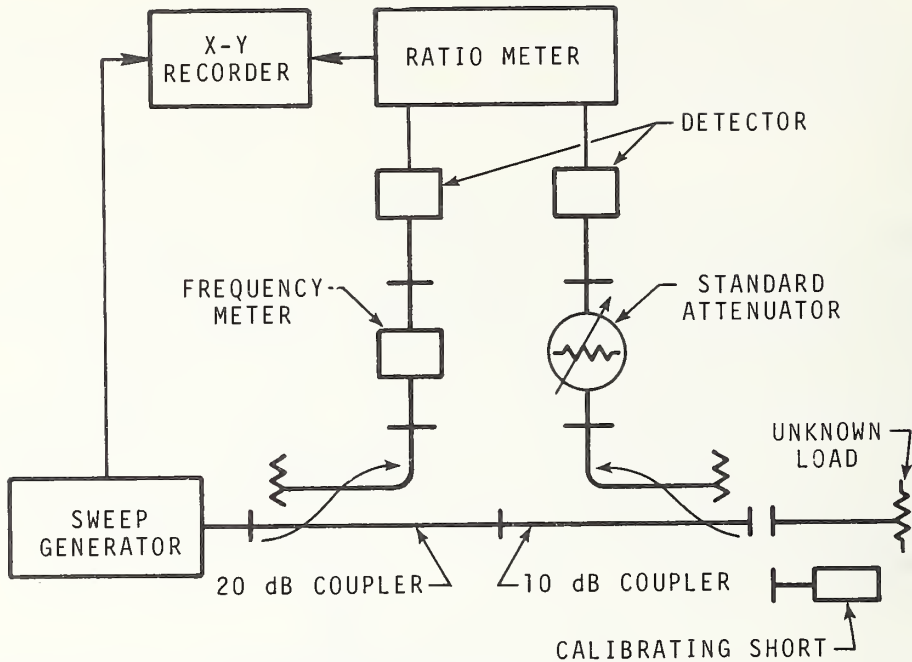


Figure 2-36. Microwave equipment set-up for making swept-frequency measurements of reflection coefficient. Use of precision attenuator in reflection arm enables a calibrated grid to be established for desired range of reflection coefficient. (Reprinted by permission: J. K. Hunton and E. Lorence, "Improved Sweep Frequency Techniques for Broadband Microwave Testing", Hewlett-Packard Journal, 12, no. 4, Dec. 1960.)

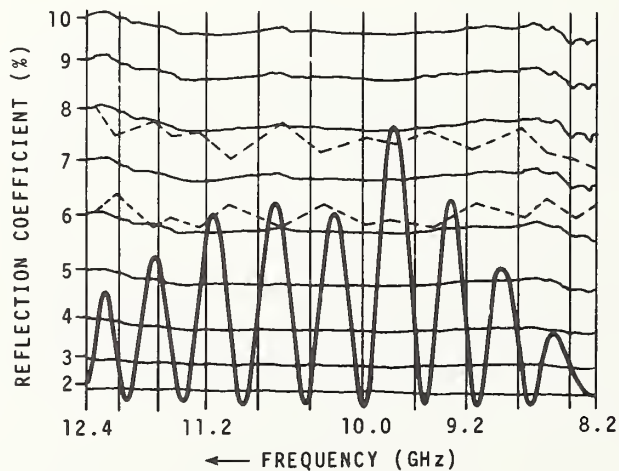


Figure 2-37. Typical swept-frequency reflection-coefficient measurement. Measurement can be recorded on transparent paper so that calibration grid, once made, can serve as an underlay for many measurements. X's show true value of three largest reflections as measured by single-frequency set-up. (Reprinted by permission: J. K. Hunton and E. Lorence, "Improved Sweep Frequency Techniques for Broadband Microwave Testing", Hewlett-Packard Journal, 12, no. 4, Dec. 1960.)

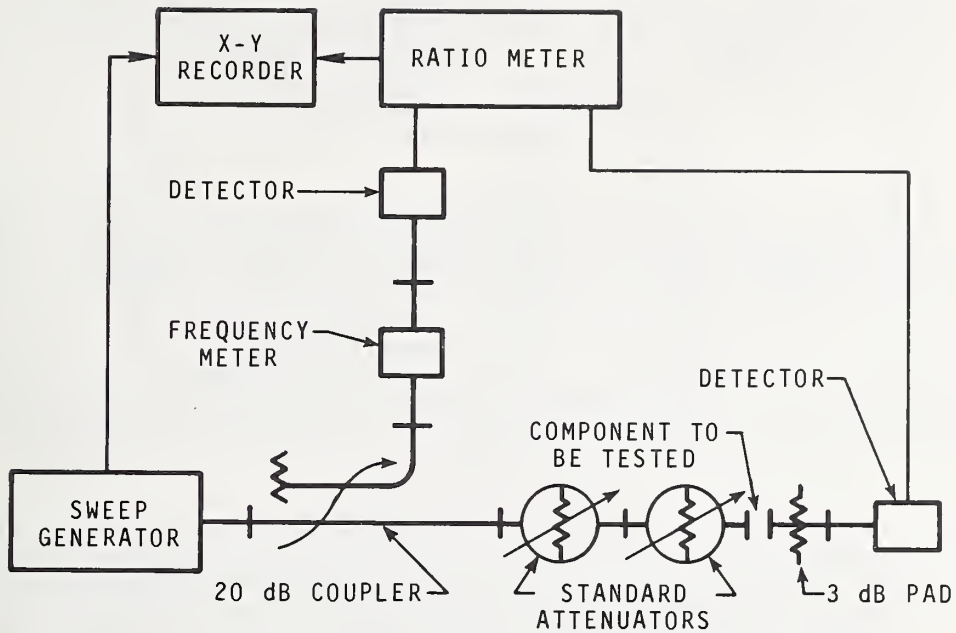


Figure 2-38. Equipment set-up for making swept-frequency measurements of attenuation. Calibration grid for attenuation measurements can be made by using one attenuator to establish desired attenuation region and second one to add small values to desired level. (Reprinted by permission: J. K. Hunton and E. Lorence, "Improved Sweep Frequency Techniques for Broadband Microwave Testing", Hewlett-Packard Journal, 12, no. 4, Dec. 1960.)

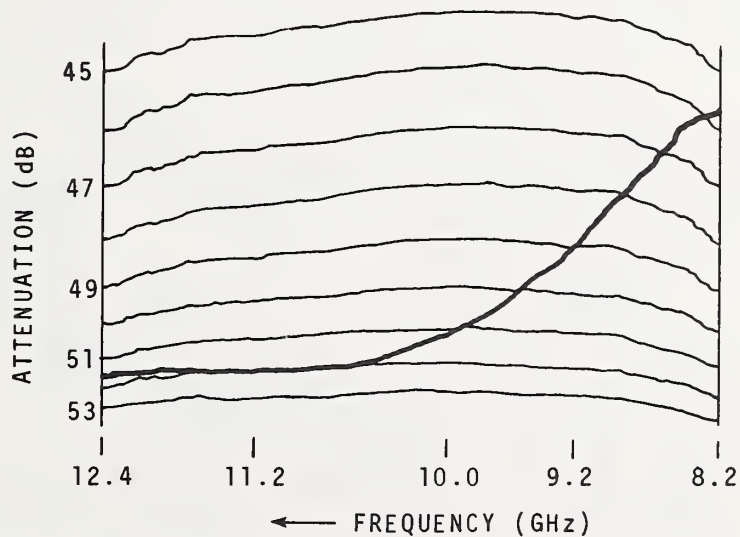


Figure 2-39. Measurement of attenuation of attenuator with dial set for 50 dB. Measurement can be recorded on transparent paper so that one calibration grid can serve for many measurements. (Reprinted by permission: J. K. Hunton and E. Lorence, "Improved Sweep Frequency Techniques for Broadband Microwave Testing", Hewlett-Packard Journal, 12, no. 4, Dec. 1960.)

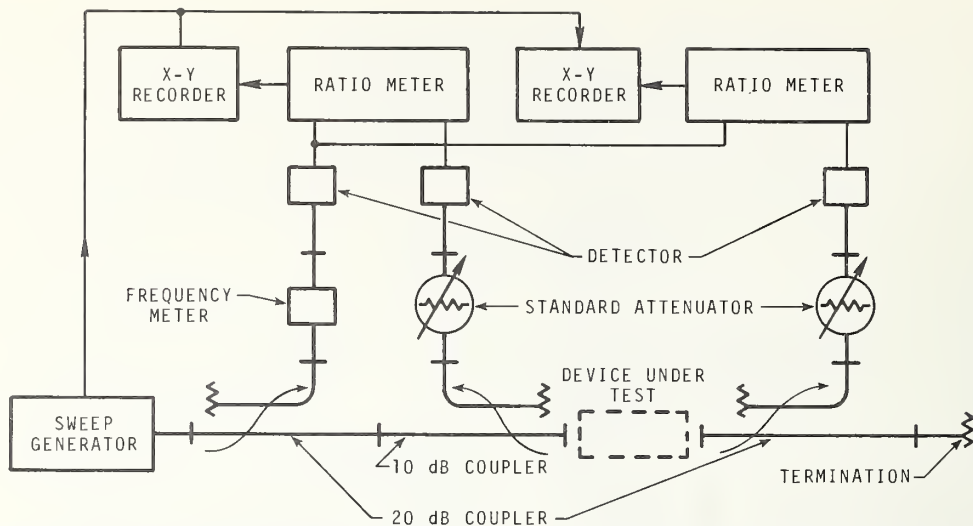


Figure 2-40. Equipment set-up for simultaneously measuring reflection and attenuation of component under test. Separate recorders are used so that grid lines for reflection coefficient and for attenuation appear on separate charts. (Reprinted by permission: J. K. Hunton and E. Lorence, "Improved Sweep Frequency Techniques for Broadband Microwave Testing", Hewlett-Packard Journal, 12, no. 4, Dec. 1960.)

The ratio meter used in these techniques measures the magnitude of the ratio of two square-law detected 1 kHz voltages. Its principle is shown in figure 2-41. Voltage E_1 is split and the phases of the components are shifted by $+90^\circ$ and -90° , respectively.

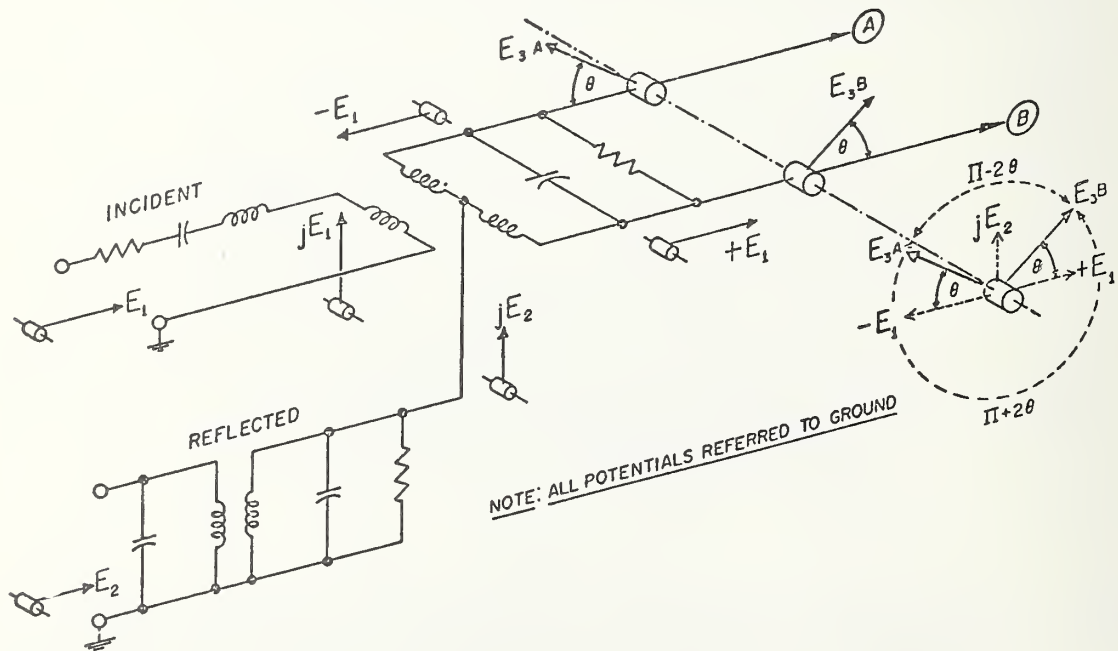


Figure 2-41. Diagram illustrating principle of ratio meter. (Reprinted by permission: Hewlett-Packard Instruction Manual, Hewlett-Packard/Operating and Service Manual, Section IV, 416A Radio Meter, printed Nov. 1961.)

The phase of voltage E_2 is shifted by 90° and added to the two components of E_1 . The resultant voltages E_A and E_B are equal in magnitude and their phase θ is determined by the equation

$$\tan \theta = \frac{E_2}{E_1} \cdot \quad (11)$$

The voltages A and B are fed to circuits which produce pulses as the voltages go through zero towards the negative direction. These pulses are applied to a flip flop circuit to produce a rectangular wave, the average value of which is proportional to θ . The output meter scale is calibrated to read $\sqrt{\tan \theta}$ which gives the desired ratio (corrected for square-law detection) of the microwave voltages before detection.

If the voltages are derived from the same source, variations in level will cause both voltage magnitudes to vary but the ratio meter indication will not change.

b. Coaxial

A swept-frequency reflectometer for the frequency ranges 20-1500 MHz and 0.5-7.0 GHz has been developed, employing broadband directional couplers having directivities greater than 40 dB for the lower range and greater than 37 dB for the higher range [89]. The directional coupler for the lower range is actually a lumped element resistive bridge shown in figure 2-42. The bridge is driven by a balanced source feeding terminals 1 and 5, and all other terminals except 7 and 8 are terminated in standard (Z_0) resistive loads. The output voltage of the detector at terminal 7 is proportional to the voltage reflection coefficient Γ of the unknown at terminal number 8 [93].

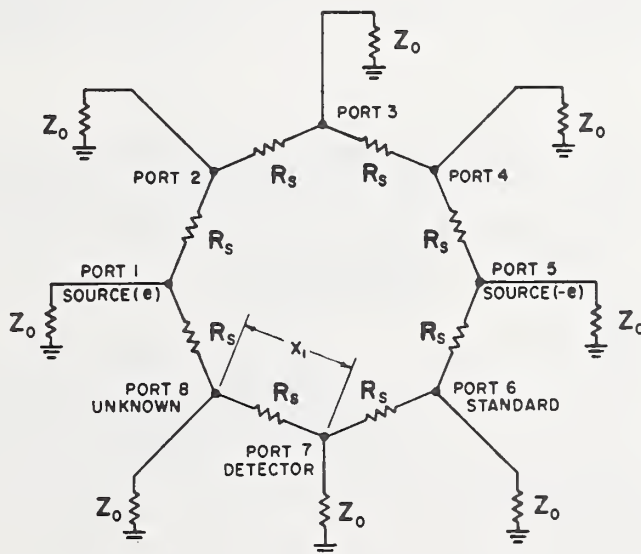


Figure 2-42. Lumped element resistive bridge. (Reprinted by permission: T. E. MacKenzie, "Some Recent Advances in Coaxial Components for Sweep-frequency Instrumentation", *Microwave Journal*, 12, no. 6, June 1969, pp. 69-77.)

In order to be able to simultaneously display reflection and transmission coefficients, the r-f circuit is arranged as shown in figure 2-43. The first directional coupler is used

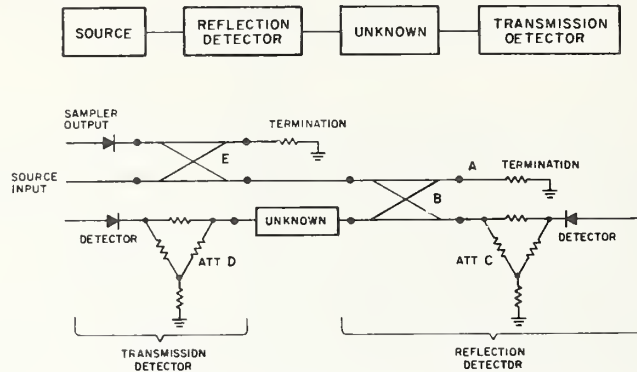


Figure 2-43. Directional-coupler arrangement. (Reprinted by permission: T. E. MacKenzie, "Some Recent Advances in Coaxial Components for Sweep-frequency Instrumentation", *Microwave Journal*, 12, no. 6, June 1969, pp. 69-77.)

for source leveling. Resistance-loaded diode detectors operate with square-law characteristics at low and moderate signal levels. Their 10 kHz demodulated output is rectified by a synchronous detector which is gated and holds sampled voltages on a storage capacitor. A d-c buffer amplifier provides d-c for display and metering. A block diagram is shown in figure 2-44.

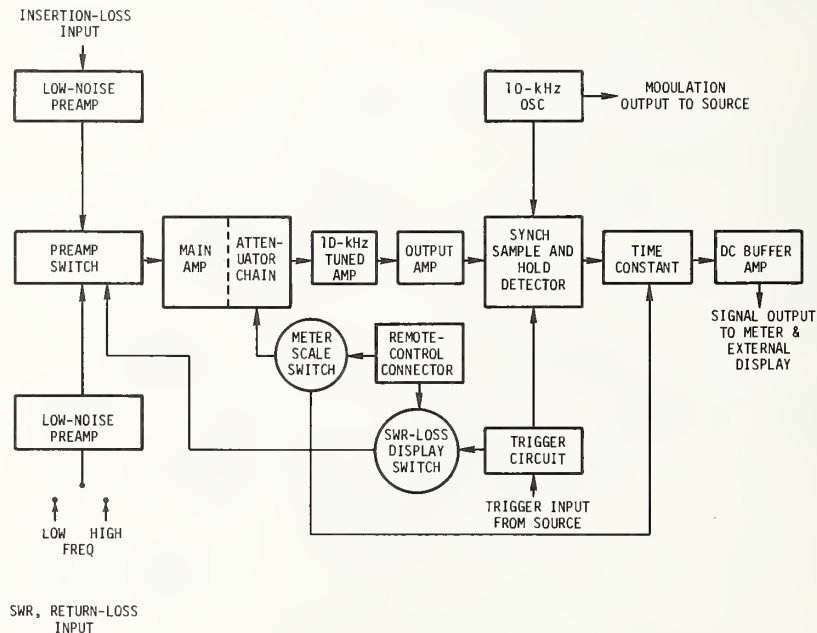


Figure 2-44. Synchronous detector block diagram. (Reprinted by permission: T. E. MacKenzie, J. F. Gilmore, and M. Khazam, "The New Sweep-frequency Reflectometer", *General Radio Experimenter*, 43, no's. 3 and 4, March-April 1969, pp. 3-14.)

2.6. Gain or Loss Versus Frequency

An early (1933) recording transmission measuring system was developed to operate at audio frequencies [4]. A motor driven oscillator swept through the frequency range while a strip chart recorder made a record of the receiver output. The source was leveled and a frequency marker was automatically put on the record by means of a tuned circuit. A block diagram of the system is shown in figure 2-45. This system demonstrated some of the advantages of automatic measurement and was a precursor for the modern sophisticated systems which later evolved.

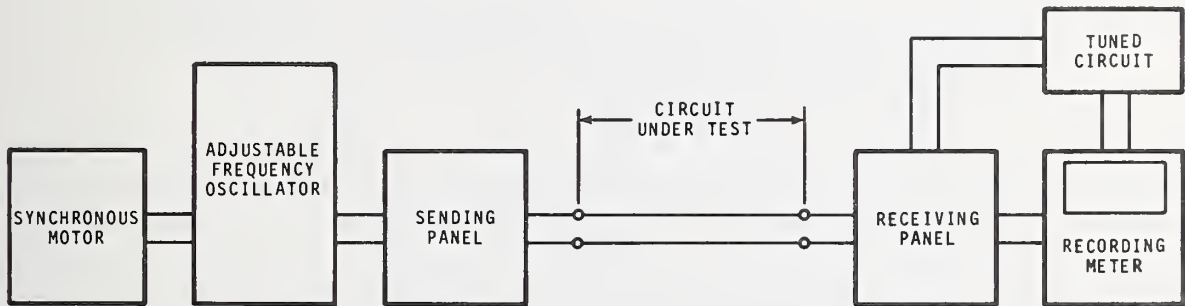


Figure 2-45. Schematic arrangement of recording system. (Reprinted by permission: F. H. Best, "A Recording Transmission Measuring System for Telephone Circuit Testing", Bell System Technical Journal, 12, no. 1, January issue, pp. 22-34. Copyright 1933, American Telephone and Telegraph Company.)

2.7. Display of Complex Z or Γ

a. Multiple Probes

Up to this point, we have discussed partial automation of measurement of complex Z or Γ , or of only the magnitude of Z or Γ by the following techniques. The voltage standing wave is sampled by:

- (a) Moving a probe along a slot.
- (b) Moving the standing wave past a fixed probe.
- (c) Moving the standing wave past two fixed probes.
- (d) Transforming the standing wave to an elliptically polarized magnetic field and rotating a magnetic field probe.

In contrast to these techniques, we now consider measurement of Z or Γ by sampling the standing wave simultaneously at three or more fixed points whose relative positions are known.

(1) Four Fixed Probes

One of the simplest methods for obtaining a display of complex Γ on a CRO was reported in 1947 [11]. As shown in figure 2-46, the differences in the rectified dc outputs of two

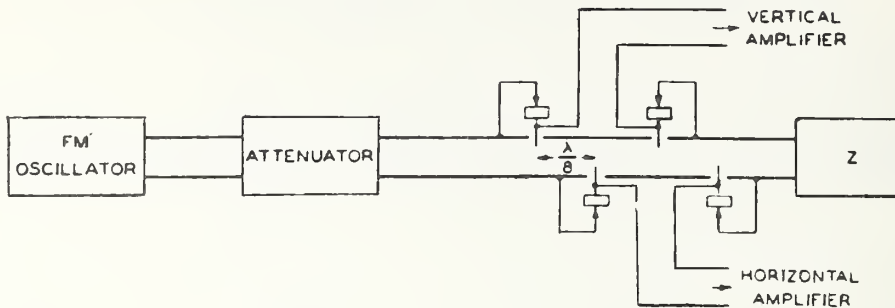


Figure 2-46. Schematic drawing of the simple four-probe method. (Reprinted by permission: A. L. Samuel, "An Oscillographic Method of Presenting Impedances on the Reflection Coefficient Plane", Proc. IRE, 35, no. 11, Nov. 1947, pp. 1279-1283.)

pairs of probes (the four probes spaced $\lambda_G/8$ apart along the center of the broadwall of a rectangular waveguide) are fed to the vertical and horizontal dc amplifiers, respectively of an oscilloscope. Suppose that the incident and reflected voltage waves have magnitudes V_I and V_R and phase difference θ . One of the CRO deflections is proportional to $V_R \sin \theta$, and the other is proportional to $V_R \cos \theta$ (in the ideal case), so that a spot is produced on the screen in the same relative position that Γ would have in the complex plane. It is assumed that probe loading is negligible, that the source is non-reflecting, that the probes and detectors are identical and square-law. Departures from these conditions will cause errors.

If the frequency is swept, additional errors will be introduced because the probe spacing will depart from the correct value as the frequency changes from the design frequency. A change in signal level during sweeping can introduce additional error. If the frequency is not swept more than 5 percent, it is claimed that one can hold the total uncertainty in $|\Gamma|$ within 5 percent.

Instead of using four probes, it is possible to use directional couplers and hybrid junctions to achieve the same results as shown in figure 2-47.

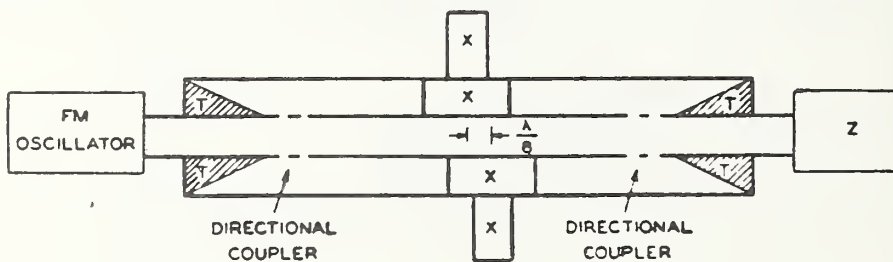


Figure 2-47. A circuit employing hybrid junctions to perform the required additions and subtractions. (x denotes detector attached to arm of hybrid junction.) (Reprinted by permission: A. L. Samuel, "An Oscillographic Method of Presenting Impedances on the Reflection Coefficient Plane", Proc. IRE. 35, no. 11, Nov. 1947, pp. 1279-1283.)

If one desires the transmission coefficient S_{21} of a 2-port, the arrangement in figure 2-48 is suggested. However, the main advantage of this technique lies in its simplicity and ease of setting up in the form shown in figure 2-46.

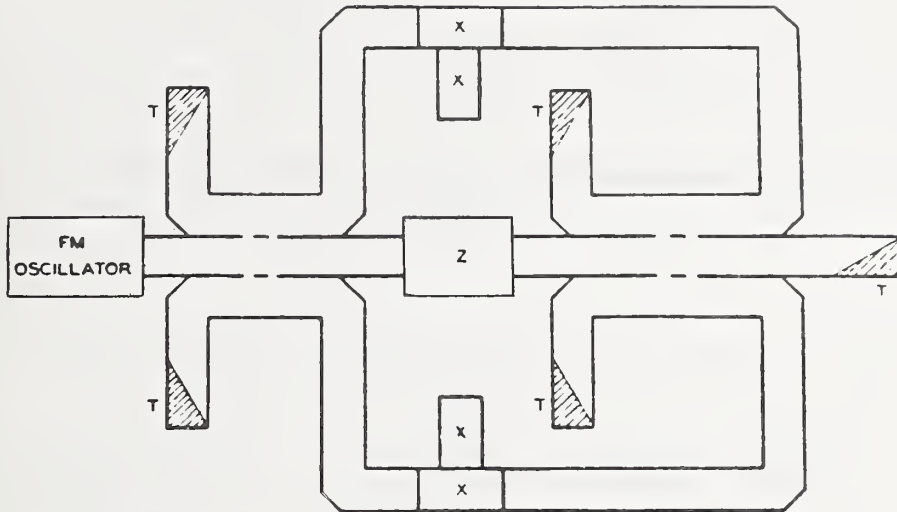


Figure 2-48. Transmission-measuring circuit based on the same principles. (Reprinted by permission: A. L. Samuel, "An Oscillographic Method of Presenting Impedances on the Reflection Coefficient Plane", Proc. IRE, 35, no. 11, Nov. 1947, pp. 1279-1283.)

A later (1958) version of the four-probe technique achieves a 10 percent sweep at X-band by improved source leveling and claims the total uncertainties in $|\Gamma|$ are within ± 4 percent, and, in phase of Γ within $\pm 2^\circ$ [39]. The sum of a pair of probe voltages is proportional to $V_T^2 (1 + |\Gamma|^2)$ and is held constant by comparing it to a standard reference voltage to derive an error signal which is applied to a ferrite attenuator.

A still later (1963) version of the 4-probe technique used wall current detectors and operated on a swept frequency bandwidth of 10 percent at X-band [60]. It was stated that because of the simplicity of the principle, it could easily be scaled down in size for use at millimeter waves.

(2) Three (or five) Fixed Probes

Instead of using four fixed probes and taking the difference of detector outputs from probe pairs, a more complicated system was developed for combining the square-law detected outputs from three fixed probes [57]. The advantage was stated to be more broadband operation without introducing inherent error due to incorrect probe spacing at other than the design frequency.

The three probes are equally spaced a distance ℓ apart as shown in figure 2-49. The angular spacing $\theta = 2\pi\ell/\lambda_G$. The voltage reflection coefficient of the load referred to

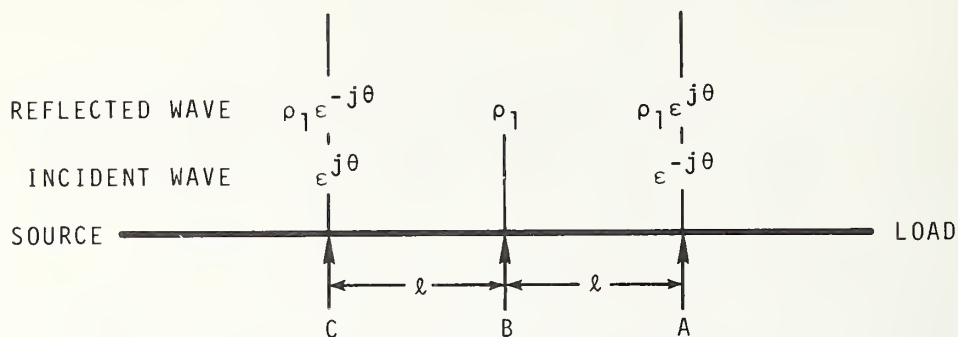


Figure 2-49. Arrangement of three probes in the measuring section.

probe position B is $|\Gamma|e^{j\psi}$. The three square-law detected probe voltages are:

$$V_B = K(1 + |\Gamma|^2 + 2|\Gamma| \cos \psi) \quad (12)$$

$$V_A = K(1 + |\Gamma|^2 + 2|\Gamma| \cos(\psi + 2\theta)) \quad (13)$$

$$V_C = K(1 + |\Gamma|^2 + 2|\Gamma| \cos(\psi - 2\theta)) \quad (14)$$

where K is a constant of proportionality depending upon the probe coupling and detector sensitivity. It is assumed that K is the same for all three probes. It can be shown that

$$|\Gamma| \sin \psi = \frac{V_C - V_A}{4K \sin 2\theta}, \quad (15)$$

and

$$|\Gamma| \cos \psi = \frac{1}{4K \sin^2 \theta} \left(V_B - \frac{V_A + V_C}{2} \right). \quad (16)$$

It is evident that the above combinations of detected probe voltages will yield suitable CRO deflection voltages to produce a visual display of complex Γ . Calibration is accomplished by appropriate amplifier gain adjustments when the load is replaced by a non-reflecting termination and by a sliding short-circuit. When operating with swept-frequency an automatic level control should be used which compensates for variations with frequency of probe and detector characteristics.

If two more probes are added and the spacing between probes is chosen to be $\lambda_G/8$,

$$|\Gamma| \cos \psi = \frac{1}{4K^2 \sin 2\theta} \left(V_B - \frac{V'_A + V'_C}{2} \right), \quad (17)$$

where V'_A and V'_C are voltages from probes at load and source ends, respectively. Then the gains required for both deflection circuits will vary only moderately with frequency over an appreciable range.

The system diagram shown in figure 2-50 is intended for spot-frequency operation and modification for swept-frequency use was thought possible, but was not done.

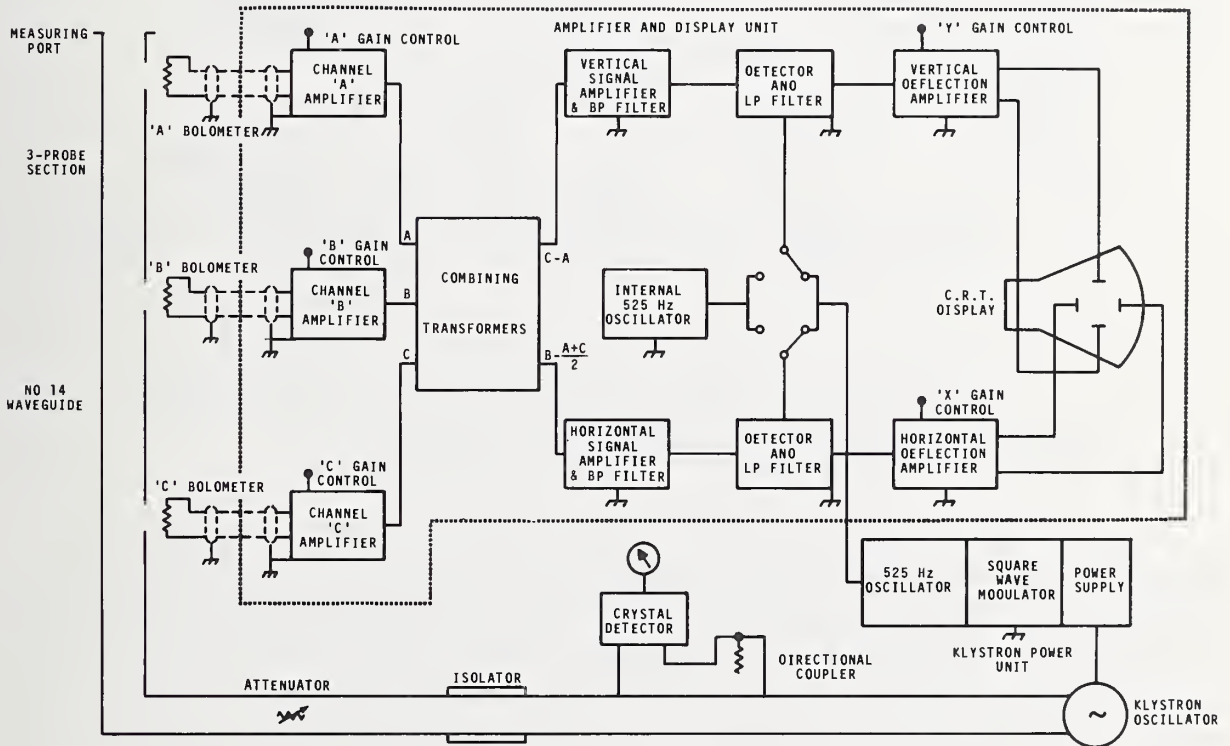


Figure 2-50. Schematic of reflection coefficient display equipment.

b. Directional Couplers and Hybrids

(1) Semi-automatic Diagram

A simple system for visually displaying complex Γ at a single frequency within the range 30 - 300 MHz is shown in figure 2-51. It was described in 1955 [31].

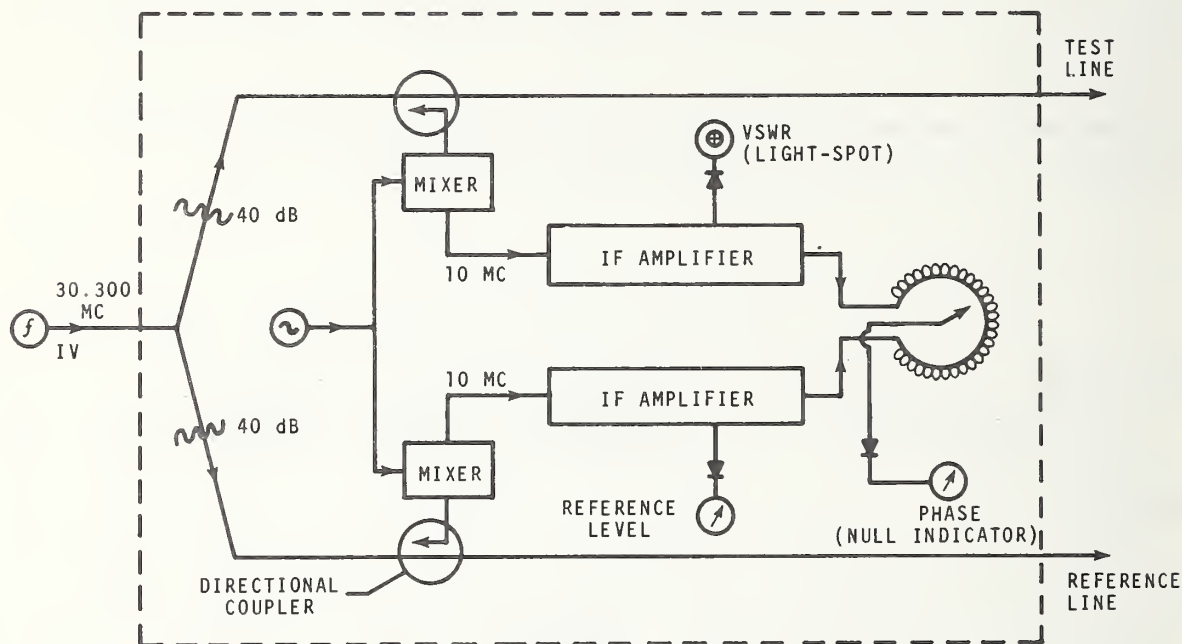


Figure 2-51. Diagram of semi-automatic frequency Γ -plotter. (Reprinted by permission: R. C. Hess, "The Diagram, A Direct Reading Instrument for Graphic Presentation of Complex Impedances and Admittances", IRE Con. Record, 3, part 10, 1955, pp. 23-25.)

The signal is split into two channels, one terminated in the test item and the other terminated by a sliding short-circuit. Directional couplers (directivity > 50 dB) feed reflected signal components to mixers and two 10 MHz I-F channels are obtained. A portion of each I-F signal is detected to give relative levels (one activates a light-spot galvanometer) and the other portions feed opposite ends of a coiled, circular delay line. A capacitively coupled probe (mechanically coupled to the Smith Chart Screen) is rotated to the position for null output to provide phase in formation. Operation is semi-automatic in that the angular position of the Smith Chart Screen is adjusted manually.

(2) Servo Control

A panoramic impedance plotter was developed in 1952 [22] to plot complex Γ on a servo-controlled recorder turntable. A variable frequency source operated between 900 and 1300 MHz. A hybrid ring phase comparator operating at 2650 MHz developed an error signal to operate the turntable servo. A bolometer bridge output fed the recorder pen servo. Broadband directional couplers were used to separate incident and reflected signal components.

A somewhat similar system operating from 8.4 to 9.9 GHz was described in 1954 [27]. It used directional couplers to separate incident and reflected components of a 60 Hz square-wave modulated signal. As shown in figure 2-52, hybrid junctions were used to split these

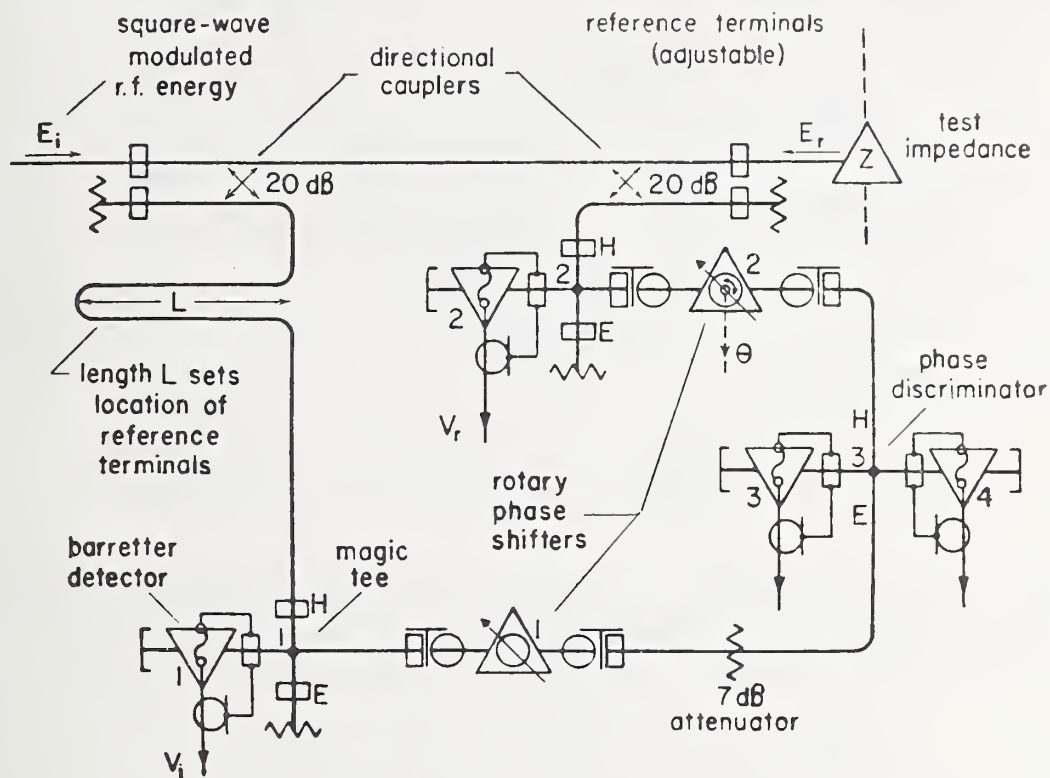


Figure 2-52. RF impedance circuit schematic. (Reprinted by permission: W. F. Gabriel, "An Automatic Impedance Recorder for X-band", Proc. IRE, 42, no. 9, Sept. 1954, pp. 1410-1421.)

signal components so that simultaneously magnitude and phase detectors could be operated. The magnitude and phase servo loops shown in figures 2-53 and 2-54 operated at 60 Hz and controlled a turntable and recorder pen. Frequency sweep and frequency indication are performed manually. Approximately 10-15 minutes are required to obtain a plot of Γ over the frequency range of the equipment.

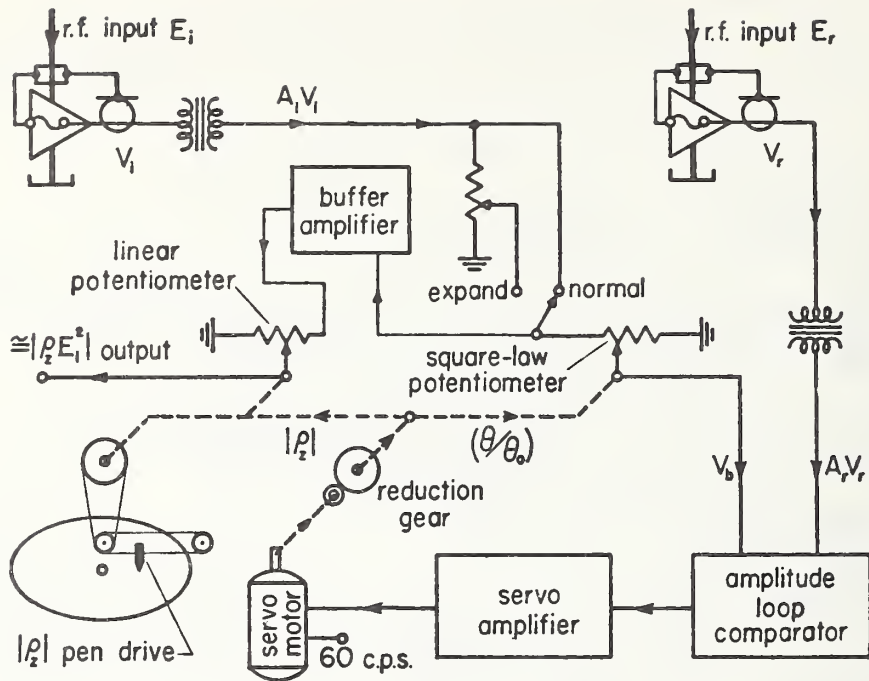


Figure 2-53. Magnitude servo loop. (Reprinted by permission: W. F. Gabriel, "An Automatic Impedance Recorder for X-band", Proc. IRE, 42, no. 9, Sept. 1954, pp. 1410-1421.)

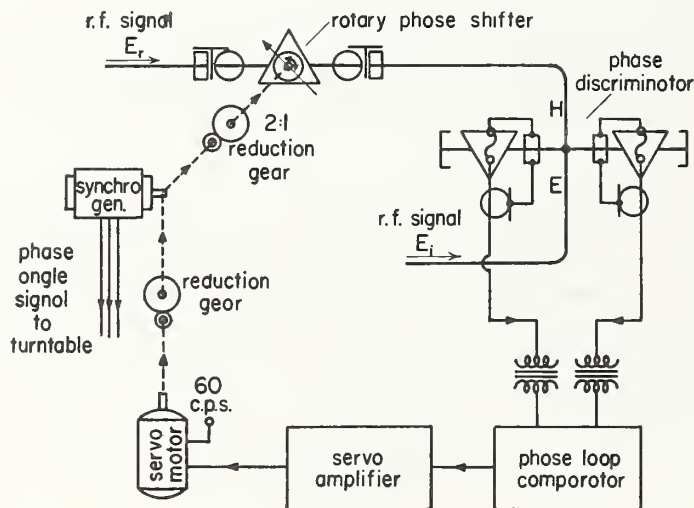


Figure 2-54. Phase servo loop. (Reprinted by permission: W. F. Gabriel, "An Automatic Impedance Recorder for X-band", Proc. IRE, 42, no. 9, Sept. 1954, pp. 1410-1421.)

(3) Balanced Modulator

An early swept frequency system (8.8 - 10 GHz) for displaying Γ on a CRO was described in 1951 [18]. A rotating phase shifter was used to produce a "local oscillator" signal 220 Hz away from the source frequency which was swept mechanically, once every two seconds. The 220 Hz driving energy for the rotating phase shifter was derived from an oscillator which also furnished the reference signals for balanced modulator types of phase sensitive detectors which fed the deflection amplifiers of a CRO. Although details are lacking, this portion of the circuit appears similar to an earlier system [5]. At fixed frequencies, a null balance method using an audio attenuator and phase shifter were used to obtain increased accuracy. The circuit is shown in figure 2-55 and incorporated one of the first rotary vane attenuators. It was noted that the system could also be used to measure complex transmission coefficients by connecting the item under test directly between the output and the signal input to the mixer.

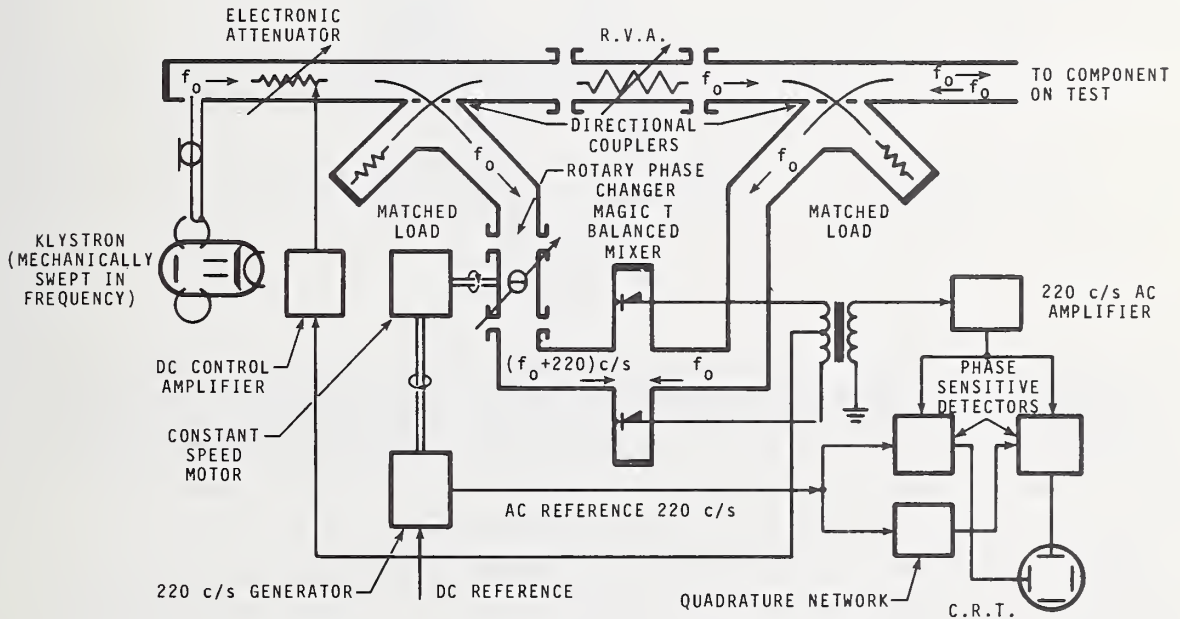


Figure 2-55. Circuit diagram.

Another system which appears to use the balanced modulator circuit [1,3,5] was developed in 1953 [23]. It displays Γ on a CRO which has a Smith Chart overlay. It sweeps over 100-200 MHz or 200-400 MHz. Two tracking local oscillators produce I-F's of 40 MHz and 5 MHz. As shown in figure 2-56, voltages proportional to the direct and reflected waves are

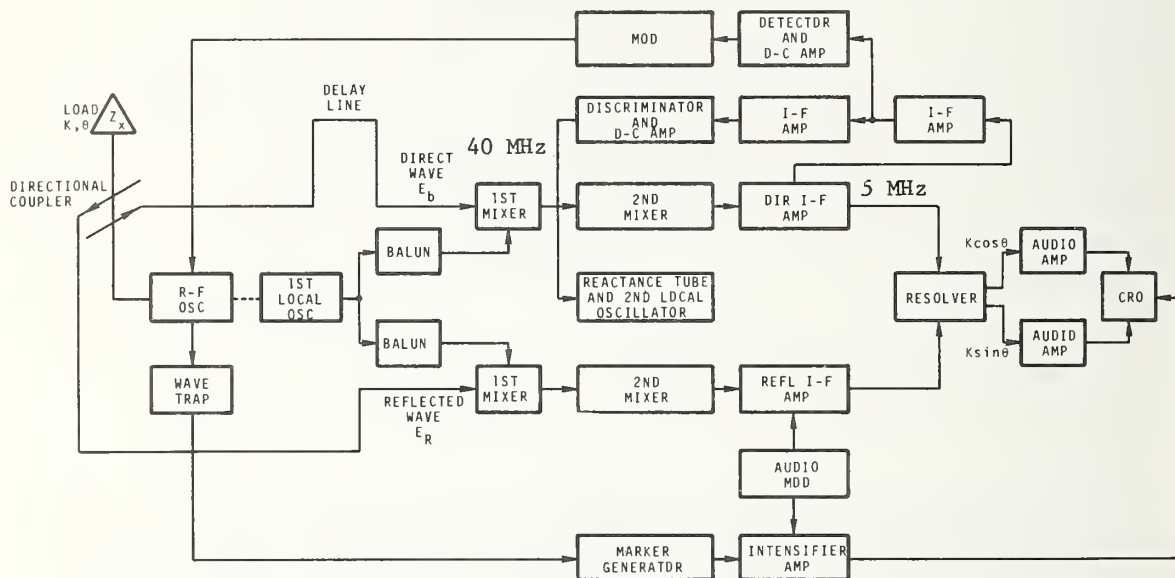


Figure 2-56. Automatic Smith Chart impedance plotter.

obtained from a directional coupler. The direct wave is maintained at a constant level by an AVC circuit so that the reflected wave magnitude is proportional to $|\Gamma|$. It is split into two channels and applied to two phase-sensitive detectors (probably the balanced modulator circuit) whose bias signals are obtained from the direct wave and are in quadrature. The detector outputs are proportional to the rectangular components of Γ .

Instead of operating the balanced modulator circuit at I-F, it was used directly at 8.2-12.4 GHz in a system developed in 1956 [35]. The source is swept at 20-50 Hz and a visual display of complex Γ is obtained on a medium persistence screen of a CRO. The block diagram shown in figure 2-57 contains a leveling arrangement and a delay line to equalize the phase shift in the two channels. Calibration (gain adjustment) is accomplished using either a short-circuit termination in place of the load or a standard mismatch having a calculable VSWR of 2.0 (or close to this figure).

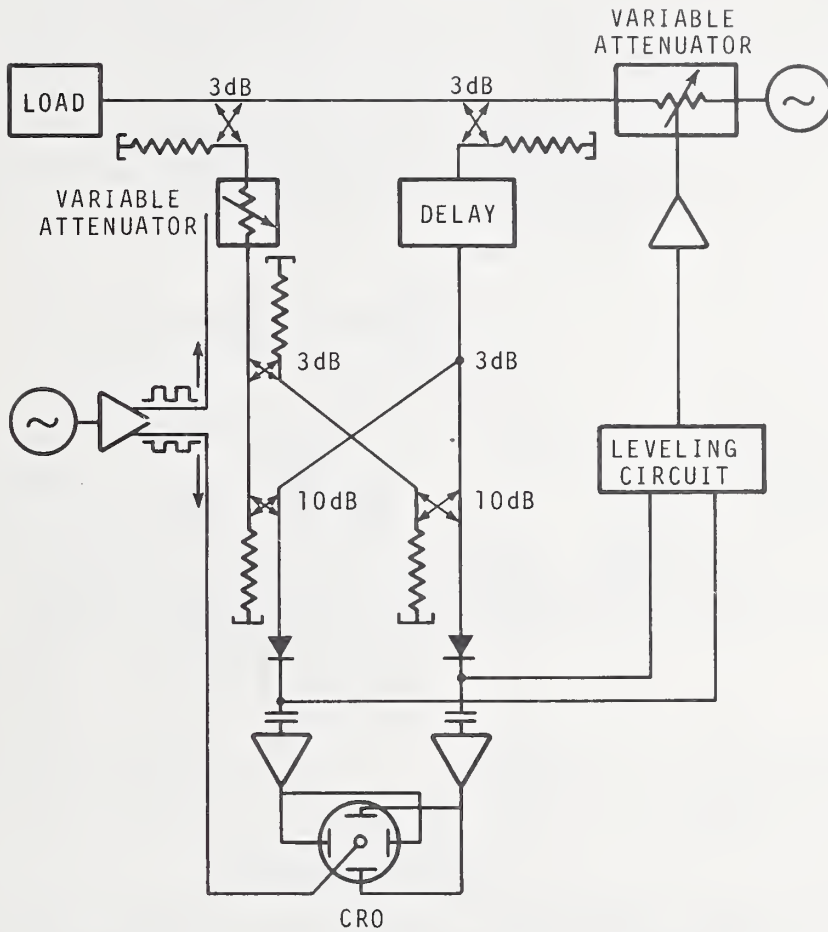


Figure 2-57. Complete block diagram. (Reprinted by permission: J. P. Vinding, "The Z-scope, An Automatic Impedance Plotter", IRE Con. Record, 4, part 5, 1956, pp. 178-183.)

(4) Hybrid Tees

One of the first swept frequency systems employing the balanced modulator circuit at microwave frequencies was described in 1955 [30] and used seven hybrid tees. The required 90° phase shift is accomplished in two 45° steps. A special waveguide section was built in such a way that the phase shift was insensitive to frequency variations over a 12 percent bandwidth (8.5–9.6 GHz). The simplified circuit of figure 2-58 shows five hybrid tees and two more are contained in the product detectors which use the same principle as the thermionic meter circuit patented in 1926 [1]. It was stated [34] that because of the complexity of this system it could not be expected to yield results as accurate as the slotted line.

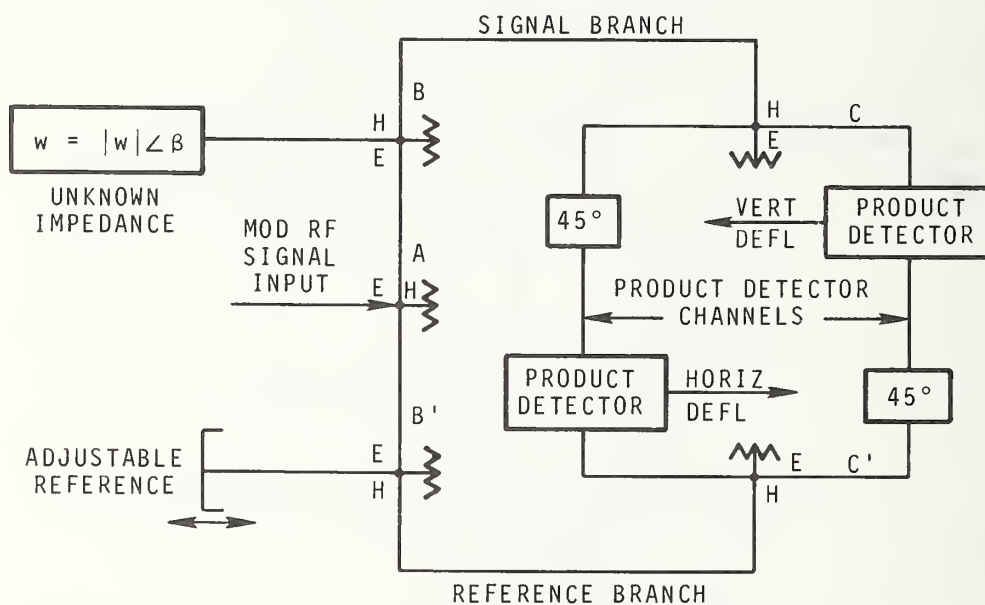


Figure 2-58. Waveguide impedance meter. (Reprinted by permission: H. L. Bachman, "A Waveguide Impedance Meter for the Automatic Display of Complex Reflection Coefficient", IRE Trans. on MTT, 3, no. 1, Jan. 1955, pp. 22-30.)

c. Long Line, Variable Frequency

(1) Swept Frequency

A simple swept frequency system developed in 1966 [72] made use of a long line to sweep the standing wave past a fixed probe. The audio frequency detected probe output was split and fed to two phase detectors which also received two detected signals (one shifted 90° in phase) from a probe in a reference delay line. As shown in figure 2-59, the d-c outputs of the phase detectors were fed to deflection circuits of a CRO to provide visual display of Γ or Z with a Smith Chart overlay. The circuit appears to be the familiar [5] balanced modulator type for obtaining a polar display. A display of Γ can also be obtained on an X-Y recorder.

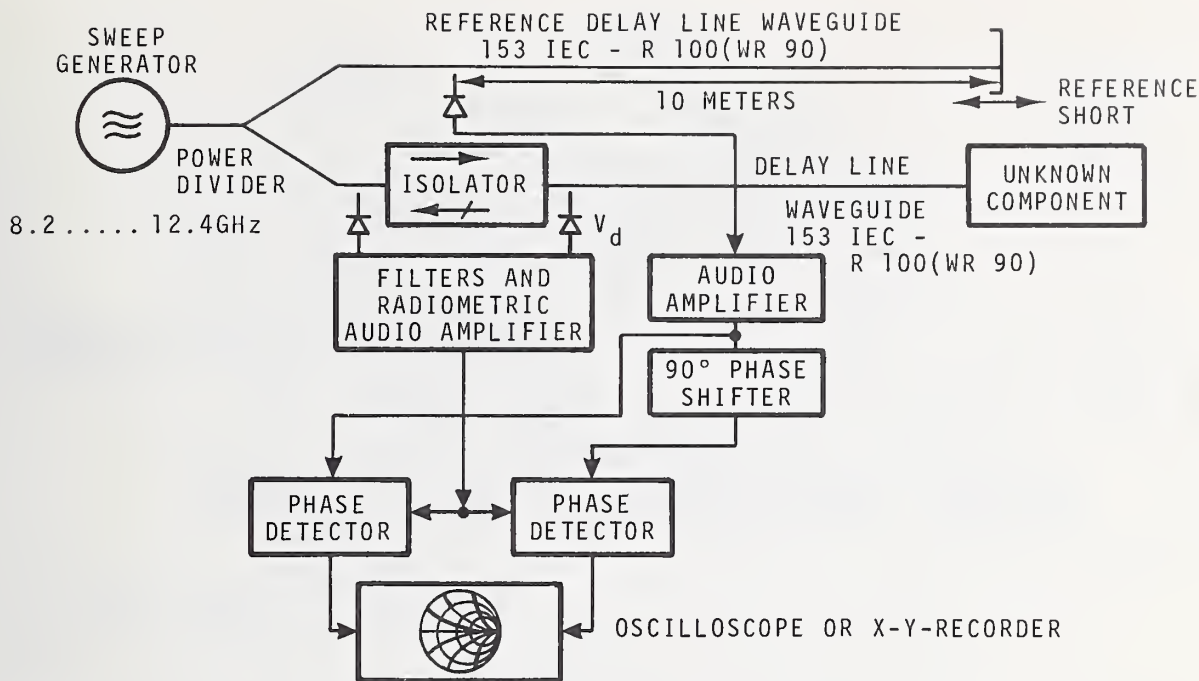


Figure 2-59. Block diagram of the Smith chart plotter. (Reprinted by permission: C. Mahle and G. Epprecht, "Reflection Measurements with Broadband Frequency Modulation Using Long Transmission Lines", IEEE Trans. on MTT, 14, no. 10, Oct. 1966, pp. 496-497.)

(2) Stepped Frequency

An interesting and original technique called the comparison reflectometer was developed in 1967 [77]. Although its main use was to measure the distribution of discontinuities producing small reflections along a moderate length (1 meter or so) of low-loss waveguide, it also had the capability to measure the magnitudes and phases of the reflection coefficients. A number of ideas were incorporated into the system for automatically stepping the frequency and for obtaining the data on punched paper tape for computer processing.

As shown in figure 2-60, a conventional reflectometer is used to measure the magnitude $|\Gamma|$ of the voltage reflection coefficient of the 2-port reference terminated in the component under test. The component under test is connected to the reference reflection by a length of precision waveguide (usually not less than 10 cm for IEC-R-100 or WR-90 waveguide). The 2-port reference consisted of a step in the waveguide height for which the voltage reflection coefficient Γ_r is calculable and relatively insensitive to frequency changes. As the frequency varies, the phases of the various reflections from the component under test, referred to the plane of the reference reflection, vary a full cycle or more, depending upon their distances from the 2-port reference. The resulting data (essentially $|\Gamma|^2$ versus the wave number $v = 1/\lambda_G$) is a complicated wave having various frequency components. The contributions at different frequencies (depending upon the distance from the 2-port reference) are determined by Fourier Analysis of the waveform.

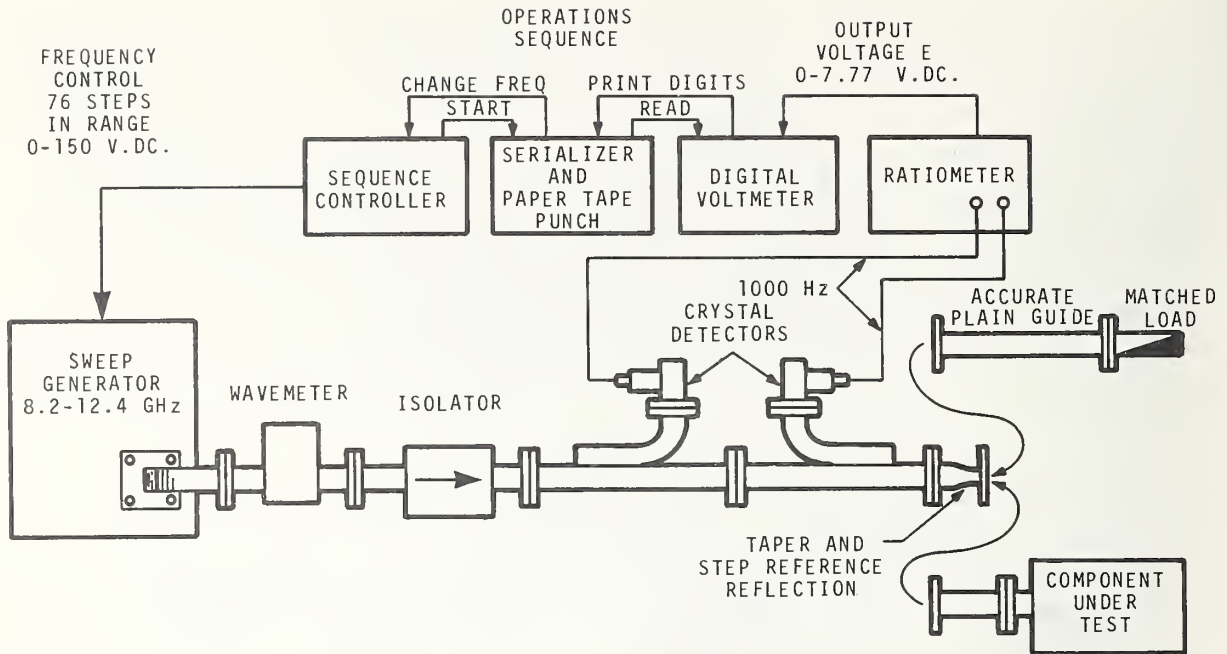


Figure 2-60. A block diagram of the comparison reflectometer used for locating and measuring reflections in X-band waveguide. (Reprinted by permission: D. L. Hollway, "The Comparison Reflectometer", IEEE Trans. on MTT 15, no. 4, April 1967, pp. 250-259.)

There are two methods used to remove background fluctuations from the output trace of the reflectometer. (Such fluctuations could result from imperfections in the components, for example, from the finite directivities of the directional couplers.)

1) Since the chief fluctuations usually appear within 20 cm of the reference, in R-100 waveguide, a 20 cm waveguide is inserted between the reference reflection and the component.

2) A substitution technique is used in which data is collected during two separate runs—one without, and the other with, the 2-port component under test connected to the instrument. The instrumental reflections are present in both runs and can be removed during computation.

It is assumed that the reflections are small, do not significantly interact, and are independent of frequency. The effect of violations of these assumptions on the accuracy of measurement has not been thoroughly investigated. One can see that a reflection that varies slowly with frequency can be measured more accurately with this technique than one which is strongly frequency dependent. However, it would be difficult to estimate the relative accuracies. As shown in figure 2-61, results of measurements of Γ_T of a test item located 30 cm from Γ_r compared fairly well at various frequencies with slotted line measurements. If it is desirable to measure components in relatively narrow frequency bands, a sufficiently long plain guide must be used to obtain at least one complete cycle in the band chosen. (Usually more cycles are needed in order to get away from additional "noise" in the low frequency end of the spectrum.)

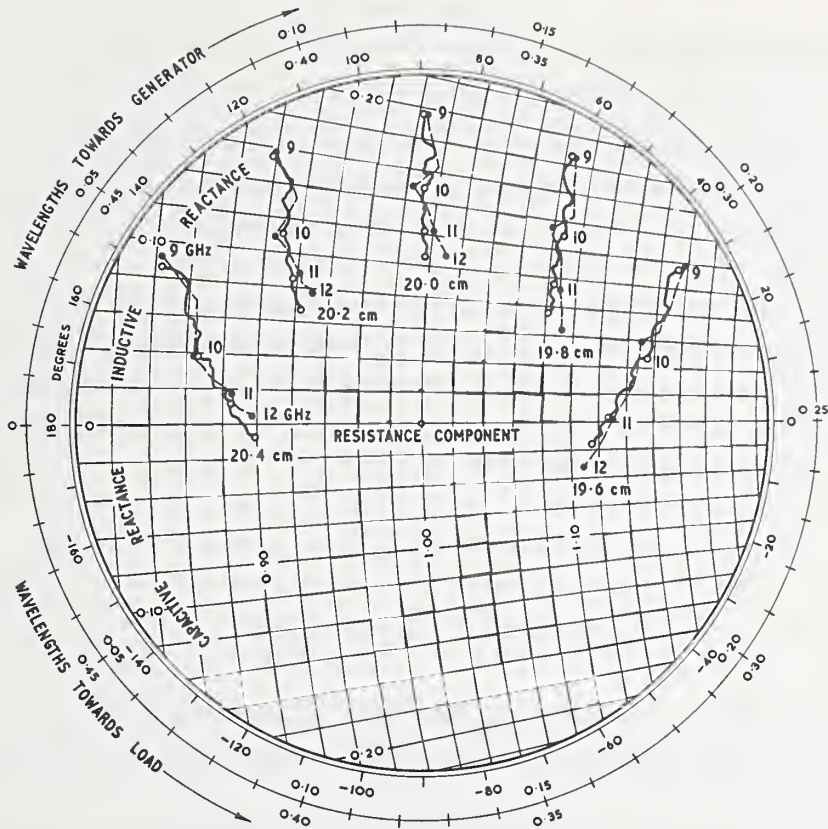


Figure 2-61. The reflection coefficient of an inductive iris shown as a function of frequency at different distances. The full lines, plotted by the comparison reflectometer, agree closely with the standing-wave impedance measurements, shown dotted. (Reprinted by permission: D. L. Hollway, "The Comparison Reflectometer", IEEE Trans. on MTT, 15, no. 4, April 1967, pp. 250-259.)

As the computation includes a correction for the waveguide loss and as the calibration can easily be checked, the loss in accuracy is not great. One can see that the smaller the frequency interval required (the greater the distance), the less Γ_T will vary, and the more the assumptions will be satisfied. However, the accuracy of measurement of Γ_T decreases as the distance between the discontinuity and the reference reflection diminishes.

Within the above stated limitations, the method gives finer resolution than narrow band Time Domain Reflectometry and for small reflections, the errors do not appear to be serious. If the reflection coefficients do not vary too rapidly, with frequency, it is possible to obtain both magnitudes and phases of reflection coefficients versus frequency to acceptable accuracy.

A coaxial version of the comparison reflectometer has not yet been described. Although it would be somewhat more difficult to construct than in rectangular waveguide, it would still be quite practical.

d. Rotating Slot Coupler

This method is described in 2.3.b.(1).

e. Z at 1592 Hz

As has been seen, automatic techniques developed for measurements at low frequencies are often applicable at high frequencies. Thus, the techniques developed for automatic impedance measurement at 1592 Hz for the VAST (Versatile Avionic Shop Test) system are of wider interest [76].

The voltage across the device under test and the current through it are sampled at their peak values and the voltage is sampled at the time when the current passes through zero. These times T1, T2, and T3, are determined by using a system "clock" crystal oscillator and counting the correct number of clock pulses starting from a zero crossing of the wave. One can determine the impedance from the relationships

$$|Z| = \frac{E(T2)}{I(T1)}, \quad (18)$$

$$\text{and } \omega L \text{ or } \omega c = \frac{E(T3)}{I(T1)}, \frac{-I(T1)}{E(T3)}. \quad (19)$$

The angle by which the voltage leads the current (the phase angle of Z) is determined by counting the time period between zero crossings of the voltage and current wave forms and converting to degrees.

Since the times T1, T2, and T3 are generally different, the sampled voltage and current must be held until they can be digitized and their ratio determined. This is done in the conventional way by charging a capacitor during the sampling time. A digital/Analog converter is employed which uses ladder circuits with resistors weighted in BCD 8421 code. The output goes to a comparator having digital readout.

Errors in resistance, inductance, and capacitance are less than 3% over a wide range of values, and are due to digitizer error and transient noise effects.

2.8. Phase Shift

In the 1960's and before, interest in microwave automatic phase measurements was stimulated by the development of chirp radar systems, phased array antennas, linear electron accelerators, etc. [50]. Of particular interest were departures from a linear phase-frequency characteristic which could cause delay distortion. (See also section 2.10.) A bibliography of phase measurement techniques was published in 1967 [78].

a. Single Sideband, Suppressed Carrier, Quadrature Method

In 1957, the need to measure phase in microwave antenna systems led to the development of an automatic phase-measuring circuit [37]. A rather complicated microwave circuit was used to generate a single sideband plus carrier reference signal. The equal amplitude and 90° phase adjustments were accomplished manually at each operating frequency. The received signal whose phase was to be measured was added and subtracted to the reference before detection by two detectors. The detected audio signal contained the phase information and this was read out by an audio frequency phase meter. Although this method was not adapted to swept frequency operation, it did give continuous readout of phase difference between two signals and could be used with a recorder for monitoring purposes. The limits of accuracy were stated to be $\pm 3^\circ$ in the range 10 to 180° .

b. Modulated Sub-carrier System

In an automatic swept-frequency system, it is desired that the phase difference between two signals be measured by a method which is insensitive to the relative magnitudes of the two signals. This was accomplished in the modulated sub-carrier technique in 1960 [48], using the following principles.

As shown in figure 2-62, certain phase relationships are indicated by a null in the detected modulation voltage at the fundamental modulation frequency. This null is independent of the relative magnitudes of carrier and sub-carrier signals. An arrangement of equipment for measuring phase shift is shown in figure 2-63.

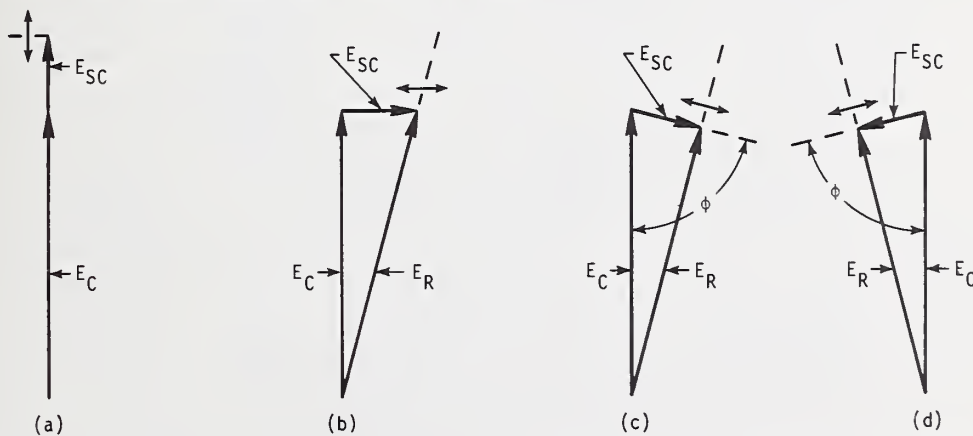


Figure 2-62. Resultant signal at detector for certain phase relationships between carrier E_C and amplitude modulated subcarrier E_{SC} ; a) E_C and E_{SC} in phase b) E_C and E_{SC} in quadrature, c) and d) E_{SC} and E_R in quadrature, the conditions for no amplitude modulation of the resultant at the fundamental modulation frequency.

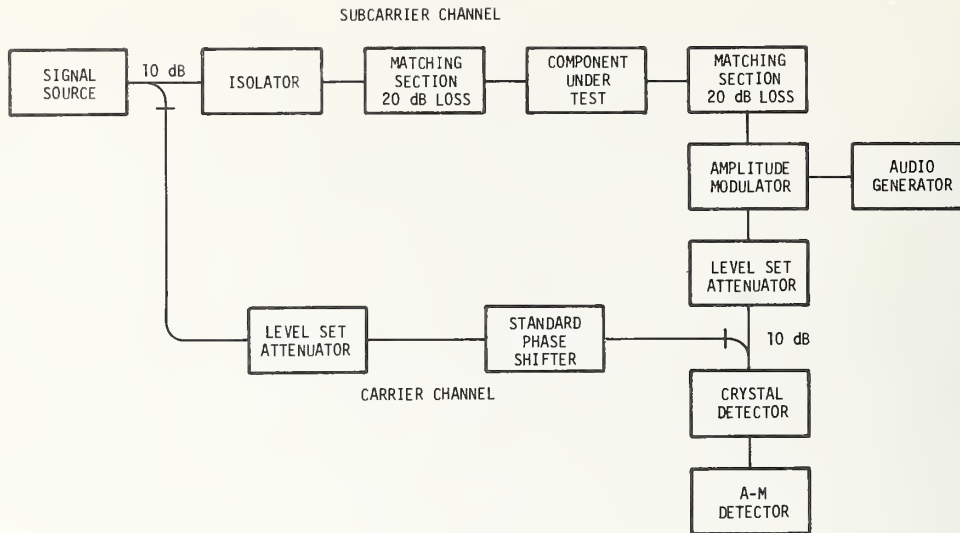


Figure 2-63. Arrangement of equipment for microwave phase shift measurements. (Reprinted by permission: G. E. Schafer, "A Modulated Subcarrier Technique of Measuring Microwave Phase Shift", IRE Trans. on Instr. 9, no. 2, Sept. 1960, pp. 217-219.)

In 1965, an automatic swept-frequency system using the above principles was described [67]. Errors were discussed and performance data was given at a frequency of 9001 MHz. A null-seeking servo system was used to automatically set the reference microwave phase shifter. Linear position potentiometers were used to indicate the dial settings of the reference phase shifter and the device under test, and the outputs were fed to an X-Y recorder. As the device under test (such as a rotary vane attenuator) was varied, a plot was automatically obtained of its phase shift. The error limits were claimed to be $\pm 0.1^\circ$. The system was not intended for swept-frequency operation, but for continuous monitoring of phase changes at one frequency.

c. Balance-modulated Sub-carrier, Quadrature and Ratio Technique

In 1961, a method for sweep-frequency presentation of phase shifts of 2-port components was described [50]. The phase indication was independent of the relative magnitudes of the signals in the reference and measurement channels. As shown in figures 2-64 and 2-65, a balanced modulator was used to amplitude modulate the sub-carrier in such a way that only the sidebands appeared. The modulated signal was split and the split portions arrived at the detectors in quadrature due to the inherent 90° phase difference between a 3 dB directional coupler output and an E-H Tee, while the carrier signals arrived in phase. As shown in figure 2-65, the signals at the detector were in general both phase and amplitude modulated, but the detectors responded only to the amplitude modulation component. Thus one detector output was proportional to $\sin \theta$, and the other to $\cos \theta$, where θ was the phase difference between the carrier in the reference channel and the subcarrier in the measurement channel. Upon applying the detector outputs to a ratio meter, an indication proportional to $\tan \theta$ was obtained. This indication is independent of the relative magnitudes of the signals from the two channels at the detectors.

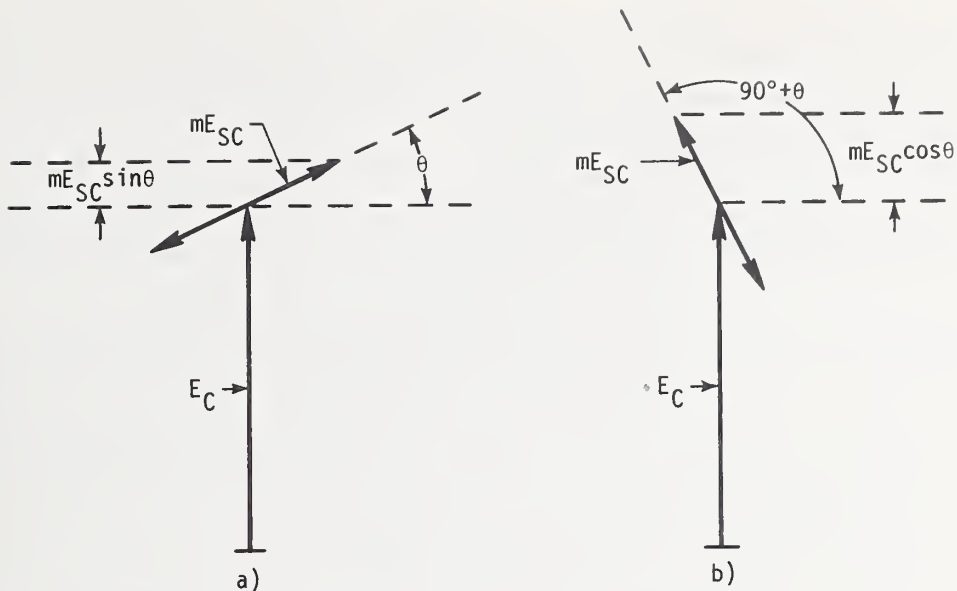


Figure 2-64. Combination of carrier E_C and modulated subcarrier mE_{SC} at detectors a) at detector no. 1, resultant amplitude modulation component at fundamental modulating frequency is $mE_{SC} \sin \theta$, and b) at detector no. 2, resultant amplitude modulation component at fundamental modulating frequency is $mE_{SC} \cos \theta$.

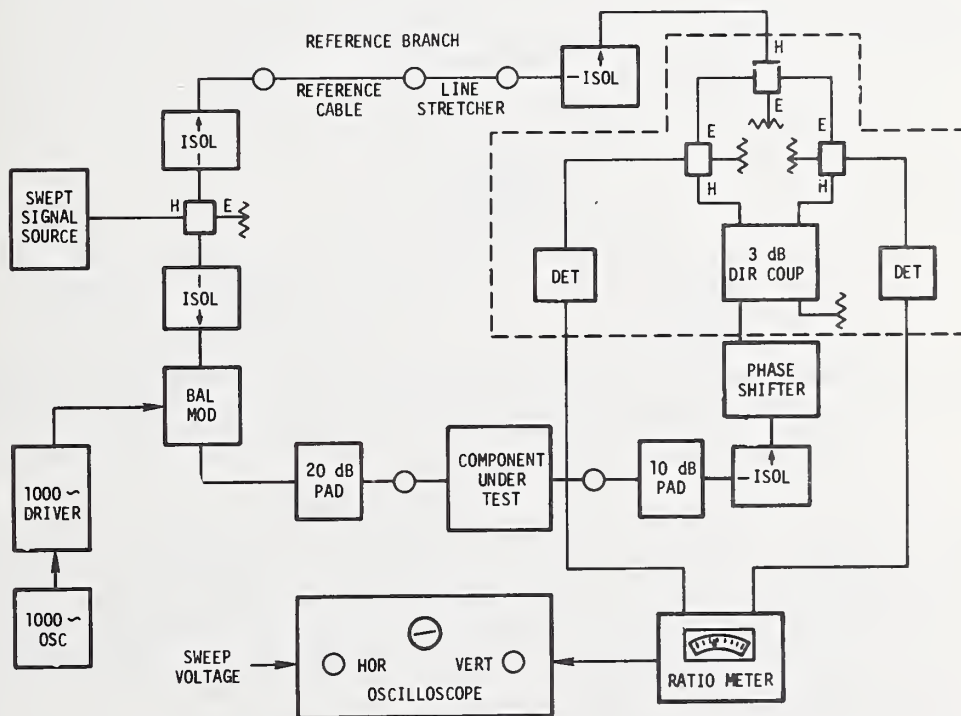


Figure 2-65. Block diagram of phase measurement system. (Reprinted by permission: S. B. Cohn and H. G. Oltman, "A Precision Microwave Phase-measurement System with Sweep Presentation", IRE Intern'l. Con. Record, part 3, March 1961, pp. 147-150.)

In order to keep the measured phase difference θ small over the frequency band of interest, a section of transmission line having a known, linear phase versus frequency characteristic was chosen to have nearly the same total phase variation as the item under test, and inserted in the reference channel.

In 1964, the above principles were used to construct commercially available automatic microwave phase measurement systems operating at 1.2 - 1.4 GHz, 3.0 - 3.6 GHz, and 8.5 - 9.6 GHz. A discussion of errors was given and performance data were shown [64].

d. Two-probe Phase Detector on Slotted Line

An automated system for measuring microwave gain and phase versus frequency was described in 1963 [61]. It was based upon the spaced pair of probes phase detector introduced in 1961 [51]. The reference and unknown signals are fed into the opposite ends of a slotted line having two spaced probes. The difference in the probe outputs is proportional to the sine of the phase difference of the two signals at the center position of the two probes. For swept frequency operation where the signal level may be varying substantially, a phase null tracking system is employed as shown in figure 2-66. A servo system automatically moves the pair of probes to the position for null output, and this is independent of the relative signal levels. The phase shift versus frequency can be read out on an X-Y recorder.

As in the previous method (2.8.c.), a phase shift unit having known phase-frequency characteristics is used in the reference channel so that it is only necessary to measure small differences in phase shift between the reference unit and the unit under test.

The measurement system can operate over 10:1 frequency ranges.

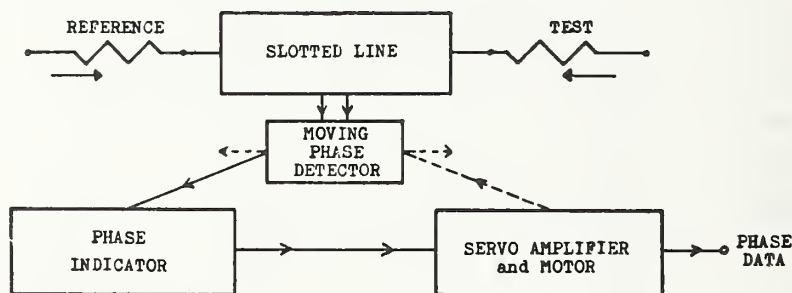


Figure 2-66. Null tracking with movable phase detector. (Reprinted by permission: P. Lacy, "Automated Measurement of the Phase and Transmission Characteristics of Microwave Amplifiers", IEEE Intern'l. Con. Rec., part 3, March 1963, pp. 119-125).

e. Pulsed Signal Technique

A phase measurement technique for pulsed RF signals was developed to obtain stability data on pulsed magnetrons, klystrons, traveling wave tube amplifiers, etc. [62]. It employed the familiar balanced modulator circuit [1,3,5] with a 90° phase shift in the signal applied to one of the modulators. A VHF clock oscillator was used to time a blanking signal to the oscilloscope for a timing reference.

No analysis of errors was made, but the accuracy under CW operation was checked using a stable CW oscillator. Under pulsed operation, the system was capable of distinguishing between stable pulsed magnetron sources and unstable ones, but no quantitative conclusions about the accuracy were possible.

2.9. Complex S_{21}

a. Fourier Techniques

The use of pulses or square waves in quickly determining the properties of linear 2-ports was discussed [6,7] in 1939 and 1942. It was stated in 1942:

"It is often desired to determine the characteristics of a circuit, for example an amplifier, over its entire working frequency range. As often done point by point, this is a rather tedious procedure,¹ and if various circuit modifications are being tried, considerable time is consumed in determining the overall effect of each modification."

"It has been seen that pulses contain all frequencies, and rectangular periodic waves contain many multiple frequencies and hence offer the possibility, when applied to a circuit to be tested, of indicating at once practically the entire frequency characteristic--at least to the extent to which the user is capable of interpreting the results."

Both magnitudes and phases of the complex amplitudes of the components of an input pulse or square wave can be obtained by Fourier Analysis of the waveform. A similar analysis of the output waveform will enable one to determine the transfer characteristics of each component frequency of a linear network.

(1) Square Wave Testing

An excellent discussion of square wave testing was given in 1939 [6]. The work was no doubt stimulated by the development of television receivers at RCA, where the technique was very useful in adjusting compensating circuits in video amplifiers under operating conditions. The further value of this technique in determining both magnitudes and phases of transmission coefficients of 2-ports was well-understood and explained, but not widely exploited. The required analysis of data was at that time rather time-consuming, but today could be handled more quickly with modern computers. It was stated [6] that:

"In general, the frequency characteristic of any circuit, for frequencies at and above the frequency of the square wave, can be obtained by dividing each term in the harmonic series which represents the output wave by the corresponding term of the series which represents the input wave. When the input can safely be assumed to be square this process takes the form of multiplying each term at the output series by n . The wave analysis may be performed by calculation, if an expression for the observed wave form can be obtained, or by graphical methods if an accurate graph of the wave can be plotted. Information on several methods of wave analysis will be found in standard engineering and mathematic texts. Calculation of the phase characteristic is similarly determined from the phase angles obtained from the wave analysis, correcting, if necessary, for any phase differences between various components of the input wave."

¹Although point-by-point measurements may have been slow and tedious in 1942, they can now be fast and accurate using computer controlled automatic measuring systems.

The choice of the input waveform is important in facilitating the analysis. A symmetrical square wave contains only odd harmonics as shown by the following equation

$$e = \frac{4E}{\pi} \sum_{n=1}^{n=\infty} \frac{1}{n} \sin n (\omega t + \phi). \quad (20)$$

The use of non-symmetrical square waves enables one to introduce more frequency components as stated [6] below:

"Waves whose time intervals are unequal contain even as well as odd harmonics. The output wave shapes obtained with input waves of the type shown in figures 18, 19 and 20 (of ref. [6]) will in most cases be similar to the wave shapes obtained by means of symmetrical waves. The shape of the output wave over the long interval T, being similar to that obtained by means of a symmetrical wave whose period is 2 T, while the shape over the short interval T₂ will be similar to that obtained by the use of a symmetrical wave whose period is 2 T₂. Thus, changing the positive and negative time intervals may be considered equivalent to using square waves of different frequencies at the same time."

"The general expression for a rectangular wave is:

$$E = \sum_{n=1}^{n=\infty} E_n \cos (n\omega t + \phi_n)$$

$$E_n = \frac{4D}{n\pi} \sin \frac{n\pi}{b}, \text{ where } \phi_n = 0 \quad (21)$$

and b is the ratio of the full period to the shorter duration. It can be seen that the amplitude of any harmonic whose number is an integral multiple of b will be zero, and that the successive groups of harmonics, lying between those whose amplitude is zero, are of opposite polarity (reversed in phase)."

"The wave shown in figure 2-67 is square, having b = 2. In this special case, the phase of all the components can be made to coincide by choosing the origin at the beginning of the rise rather than at the center of the positive portion of the wave and by plotting sine components rather than cosines. In general, it will be found that most wave analyses can be considerably simplified by proper choice of origin."

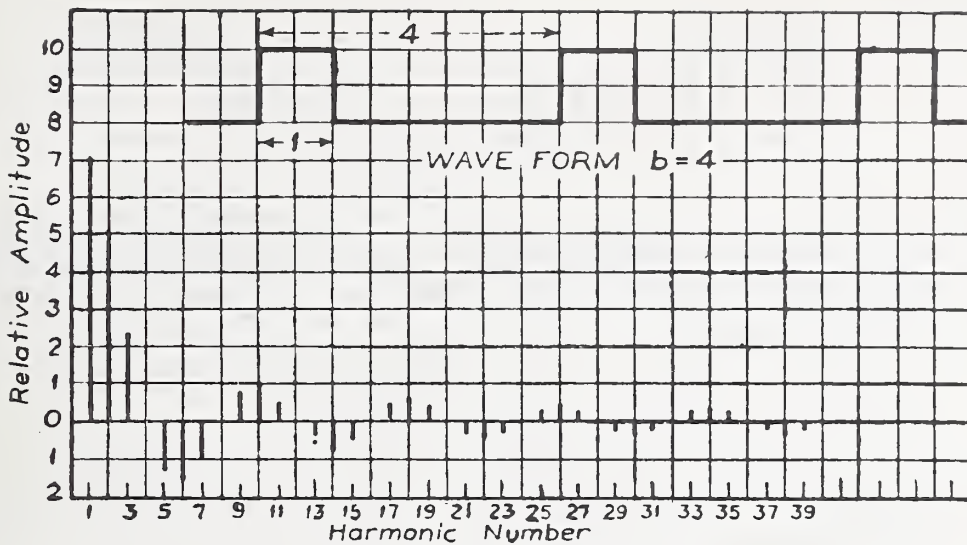


Figure 2-67. Symmetrical square wave.

"Output waves which are symmetrical with respect to time but whose positive and negative half cycles are unsymmetrical indicate the presence of non-linear distortion in the circuit. This effect is not usually noticeable unless oscillations are present in the wave shape. Where the amplitude of the wave trains at top and bottom are unequal, some non-linear distortion is indicated. Oscillations on only one side of the wave is usually indicative of saturation or cut-off in the equipment under test."

Although square wave testing was apparently only applied to the determination of transmission coefficients, it could in principle also be applied to the determination of reflection coefficients.

(2) Pulse Testing

The use of a non-periodic pulse is an extension of square-wave testing in which the pulse is represented by a Fourier Integral

$$e = \int_{-\infty}^{\infty} F(\omega) e^{j\omega t} d\omega. \quad (22)$$

This is the sum of an infinite number of components, each of amplitude $F(\omega)d\omega$ spaced infinitely close together. All frequencies are present in the pulse. With such an input, the output current of a network is

$$i = \int_{-\infty}^{\infty} F(\omega) \underline{Y}(\omega) e^{j\omega t} d\omega. \quad (23)$$

Thus, one can determine the transfer admittance function if the response is determined corresponding to a known input pulse [7].

b. Other Applications

Techniques of Fourier Analysis have been used in the comparison reflectometer (see 2.7.c [77]) and in time domain automatic network analysis [86, 105, 142, 147, 148, 150]. It should also be noted that these techniques are employed in obtaining time domain information from frequency domain data, and vice-versa.

(1) I-F Substitution

Some automatic features were provided in a test set developed in 1949 at BTL to measure complex transmission factors of networks [15]. The system operated over a frequency range of 50-3600 kHz, and had an intermediate frequency of 31 kHz. Automatic frequency control featuring combined phase and frequency sensitive control were applied to the master oscillator. The local oscillator was slave to the master oscillator and maintained the 31 kHz difference frequency.

As shown in figure 2-68, the phase and transmission standards operated only at (31 kHz = 31 kc). Line lengths in the channels were balanced so that a frequency insensitive null could be obtained when the unknown was replaced by a "coaxial strap" (a straight-through connection). The master oscillator could then be swept through its entire range for rapid appraisal of network performance by observation of the phase and transmission difference indicators.

At single-frequency operation, the switching and null adjusting were done manually. However, this circuit was the precursor of later BTL test sets that were more fully automated.

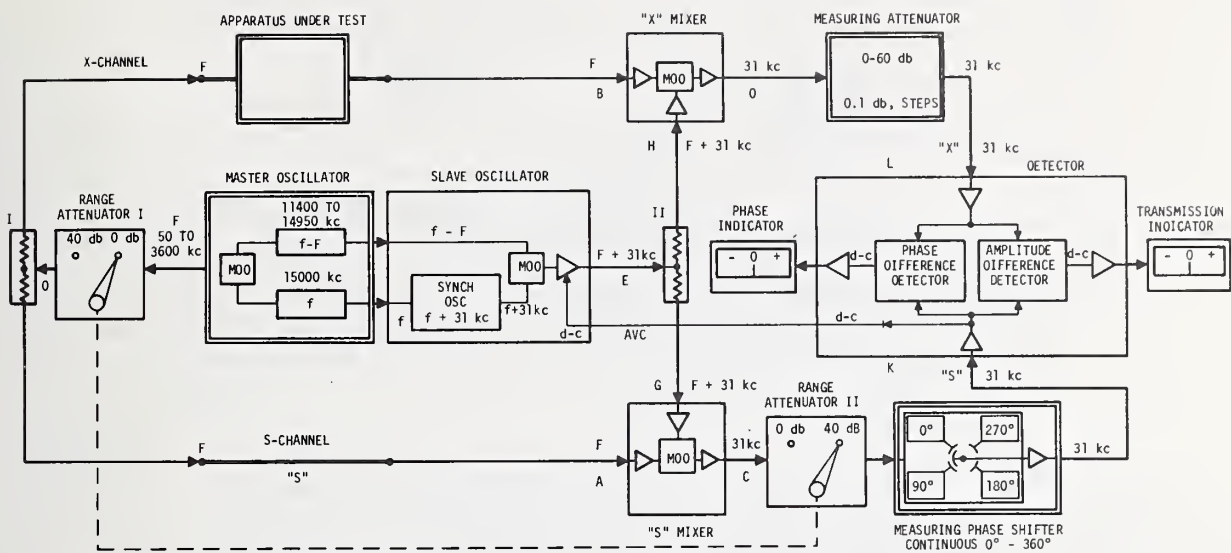


Figure 2-68. Block schematic of the phase and transmission measurement system. (Reprinted by permission: D. A. Alsberg and D. Leed, "A Precise Direct Reading Phase and Transmission Measuring System for Video Frequencies", Bell System Technical Journal, 28, no. 1, April issue, pp. 221-238. Copyright 1949, American Telephone and Telegraph Company.)

(2) Balanced Modulator Circuits

One of the earliest automatic systems for measuring the complex transmission coefficient of networks was developed at BTL in 1933 [5]. The motivation for the development was to reduce the time and tedium required to measure the complex transfer factor of amplifiers over a wide range of frequencies in order to verify and apply Nyquist's criterion for stability. For this reason, an automatic method of visual presentation was developed. Although it operated mainly at audio frequencies, it introduced basic circuits which have been used again many times at higher frequencies and is in use today in computer-controlled automatic network analyzers.

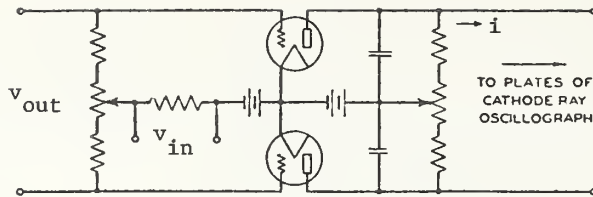


Figure 2-69. Circuit of a vacuum tube wattmeter used to provide a rectified potential proportional to the product of the two impressed grid potentials (both of the same frequency) multiplied by the cosine of the phase angle between them. (Reprinted by permission: E. Peterson, J. G. Kreer and L. A. Ware, "Regeneration Theory and Experiment", Bell System Technical Journal, 13, October issue, pp. 680-700. Copyright 1934, American Telephone and Telegraph Company.)

Because of their importance, the basic circuits [1,3,5] will be described. As shown in figure 2-69, a balanced modulator type of circuit is used in which the modulating and carrier frequencies are the same. It was called a wattmeter [3,5] because it could be used to measure power. The rectified output was proportional to $v_{in} v_{out} \cos \theta$, where θ is the phase angle between the two voltages. The circuit is used in automatic measuring systems to provide dc voltages which can be used to display on an oscilloscope the magnitude and phase of a sinusoidal voltage. (In some modern automatic network analyzers, these d-c voltages are digitized by an interface unit and fed to a computer for storage, analysis, and error correction.)

In operation, a reference voltage v_{in} is the input to the circuit under test and is also applied in phase to both grids of the modulator tubes, as shown in figure 2-69. The output voltage v_o of the circuit under test is applied in push-pull to the grids. The rectified output current (i_1) in the plate circuit is then

$$i_1 = k |v_{in} v_o| \cos \theta, \quad (24)$$

where k is a constant of proportionality, and θ is the phase difference between v_{in} and v_o .

Another balanced modulator circuit is employed as shown in figure 2-70 and operates in a similar way except that the input voltage v_{in} is shifted in phase minus 90° before being applied in phase to both grids of the modulator tubes. The rectified output current (i_2) in the plate circuit is

$$i_2 = k |v_{in} v_o| \sin \theta. \quad (25)$$

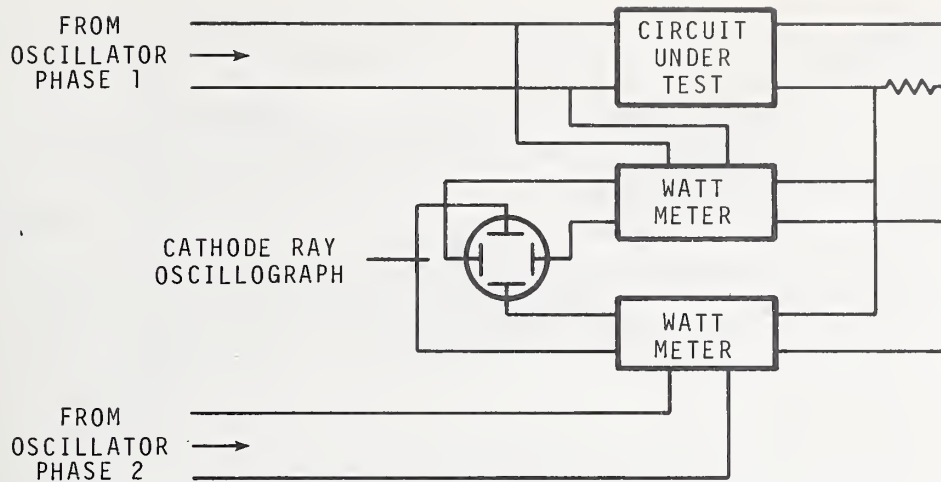


Figure 2-70. Schematic diagram of the circuit used to plot the transfer factor diagram on the screen of a cathode ray oscillograph. (Reprinted by permission: E. Peterson, J. G. Kreer and L. A. Ware, "Regeneration Theory and Experiment", Bell System Technical Journal, 13, October issue, pp. 680-700. Copyright 1934, American Telephone and Telegraph Company.)

These two currents can be used to produce a visual display on a cathode ray oscilloscope of the complex transfer factor T of the circuit under test.

We define²

$$T = \frac{v_o}{v_{in}} = \left| \frac{v_o}{v_{in}} \right| e^{j\theta}. \quad (26)$$

The real part of T is

$$\text{Re}(T) = \left| \frac{v_o}{v_{in}} \right| \cos \theta, \quad (27)$$

and the imaginary part is

$$\text{Im}(T) = \left| \frac{v_o}{v_{in}} \right| \sin \theta. \quad (28)$$

We note that

$$i_1 = k \left| v_{in} \right|^2 \cdot \text{Re}(T), \quad (29)$$

and

$$i_2 = k \left| v_{in} \right|^2 \cdot \text{Im}(T). \quad (30)$$

The display on the oscilloscope is then proportional to the transfer factor T and exhibits its picture in the complex plane.

²It can be shown that the transfer factor is related to the scattering coefficients of the circuit under test by $T = S_{21}/(1 + S_{11})$, if the load is non-reflecting.

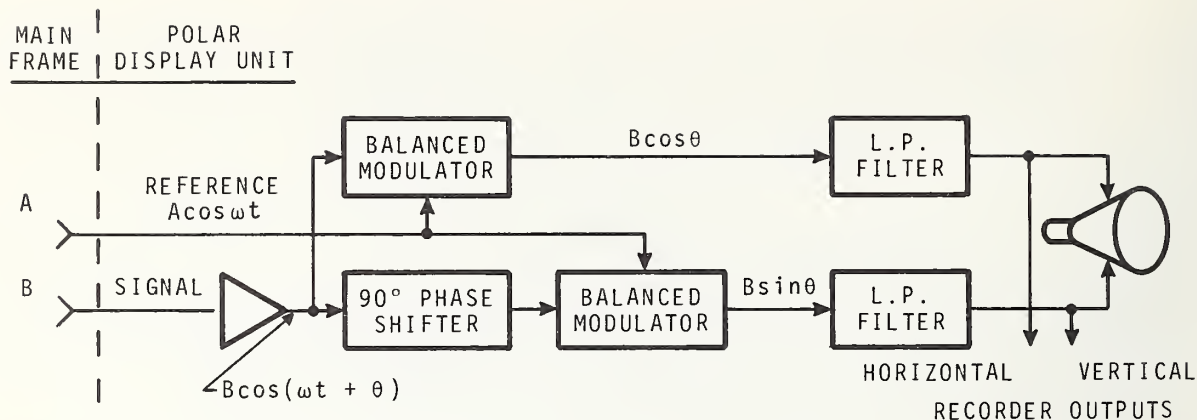


Figure 2-71. Block diagram of basic Polar Display Unit which converts polar magnitude and phase information to be presented to its self-contained CRT. (Reprinted by permission: R. W. Anderson and O. T. Dennison, "An Advanced New Network Analyzer for Sweep-measuring Amplitude and Phase from 0.1 to 12.4 GHz", Hewlett-Packard Journal, 18, no. 6, Feb. 1967.)

As shown in figure 2-71, the balanced modulator circuit was used in the Polar Display Unit of a 1967 Network Analyzer [74] and is used today in modern Automatic Network Analyzers.

One notes that correct operation of this circuit requires square-law detection and matched detectors. Deviations from these requirements produce "detector errors". It is also essential that an exact 90° phase shift is produced in v_{in} before applying it to one of the balanced modulator circuits. A deviation from this requirement produces what is called "quadrature error".

2.10. Envelope Delay

a. Carrier Phase Shift Versus Frequency

An automatic measuring system that is capable of measuring transmission phase shift ($\arg S_{21}$) versus frequency can also measure group delay τ_G . If one defines

$$\tau_G = - \frac{d\psi_{21}}{d\omega}, \quad \text{where } \psi_{21} = \arg S_{21}, \quad (31)$$

one can calculate τ_G from the slope of the ψ_{21} versus frequency curve. If ψ_{21} is measured in degrees at closely spaced discrete frequencies f_L , f , and f_H in GHz as shown in figure 2-72, then the calculated τ_G at frequency f is

$$\tau_G = \frac{[(\psi_{21})_L - (\psi_{21})_H]}{360 (f_H - f_L)} \text{ ns.} \quad (32)$$

Although this result is well-known, it may be unfamiliar to many metrologists who have not actually had to measure group delay.

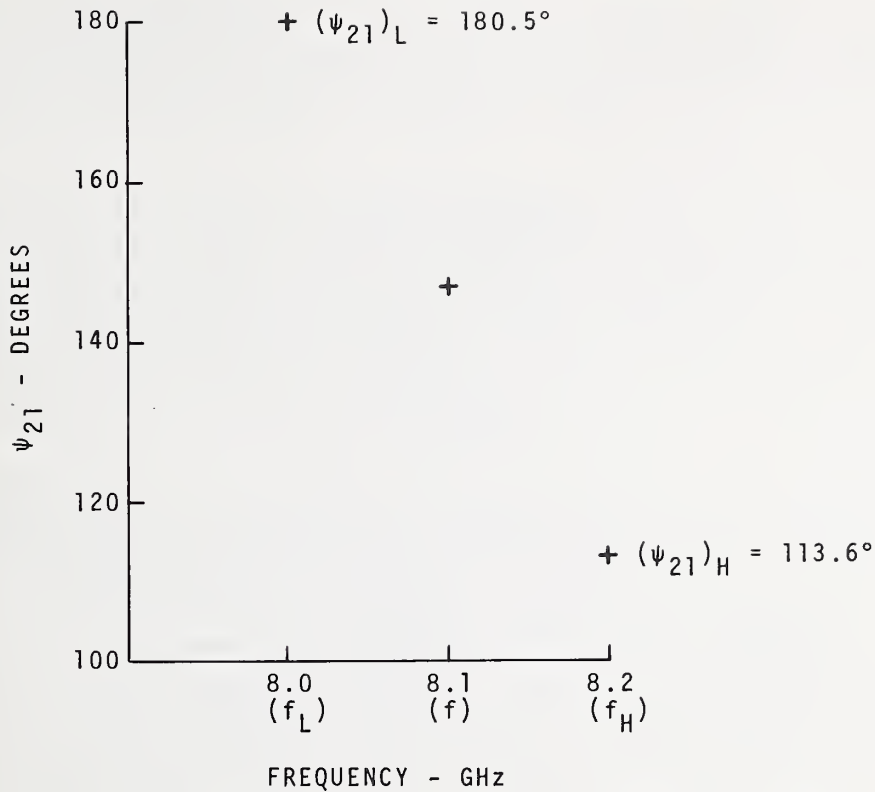


Figure 2-72. Measured ψ_{21} at three closely spaced frequencies.

For example, if

$$(\psi_{21})_L = 180.5^\circ,$$

$$(\psi_{21})_H = 113.6^\circ,$$

$$f_H = 8.2 \text{ GHz},$$

$$f = 8.1 \text{ GHz},$$

and $f_L = 8.0 \text{ GHz},$

$$\tau_G = 0.929 \text{ ns}.$$

In computer-controlled automatic measuring systems, this calculation is part of the computer program and the result is printed out automatically.

The assumption is made that the phase shift is linear with frequency over the range f_L to f_H .

b. Phase Shift of Envelope

The phase shift of a modulation envelope at 1.39 MHz was automatically measured in 1964 [65] in order to measure group delay. A self-balancing phase meter having a servo-controlled phase shifter was used with an X-Y plotter to obtain a recorded display of time delay versus frequency from 2 to 4 GHz. A reference run without the test item gives the residual time delay of the system.

A straightforward swept-frequency system to measure the phase shift of a sinusoidal modulating envelope was described in 1972 [114]. It used a levelled sweep oscillator operating around 4 GHz. The modulating frequency of 2.78 MHz resulted in 1° of phase shift for 1 ns of group delay. The modulated signal was sampled and detected before and after passage through the device under test. As shown in figure 2-73, the phases of the two detected envelopes were compared in a vector voltmeter and their phase difference displayed on an X-Y recorder.

With the device removed from the system, the phase zero of the vector voltmeter was moved in equal increments to put on calibration lines. The values of group delay at individual frequencies are then obtained by measurements on the plotted curve.

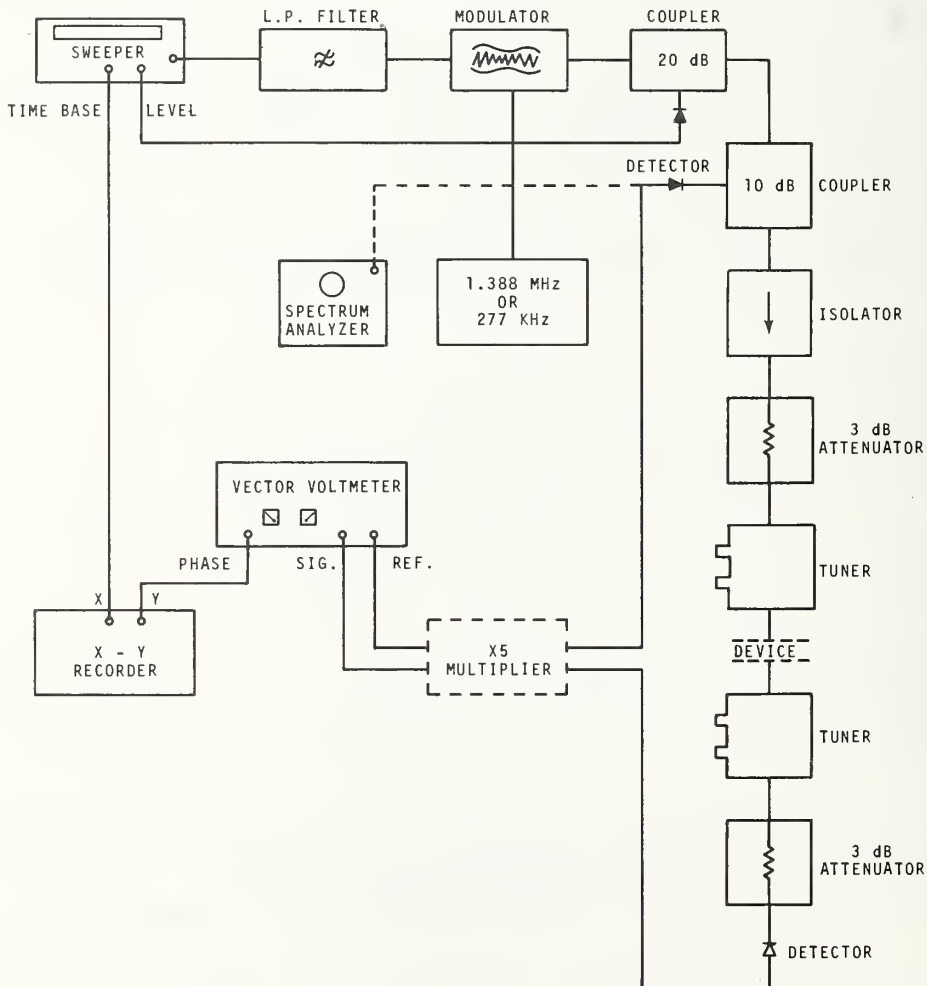


Figure 2-73. Group-delay test set.

In order to check the performance of the system, measurements were made on a tapped-resonator group-delay equalizer, which had calculable group-delay versus frequency characteristics. Agreement to within ± 0.2 ns was obtained between measured and calculated group delay.

c. Two-tone Method

It was shown in 1930 [2] that one could determine the envelope delay τ_o in seconds by measuring the phase M in degrees of a sinusoidal modulating signal having a frequency f_M . The envelope delay is approximated by

$$\tau_{\Delta} = \frac{M}{360 f_M}. \quad (33)$$

It was shown that the phase shift M is the average phase shift of the two sidebands produced by the modulating signal if the phase shift is linear with frequency over the range $f_c - f_M$ to $f_c + f_M$, where f_c is the carrier frequency.

Instead of modulating the carrier to produce sidebands, one can eliminate the carrier and generate the sidebands separately as a two-tone signal. This scheme was used in 1962 [59] to measure envelope delay in the 50 - 60 GHz range. The envelopes were recovered by detectors before and after passing the two-tone signal through the unknown path as shown in figure 2-74. A rapid switching technique and a two-channel circuit permitted one to use a delay standard and a nulling technique to achieve high accuracy and sensitivity.

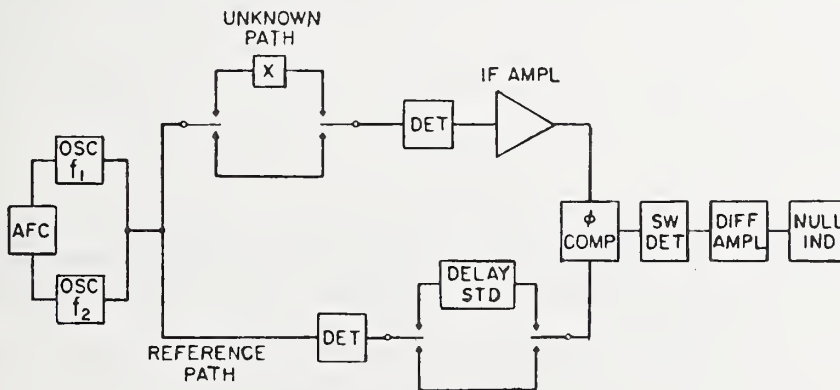


Figure 2-74. Circuit used in two-tone method to measure envelope delay. (Reprinted by permission: M. B. Chasek, "An Accurate Millimeter Wave Loss and Delay Measurement Set", IRE Trans. on MTT, 10, no. 11, Nov. 1962, pp. 521-527.)

Another version was described in 1966 [70] in which the lower sideband was filtered out prior to detection, leaving the carrier and upper sideband. (See section 2.11.d.)

d. Frequency Modulation Technique

An automatic switching method has been developed for measuring envelope delay in the 50 GHz region [97]. It is based upon the principle of measuring the phase shift of a sinusoidal modulating signal [2], but instead of amplitude modulation, frequency modulation (fm) is employed. The use of fm permits an increase in sensitivity of phase detection by multiplication of the envelope frequency. As shown in figure 2-75, the 200 kHz modulating frequency is multiplied by 49.

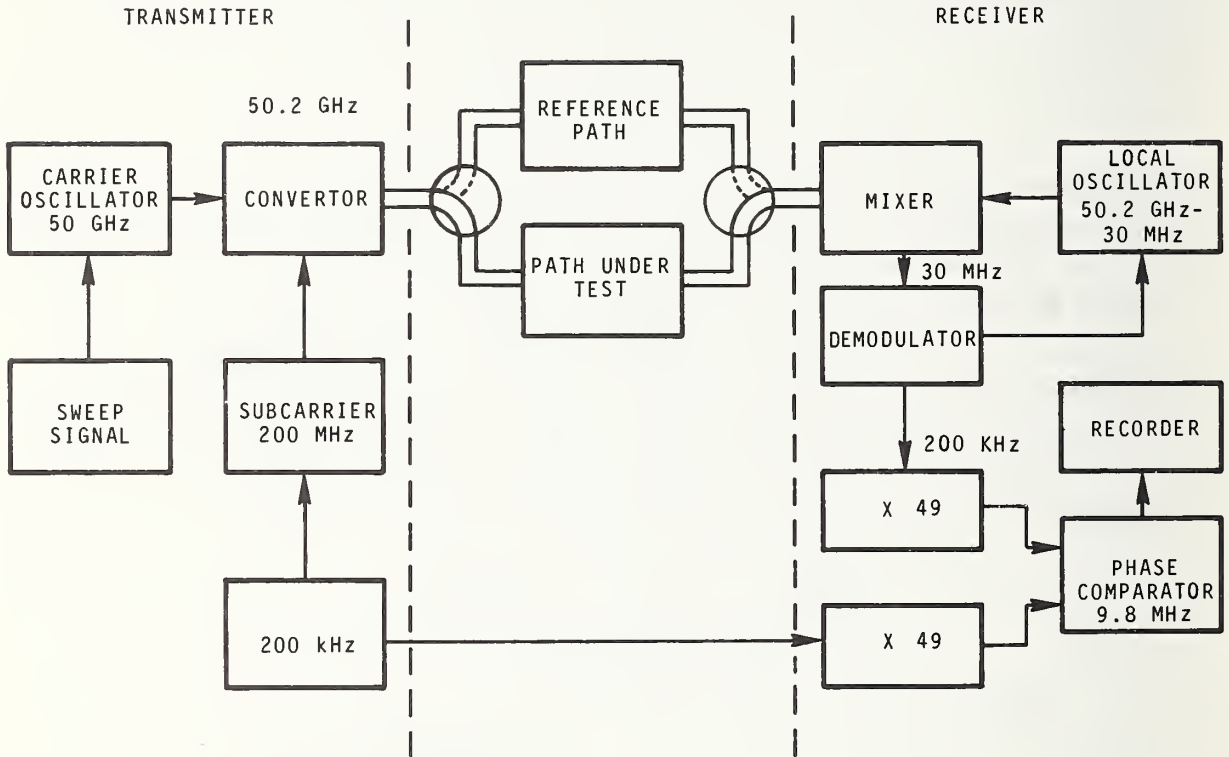


Figure 2-75. Simplified measuring-equipment block diagram. (Reprinted by permission: M. Shimba and M. Kikushima, "An Accurate Delay-time Measuring Equipment in the 50 GHz Region", IEEE Trans. on I&M, 19, no. 1, Feb. 1970, pp. 9-14.)

The phase comparator responds to the total phase shift between the modulating signal and the detected signal, but only the phase shift through the path under test is desired. Therefore, a reference path of known phase shift is provided and a rapid switching between the two paths permits one to measure only the difference in the delay times between the two paths.

e. Differentiating Phase Shift with Sawtooth Frequency Sweep

A sweep-frequency network analyzer described in 1972 [118] measured group delay by differentiating the phase shift with respect to time $d\phi/dt$, while the frequency was being linearly swept at a known constant rate $k = df/dt$. The group delay $-d\phi/d\omega$ was proportional to $\frac{1}{k}(d\phi/dt)$.

The phase detectors operated at the 80 KHz intermediate frequency, and measured the time between positive-going zero crossings in the reference channel and signal channel.

The phase noise of the signal source limits the range of group delay measurement. No data was given on range or accuracy. However, the frequency coverage consists of three sweepable ranges 0.4 to 5, 4 to 50, and 40 to 500 MHz.

2.11. Complex Reflection and/or Transmission Coefficients

a. Using Balanced Modulator

(1) Hybrid Circuit Operating at r.f.

In 1957, an automatic impedance plotter was described which introduced a coaxial hybrid circuit and a polar display unit [36]. The hybrid circuit operates like a Wheatstone bridge [120], or like a magic tee [10], in that the complex ratio of the output to input voltages is

$$\frac{E_o}{E_I} = \frac{\Gamma_L}{8}, \quad (34)$$

where Γ_L is the voltage reflection coefficient of the unit under test, and it is assumed that both signal source and detector are non-reflecting. The corresponding relationship for an ideal magic tee is

$$\frac{E_o}{E_I} = \frac{\Gamma_L}{2}. \quad (35)$$

Thus the hybrid circuit has 12.04 decibels loss as compared with a magic tee. However, it is more broad band in operation (50-250 MHz, and 180-900 MHz).

In order to obtain a display of complex Γ on a cathode ray oscilloscope, the familiar two channel circuit with a 90° phase shift and balanced modulators [5,18,30,35, etc.] is used.

Although the system was developed mainly as an automatic impedance plotter, it can also display complex transmission coefficients using the circuit shown in figure 2-76.

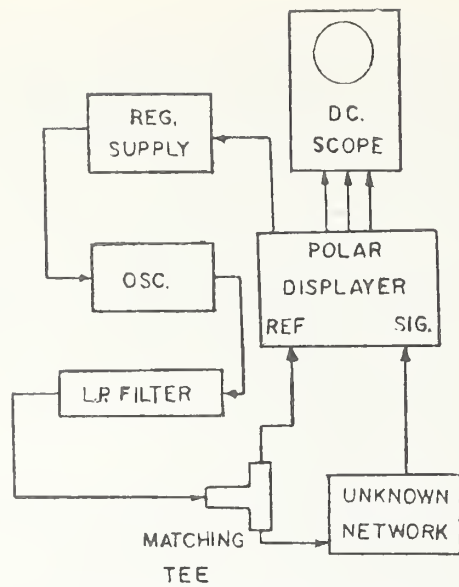


Figure 2-76. Arrangement for observing a Transfer Function. (Reprinted by permission: C. B. Watts, Jr. and A. Alford, "An Automatic Impedance Plotter Based on a Hybrid-like Network with a Very Wide Frequency Range", IRE Con. Record, 5, 1957, pp. 146-150.)

(2) I-F Input to Display Unit

The automatic swept-frequency impedance meter described in 1958 [38] also had the capability to measure transmission coefficients by changing two waveguide links. The diagram of figure 2-77 does not show details of the resolving amplifiers in the display unit, but they appear to be the familiar 2-channel balanced modulator circuit as shown in

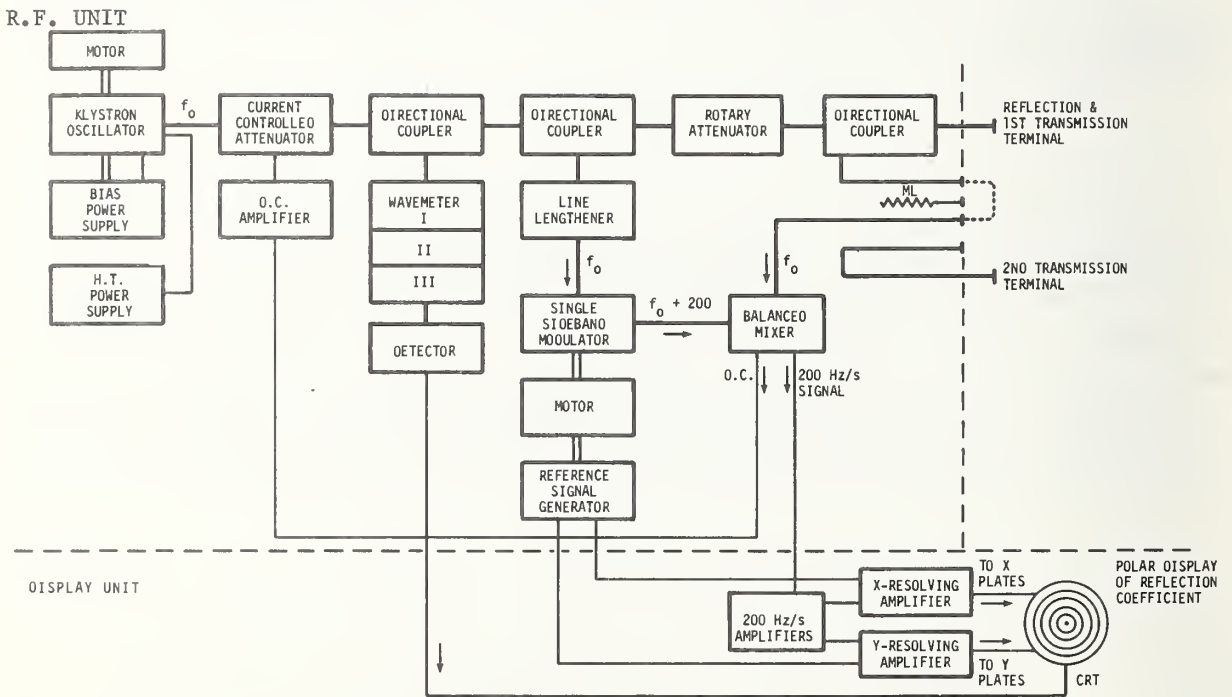


Figure 2-77. Simplified block diagram of Elliott automatic swept frequency impedance meter.

figure 2-55 from an earlier reference [18]. The system appears to be the same as that described in (2.7.b(3) p. 49) with the addition of a line stretcher to vary the position of the reference plane, and the provision for inserting a 2-port device to measure its transmission coefficient.

b. Complex V and I

A multi-frequency network analyzer was developed at the Leatherhead, Surrey (England) Research Laboratory of the Electrical Research Association in 1959 [46]. It operated at 18 frequencies within the range 0.159 to 15.9 kHz. It measured complex potential difference V between two selected points in a network and the complex current I through a selected unit. The direct phase difference ϕ between V and I as well as the products $VI \cos \phi$ and $VI \sin \phi$ could be read out on dials at the control desk.

The measurement of voltage (or current) is made by comparing the selected voltage signal from the network nodes (or shunt) with a reference signal derived from a servo-controlled potentiometer and phase shifter, whose shafts are coupled to read out dials on the control desk.

The multiplying operations are performed on a fixed frequency analog signal by means of potentiometers and a sine-cosine resolver ganged with the voltage and current bridges.

c. I-F Substitution Without Computer Control

The 5-250 MHz loss and phase set described in 1961 [53] represented another step towards the 50 Hz-250 MHz computer-operated transmission measuring set which appeared in 1969 [92]. It was based upon i-f substitution techniques used in earlier test sets [15] (2.9.b(1)) but employed a "rapid sampling" technique³ as illustrated in figure 2-78. Use of rapid comparison and null balancing greatly reduces the effects of drift in the source level or of drift in the i-f amplifiers and detectors. It also greatly relieves requirements of tracking of conversion and phase loss of the converters, since they are common to the channels being compared. "Sample and hold" circuits, in which charges were stored on capacitors, were used to facilitate the comparison of signals propagating in turn through unknown and standard paths. It also introduced the measurement of impedance by bridging [19] which extended the capability of the transmission measuring set to impedance or reflection coefficient measurements.

³In 1954, Slonczewski [26] described a transmission measuring circuit incorporating rapid switching, at a 60 Hz rate, between the unknown and a reference strap; and null balancing at the detector output.

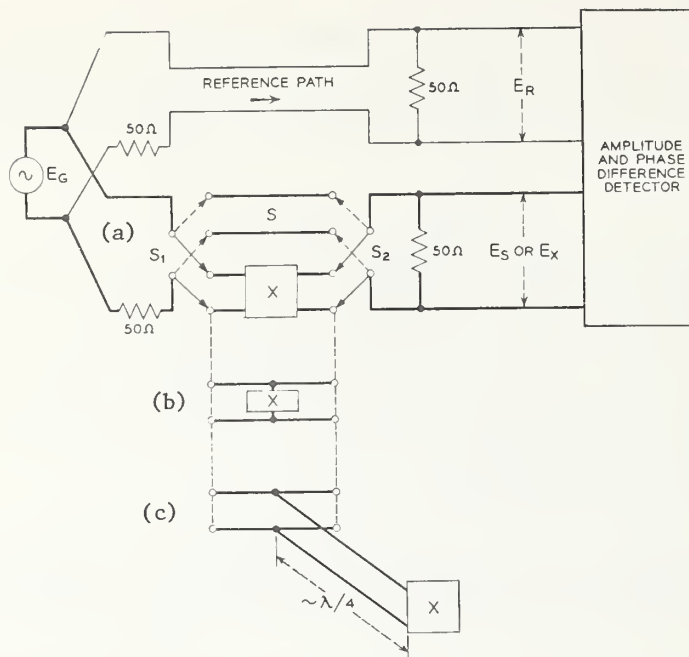


Figure 2-78. (a) Rapid comparison principle of measurement: alternatively interposing X and S between generator and load prevents errors from variations of generator level, detection sensitivity, or shift of detector operating point. (b) Impedance measurement of bridging. (c) Inversion of high impedance by $\lambda/4$ line transformer. (Reprinted by permission: D. Leed and O. Kummer, "A Loss and Phase Set for Measuring Transistor Parameters and Two-port Networks Between 5 and 250 mc", Bell System Technical Journal, 40, no. 3, May issue, pp. 841-884. Copyright 1961, American Telephone and Telegraph Company.)

Another important innovation was the calibration of the set for impedance measurements by measuring the insertion losses and phase shifts corresponding to three different known impedance standards. It was recognized that the complex transmission coefficient T was related to the impedance Z by the following linear fractional transformation

$$T = \frac{a + b Z}{1 + c Z}, \quad (36)$$

where a, b, and c are complex coefficients. These coefficients can be evaluated by measuring the complex values of T corresponding to each of three different known impedances. The simplest known impedances are a short-circuit ($Z = 0$), an open-circuit ($Z = \infty$), and a resistive non-reflecting load ($Z = 50$ ohms for the given coaxial line in use).

An off-line computer was used to do the required calculations.

Two techniques were used to check on errors.

1) Insertion loss and phase shift were measured by individual pads, and then the pads were cascade-connected and remeasured as a unit. The sums of the losses and the sums of the phase shifts were compared with the latter measurement.

2) The insertion phase shift was measured at a large number of frequencies of a precision section of coaxial line. The measured results are compared with calculated values.

The simultaneous switching of the r-f and i-f portions of the circuit are shown in figure 2-79 and the mercury relays used in the r-f portion of the circuit are shown in figure 2-80.

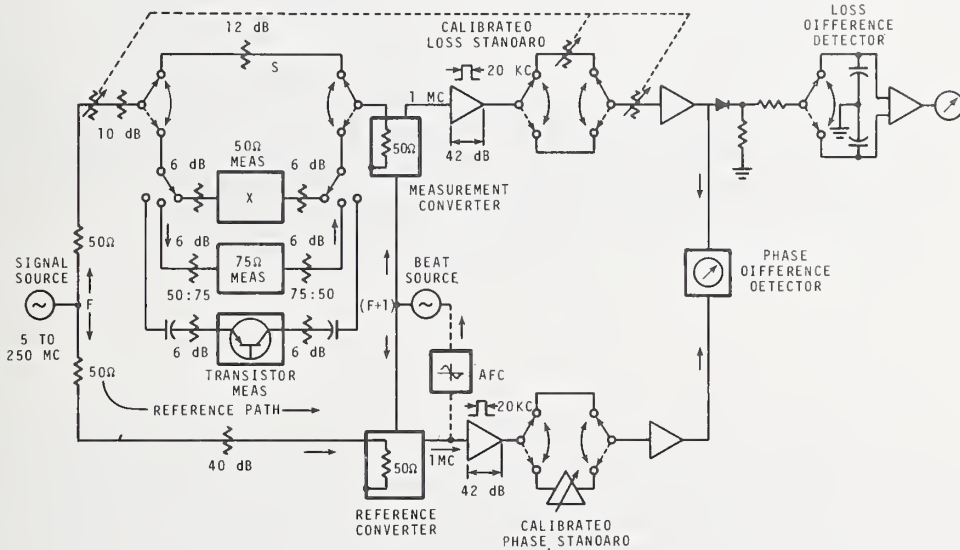


Figure 2-79. Block diagram of measurement set. Parameters of unknown are heterodyned to a constant detection frequency, where their magnitudes are read out on null-balanced, calibrated loss and phase standards. (Reprinted by permission: D. Leed and O. Kummer, "A Loss and Phase Set for Measuring Transistor Parameters and Two-port Networks Between 5 and 250 mc", Bell System Technical Journal, 40, no. 3, May issue, pp. 841-884. Copyright 1961, American Telephone and Telegraph Company.)

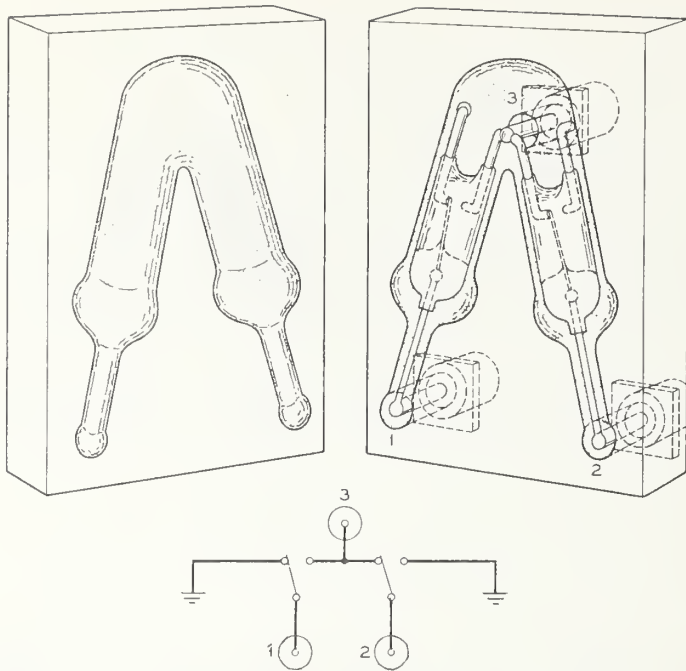


Figure 2-80. 5 to 250 mc comparison switch unit. Glass-encapsulated mercury relays are enclosed within coaxial cavities to provide 50-ohm transmission paths. (Reprinted by permission: D. Leed and O. Kummer, "A Loss and Phase Set for Measuring Transistor Parameters and Two-port Networks Between 5 and 250 mc", Bell System Technical Journal, 40, no. 3, May issue, pp. 841-884. Copyright 1961, American Telephone and Telegraph Company.)

The local oscillator was automatically controlled to maintain the i-f (1 MHz) to within 1 kHz. The loss standard was a calibrated resistive step attenuator and the phase shift standard consisted of a phase splitting network and a four-quadrant sine condenser.

The test frequency was set manually and the loss and phase shift standards were adjusted and read by the operator. A considerable measure of automatic operation using relays was introduced to make signal path changes when transferring among the various measurement modes. The modes included operation at 50 or 75 ohm impedance levels and transistor S-parameter measurements.

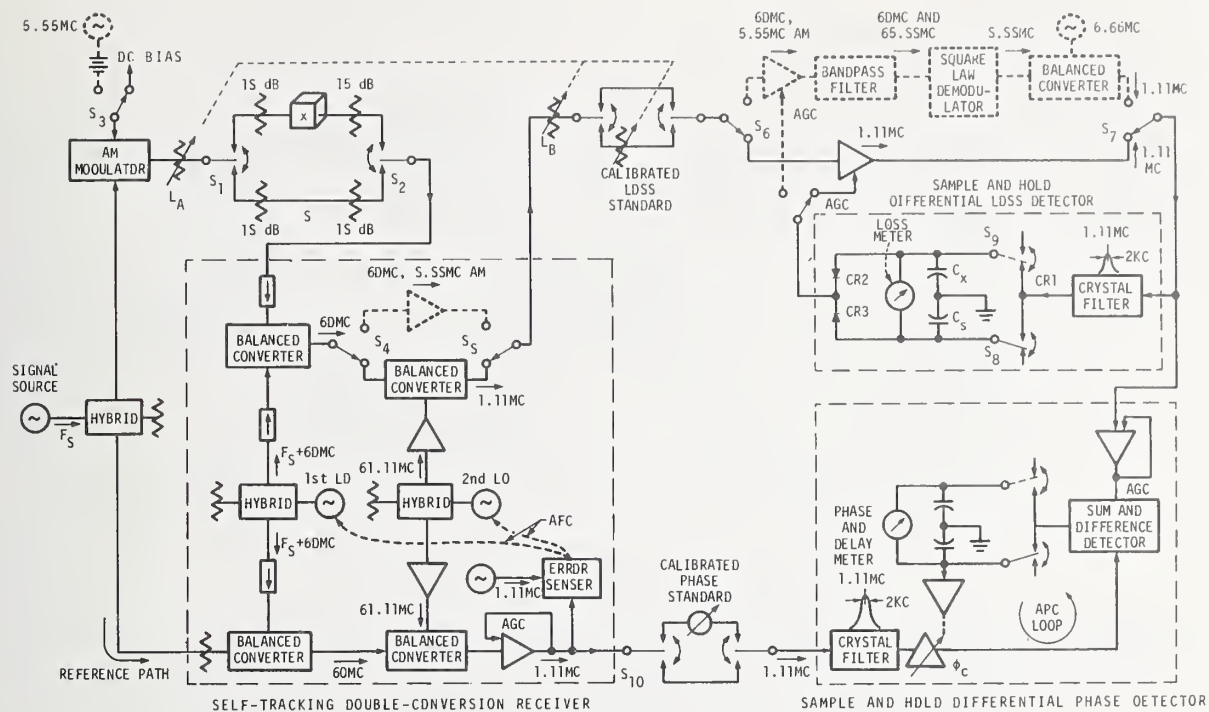


Figure 2-81. Block diagram of test set showing rapid comparison, IF substitution technique of measurement. (Reprinted by permission: D. Leed, "An Insertion Loss, Phase and Delay Measuring Set for Characterizing Transistors and Two-port Networks Between 0.25 and 4.2 gc", Bell System Technical Journal, 45, no. 3, March issue, pp. 397-440. Copyright 1966, American Telephone and Telegraph Company.)

In 1966, another test set using the I-F substitution principle was described [70]. A simplified block diagram is shown in figure 2-81. This set was similar to the previous one [53], but extended the frequency range from 250 MHz to 4.2 GHz. A number of new features were incorporated, including the measurement of non-coaxial devices including rectangular waveguide components and transistors with pig tail leads. Double conversion was employed with IF's of 60 MHz and 1.1 MHz.

Envelope delay was determined by measuring the phase shift experienced by a sinusoidal modulation envelope in its transit through the 2-port under test. Before detection the lower sideband was eliminated by filtering, so as to make the phase of the beat frequency product independent of the beating signal levels. This also reduced the "aperture error" due to non-linearity of phase shift between the sideband frequencies. The concept of "aperture error" in envelope delay measurement is illustrated in figure 2-82.

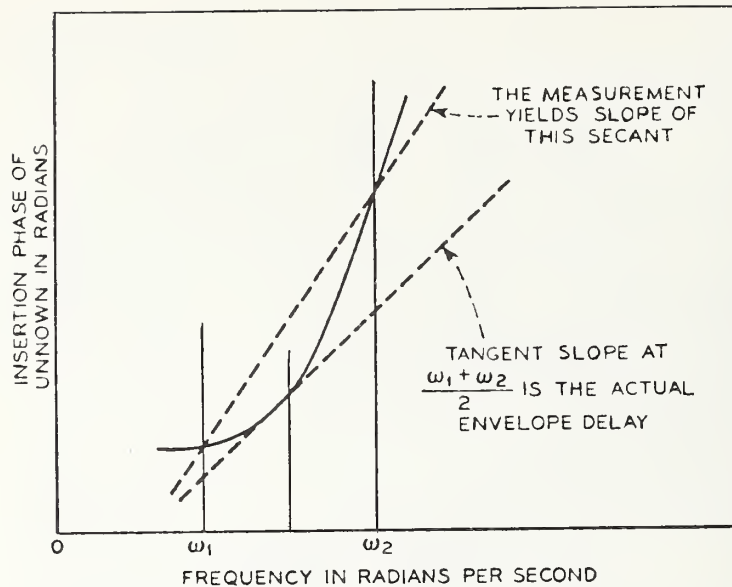


Figure 2-82. "Aperture error" in envelope delay measurement. (Reprinted by permission: D. Leed, "An Insertion Loss, Phase and Delay Measuring Set for Characterizing Transistors and Two-port Networks Between 0.25 and 4.2 gc", Bell System Technical Journal, 45, no. 3, March issue, pp. 397-440. Copyright 1966, American Telephone and Telegraph Company.)

d. Frequency Translation by Sampling

(1) Swept Frequency

In 1967, a network analyzer was described which sweep-measured the magnitude and phase of reflection and transmission coefficients over the range from 110 MHz to 12.4 GHz [74]. Double heterodyne detection was employed with I-F's of 20 MHz and 278 kHz. A technique of frequency translation by sampling was used to obtain the first I-F. In this technique, the local oscillator in the conventional heterodyne system is replaced by a pulse train generator of variable pulse repetition rate (prf). The pulses are narrow so that there is significant harmonic content at frequencies high enough to beat with the incoming signals to the mixer.

As shown in figure 2-83, a phase lock loop controls the pulse repetition frequency so that harmonic mixing occurs automatically as the source frequency is swept. As the frequency sweeps over the entire range, the phase lock loop must continually search for new harmonics of the prf and lock on for part of the sweep. The prf is variable from 60-150 MHz.

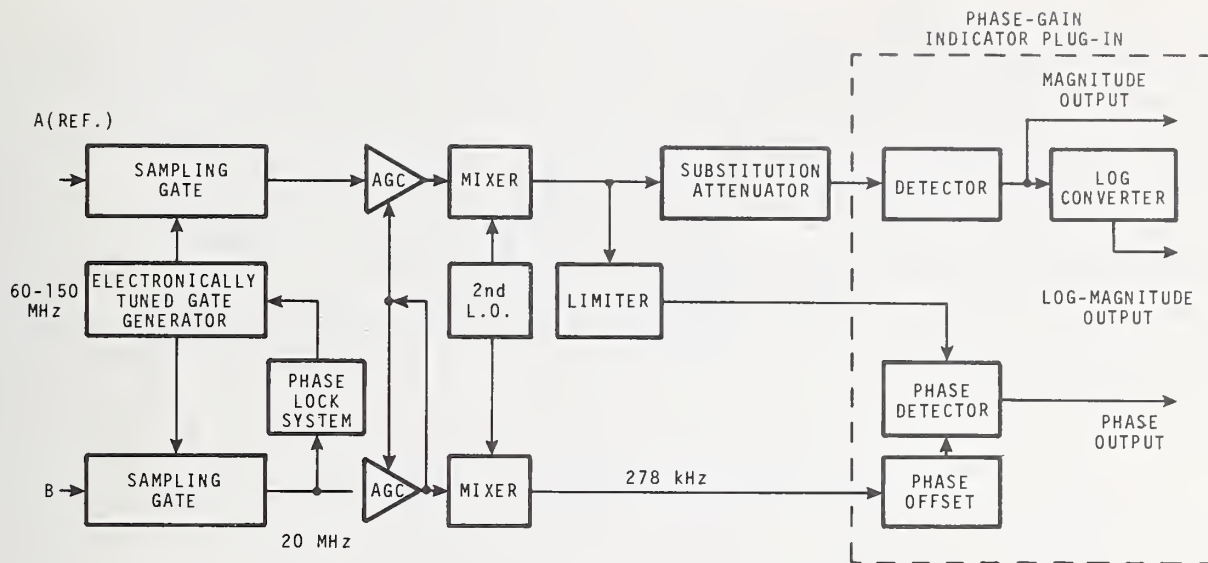


Figure 2-83. Basic system used to achieve frequency translation by a sampling technique. (Reprinted by permission: R. W. Anderson and O. T. Dennison, "An Advanced New Network Analyzer for Sweep-measuring Amplitude and Phase from 0.1 to 12.4 GHz", Hewlett-Packard Journal, 18, no. 6, Feb. 1967.)

The test and reference channels at 278 kHz are fed to the polar display unit shown in figure 2-71. It incorporates the familiar balanced modulator circuit, with a 90° phase shift in one channel [5]. This yields d-c signals proportional to the real and imaginary components of the signal in the test channel as compared with that in the reference channel. These signals can give a display on an oscilloscope or x-y recorder.

This network analyzer was the precursor of the computer-controlled automatic network analyzer, prophesied by Ely [75, 79], and described by Hackborn [84].

(2) Computer Controlled

The computer-controlled network analyzer described in 1968 [84] was an extremely significant advancement. Although it made use of previously known techniques, several functions formerly performed by a human operator were taken over by an on-line instrumentation computer. Manual adjustment of variable standards, reading of dials, and processing of data by an operator were eliminated. In addition, the calibration process by which errors were corrected, was extended.

Previously [53], calibration of a test set for impedance measurements consisted of determining the three complex parameters a , b , and c , of eq. (36), at each frequency. With the computer-controlled network analyzer, additional complex parameters are determined in order to make corrections in transmission measurements. If one assumes a flow graph model as shown in figure 2-84, one measures 5 complex factors by making

- (1) reflection coefficient measurements of three known loads; a non-reflecting termination (simulated by sliding a load having low reflection), a short-circuit, and an offset short-circuit, and
- (2) transmission coefficient measurements in each direction with the measurement ports joined together [85].

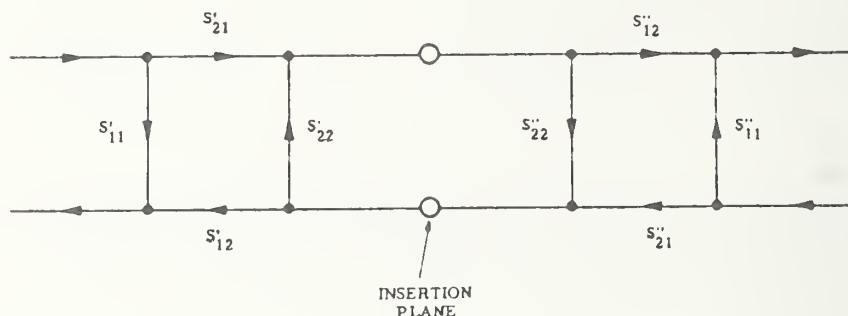


Figure 2-84. Two-port error measurement. (Reprinted by permission: S. F. Adam, "A New Precision Automatic Microwave Measurement System", IEEE Trans. on I&M, 17, no. 4, Dec. 1968, pp. 308-313.)

The entire process is speeded up because correction data is stored in the computer memory while stepping through the desired frequencies at each stage in the calibration process. The corrections are then calculated after the measurements are made, and this is done rapidly and automatically. It is extremely important that the frequency is set to the same value during the calibration and during the corresponding measurement. Since corrections are often very frequency dependent, a correction determined at one frequency would not be valid for a measurement made at a slightly different frequency.

The subject of error analysis and correction in computer-controlled network analyzers is a complicated one, although additional work has been done [83, 96, 101, 102, 103, 119, 126, 129, 131, 132, 141, 143, 145] the last word has not been said. For example, more complicated flow graph models, such as that shown in figures 2-85, 3-7, and 3-8, have been used to analyze the errors in automatic network analyzer systems [96,129]. Six complex error parameters are determined during the calibration procedure.

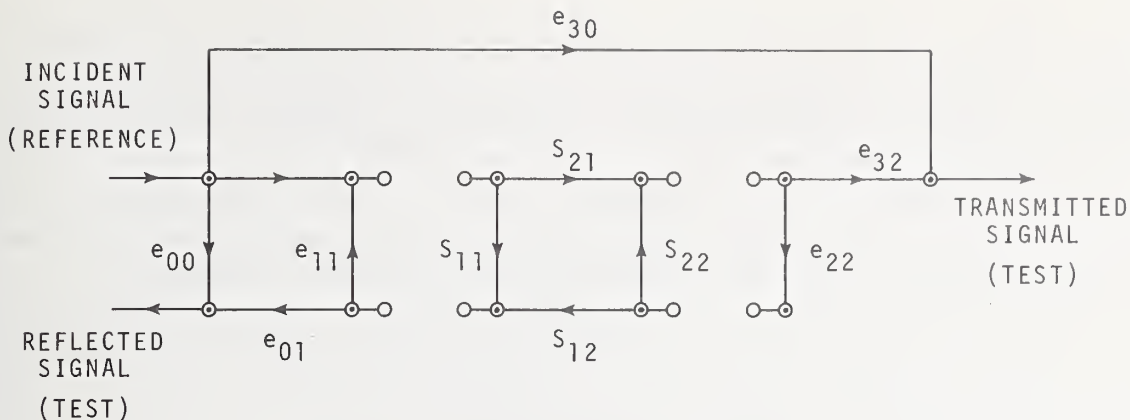


Figure 2-85. Flowgraph model of system.

e. I-F Substitution with Computer Control

In 1969, a computer-operated transmission measuring set (COTMS) for the 50 Hz - 250 MHz frequency range was described [92]. Although its development profited from previous work [53,83], considerably more automation was accomplished. Some of the features distinguishing this set from previous sets were the following:

(1) Instead of controlling the local (beat) oscillator to follow the signal oscillator, each oscillator was composed of a frequency synthesizer and a frequency multiplier, and they could be controlled with digital signals. Absolute accuracies of the output frequency, frequency changes of either oscillator, and frequency differences between the two oscillators were all within 3 parts in 10^8 .

(2) Instead of manually adjusting and reading dials of loss and phase standards, relay switched precision attenuators and quadrant selectors were used. The smallest attenuator steps were 0.01 dB, and additional resolution was obtained by feeding the differential d-c detector output to the computer via an analog-digital converter. Phase measurement was accomplished by measuring the time intervals between pulses produced by zero crossings of the IF signals. The time intervals were measured by counting pulses from a gated 100 MHz source. This digital information was fed to the computer for readout.

(3) Instead of manually connecting the network for each of four measurements required in calibration techniques associated with transistor measurements, considerable coaxial relay switching was developed. In addition, "small bore" standards were developed to apply to the transistor connection terminals.

(4) Automatic measurement and monitoring of some error sources was provided. For example, spurious products such as crosstalk, noise, 60 Hz harmonic pickup, and IF carrier leakage can be automatically measured and plotted as a function of frequency and level configuration.

(5) Improved calibration procedures and data processing techniques were developed [83]. Variation with frequency of short-circuit and open-circuit standards were taken into account. Similarly the variation of phase shift and attenuation with frequency of precision coaxial line sections was considered.

Errors due to mismatch or mistermination were avoided by measuring scattering coefficients defined with respect to the terminal impedances which prevail in the test set rather than to the nominal design impedances. If one then measures the equivalent source and load impedances at the insertion point, it is possible to transform to scattering parameters which are referred to the nominal design impedance (for example, 50 ohms).

An alternate method of correcting for test set imperfections, not requiring an iterative computational technique, has also been developed [102].

Methods of evaluating individual sources or error in COTMS by using its own automatic capability were discussed [119]. The measurement of known, stable transmission standards was proposed as a complementary way of verifying the accuracy.

3. Trends

3.1. Introduction

In order to note the trends in the development of automatic systems to measure network parameters, the status through 1972 is summarized, then more recent work is reviewed, and finally, some of the options open for future developments are mentioned. In making a survey of a rapidly developing field, one must stop at a point in time, knowing that the complete story has not, and cannot be told. However, it may be helpful, before rushing onward, to pause and look back in order to obtain perspective.

It is difficult to accurately predict future developments. Usually, one tends to extrapolate, knowing that many recent developments will be pursued further. The introduction of a new technique, or the revival of an old one may be unforeseen. Thus, the listing of options open for future developments is expected to be of limited value, and may only provide some "food for thought."

In the following, the considerations of precision and accuracy have been given the greatest priority in contrast to speed of data acquisition and low cost per measurement. The potential of automatic techniques to improve the accuracy of measurement systems continues to be of great interest to the National Bureau of Standards.

3.2. Status Through 1972

a. I-F Substitution, Comparison by Rapid Switching

A number of computer-operated transmission measurement systems (COTMS) were developed and built prior to 1973 for use by the Bell Telephone System. By careful attention to all sources of error, excellent performance was obtained. For example, some systems [107] could provide resolutions and accuracies of ± 0.002 dB, 0.01° , and 0.01 ns at frequencies from 3.7 to 4.2 GHz. A similar system had been developed for frequencies from 50-250 MHz [92]. By means of "appliques", the frequency range was extended through 12 GHz [123]. One applique covered the 1-4 GHz range and the other covered 3.6 to 12.4 GHz*.

These computer operated systems could measure network parameters with greater resolution and accuracy than any of the other automatic systems developed up to that time. In fact, the accuracy of phase measurement was as good as one could expect to do with fixed frequency, manually tuned and operated systems. This was due in part to the limitations imposed by mechanical instabilities in microwave circuitry. Somewhat greater resolution and accuracy (approximately ± 0.0001 dB), had been achieved in microwave attenuation measurements with manually tuned and operated fixed frequency measurement systems [47, 128].

*Private communication from C. F. Hempstead, Supervisor, MW Measurement Center, Bell Laboratories, North Andover, Massachusetts 01845.

b. Frequency Translation by Sampling

The automatic network analyzers developed for commercial use up to 1973 could measure magnitude and phase of network parameters at frequencies from 100 kHz to 18 GHz. The resolution of readout data was 0.01 dB, 0.1°, and 0.01 nanosecond. A set of complex error coefficients could be measured and stored and corrections made by the computer to reduce errors.

The magnitude only of reflection and transmission coefficients could be measured with an automatic spectrum analyzer over the frequency range 10 kHz to 18 GHz. The resolution was 0.03 dB and the readout resolution was 0.1 dB [108].

c. Time Domain to Frequency Domain Transformation

Based upon work described in 1968 [86], Nicolson and others developed a measurement system in 1972 using a pulse generator, sampling oscilloscope, and computer [105]. Fourier transforms were taken of the input impulse and the response to obtain frequency domain data and the ratio could give complex reflection or transmission coefficients. Up to frequencies as high as 12 GHz, the resolution was approximately ± 0.1 dB and $\pm 1^\circ$ over ranges up to almost 20 dB. The theory has been known for a long time [7], but the technology has only recently advanced sufficiently to obtain such results. The method gives better accuracy when measuring broadband networks whose impulse response is relatively short-lived, than with narrow band components (because of the excessive number of samples required).

The time required to process data over two frequency decades may be 4 to 5 minutes compared with a few seconds for frequency domain automatic network analyzers. However, the instrumentation is simpler and less costly (no microwave source is required), the ability to carry out frequency analysis of only certain regions of the time domain waveform allows the reduction of effects from unwanted reflections, and it is possible to obtain simultaneous display of time and frequency domain responses of a network.

d. Six-port Coupler

An interesting study of the possibilities of measurements of voltage, current, power, and network parameters using a six-port coupler was reported in 1972 [112].

Considerable attention was given to analysis of an arbitrary six-port having a source connected to port 1, a power meter or load connected to port 2, and power level detectors connected to arms 3, 4, 5, and 6, as shown in figure 3-1. However, it was noted that there

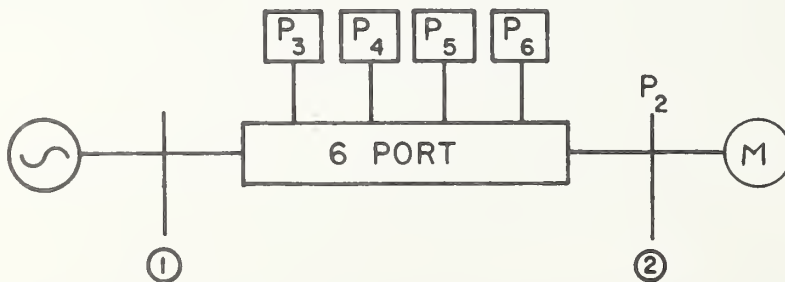


Figure 3-1. A 6-port coupler.

were several other possible measurement applications, including building an automated system around six-port couplers instead of 3 or 4-port directional couplers. Such an automated system should provide increased accuracy for measurements of Z or Γ for which $|\Gamma| > 0.4$, for example. In contrast to IF substitution techniques, only a single source would be required and only power level detectors would be required, not having any phase measurement capability. It was anticipated that Josephson junction detectors might prove extremely suitable for use with six-port couplers in automatic measurement systems.

e. Ratio Measurements Without Standards

Principles of measuring complex ratios without the use of standards were developed prior to 1973 and were referenced by Allred and Manney [124]. Additional work was reported by Somlo, Hollway, and Morgan in 1972 [111]. Although it was not at first anticipated that these techniques would be applied to automatic measurement systems, later developments have included such applications.

The technique of Somlo, Hollway, and Morgan employs a highly reproducible phase-shift step of an initially unknown value. Although this is not a "standard" in the usual sense, it is a special component which is critical to the technique. The phase shifter under test is cascade-connected with the step phase shifter or "flap" as shown in figure 3-2, and the

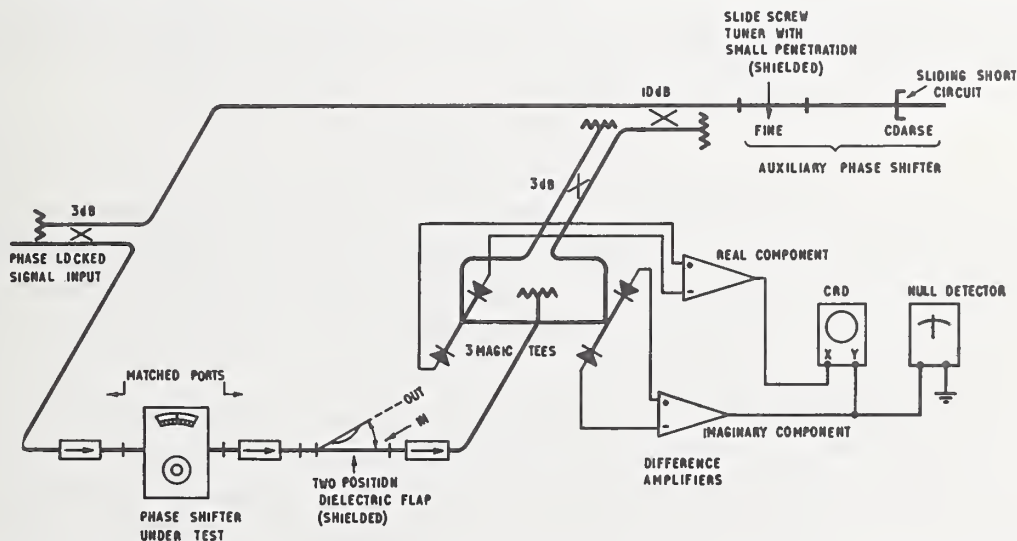


Figure 3-2. Apparatus for phase-shifter calibration. (Reprinted by permission: P. I. Somlo, D. L. Hollway, and I. G. Morgan, "The Absolute Calibration of Periodic Microwave Phase Shifter", IEEE Trans. on MTT, 20, no. 8, Aug. 1972, pp. 532-537.)

change of phase shift produced by switching the 2-position flap is measured with the phase shifter under test (PSUT). An auxiliary phase shifter is adjusted between sets of readings so that the PSUT can repeat measurements of the flap at other portions of the dial of the PSUT. Two methods of computing the error curve from the string of pairs of readings are used: Fourier analysis and interpolation. The Fourier spectrum of the computed correction curve can be used to deduce sources of error that are either electrical or mechanical in nature.

f. Calibration of Automatic Network Analyzers

In 1961, Leed and Kummer [53] introduced a calibration procedure for their 50-250 MHz loss and phase measuring set. They measured both magnitude and phase of the transmission coefficient of a 50-ohm transmission path with three known impedance standards successively bridged across it. After evaluation of the parameters in the linear equation to correct the measurements, a fourth standard impedance was bridged across the transmission path and its impedance measured as a check on the procedure. This was the forerunner of slightly more complicated calibration techniques used later with computer-controlled automatic network analyzers.

In 1968 Adam [85] described an error network whose parameters were evaluated by making measurements of both magnitude and phase of reflection and transmission coefficients with various standards connected in place. The error network was shown in figure 2-84 and did not contain the leakage path e_{30} introduced later. In 1970, Hand [96], described a calibration process using the model shown in figure 2-85. The calibration involved six measurements and the solution of the six equations and the subsequent correction of the measurement were done by the computer using an iterative process.

In 1971, Kruppa and Sodomsky [102] obtained an explicit solution to correct the measurements, making unnecessary the use of an iterative technique. Their solution applied to the network not having the leakage path. However, the leakage path was needed to take into account errors due to crosstalk between channels.

g. Interface Systems

Digitally coupled instrument systems began in the mid 1950's with the "marriage" of the frequency counter to a digital recorder. Digital data was presented in parallel form and information flow was unidirectional. Later, programmable digital voltmeters having digital inputs and outputs were introduced. Other digitally controlled instruments followed, and a variety of signal levels and logic conventions were encountered, making interconnection a difficult problem in many cases.

In the late 1960's computer control of measurement systems brought some uniformity to the interface hardware, but the overall interface network remained a star pattern with each instrument connected to the central processor or controller by its own cable and plug in I/O (Input-Output) card. Around 1970, the plug in I/O cards were included in the processor mainframe and an instrument bus structure began to take form [116]. Connecting instruments into a digitally controlled measurement system finally became simply a matter of plugging in cables [115]. The interface bus system which evolved in 1972 is illustrated in figure 3-3.

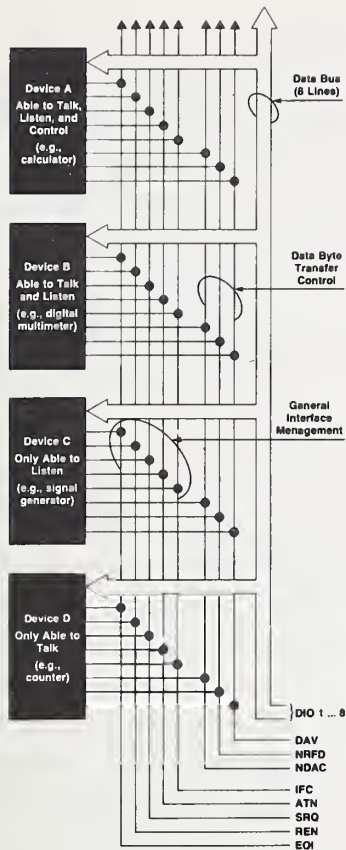


Figure 3-3. A practical interface system for electric instruments. (Reprinted by permission: Hewlett-Packard Journal, 26, no. 5, January 1975, p. 3.)

3.3. Recent Developments

a. I-F Substitution, Comparison of Rapid Switching

The number of computer operated transmission measurement systems (COTMS) has greatly increased and they have been installed at various locations including New Jersey, Georgia, North Carolina, Massachusetts, Pennsylvania, Illinois, and Missouri [123]. The basic transmission measuring system covers the frequency range 50 Hz to 1 GHz. Additional test terminals in this range can be provided by remotely located test equipment called "appliques," connected to COTMS by computer-controlled applique switches and transmission lines. Microwave appliques cover frequencies up to 20 GHz.* They operate by accepting a signal in the frequency band below 1 GHz from the central transmission measuring system and translate it up to the desired microwave test frequency. The applique then passes the microwave test signal through the network and translates it down to the band below 1 GHz for transmission to the central measuring system which measures the insertion loss and phase. Appliques for the 0.9 - 12.4 GHz range have been described [151]. Advantages of appliques include the sharing of centrally located equipment such as a computer and I-F standards, and the reduction of effects of drifts and instabilities in microwave transmission paths by the use of rapid comparison switching.

*Private communication from C. F. Hempstead.

b. Frequency Translation by Sampling

Lowered costs of core memory plus experience in the operation of many automatic measurement systems has led to improvements in software. Stored programs on paper tape have given way to magnetic tape cassettes. One can choose between 26 output parameters calculated from the measured S-parameters. Output data can be in tabular form or may appear almost instantaneously on a graphics terminal with the option to obtain a hard copy within 11 seconds [125]. Other improvements are covered in section 3.3.f. Some hardware improvements have also been made, but have not been fully described in the literature. A recent improvement in the quadrature detector results in more accurate measurements of low-loss devices, such as short sections of transmission line.

c. Time Domain to Frequency Domain Transformation

Using basically the same technique described by Nicholson et al [86,105], a time domain automatic network analyzer having greatly improved performance has been developed by Gans and Andrews [147,148,150]. It measures S-parameter versus frequency from 0 to beyond 18 GHz. The signal source is typically a tunnel diode pulse generator having a risetime of less than 20 ps. The receiver is a sampling oscilloscope having a risetime of 20 ps. A minicomputer controls the oscilloscope and stores and processes the data. The data is averaged to improve signal to noise ratio, Fourier transformed from time domain to frequency domain, and manipulated to output S-parameters. The range of power ratios measured is 60 dB for frequencies up to 4 GHz and 40 dB up to 18 GHz. Accuracy of attenuation measurements was determined to be within $\pm 2\%$ over a range of 10-40 dB at frequencies between 0.5 and 12.5 GHz. (Agreement within 1.5% was obtained with an IF substitution technique.) The accuracies obtainable in return loss measurements and in the measurement of phase have not yet been determined.

The elements of the measuring system are shown in the block diagram of figure 3-4 and a comparison of insertion loss measurements at microwave frequencies is given in figure 3-5.

Recently, Cronson, Nicholson, and Mitchel [142] have extended time domain metrology above 10 GHz to materials measurement. Actually, the S-parameters of a microwave circuit containing a sample of the material under investigation were measured, and the complex permittivity and permeability were then calculated. In order to avoid producing non-linear effects in the materials, it was necessary to employ a more complex waveform than a step or a pulse. The peak voltage was held below 0.8 v, and a short RF burst using a step recovery diode was found to provide sufficient spectral amplitude in the 9-16 GHz range. The RF burst was 400 ps wide.

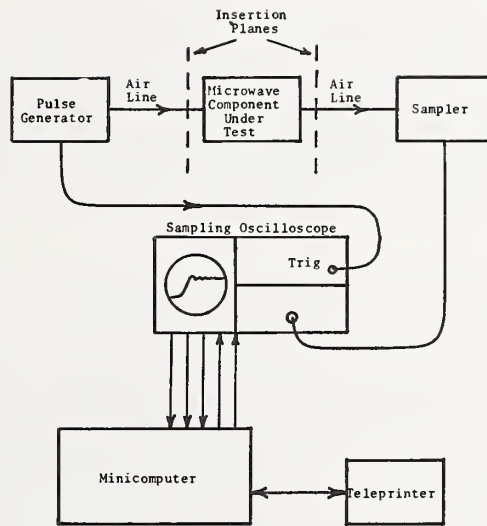


Figure 3-4. Time domain automatic network analyzer (TDANA) basic block diagram.

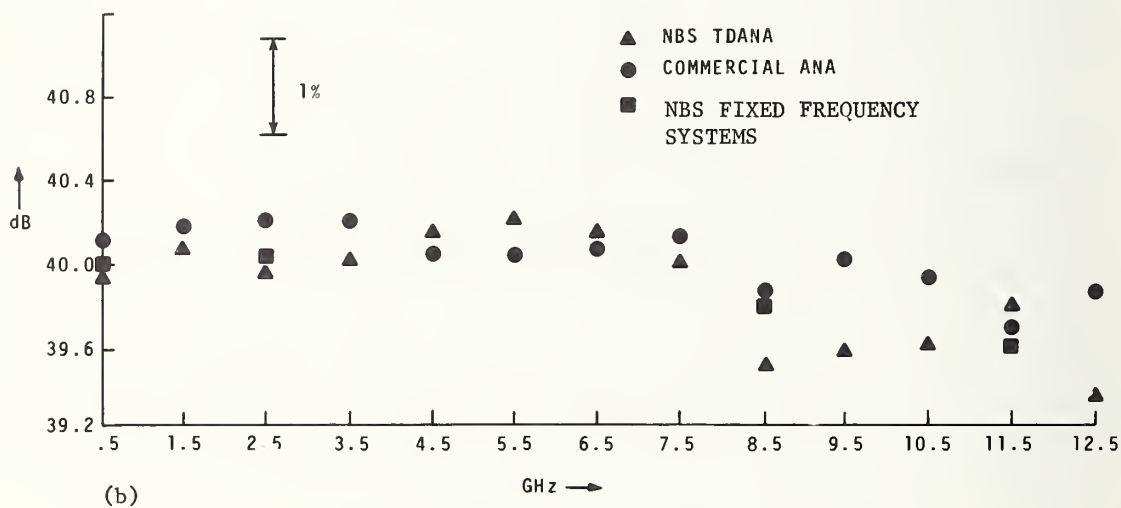
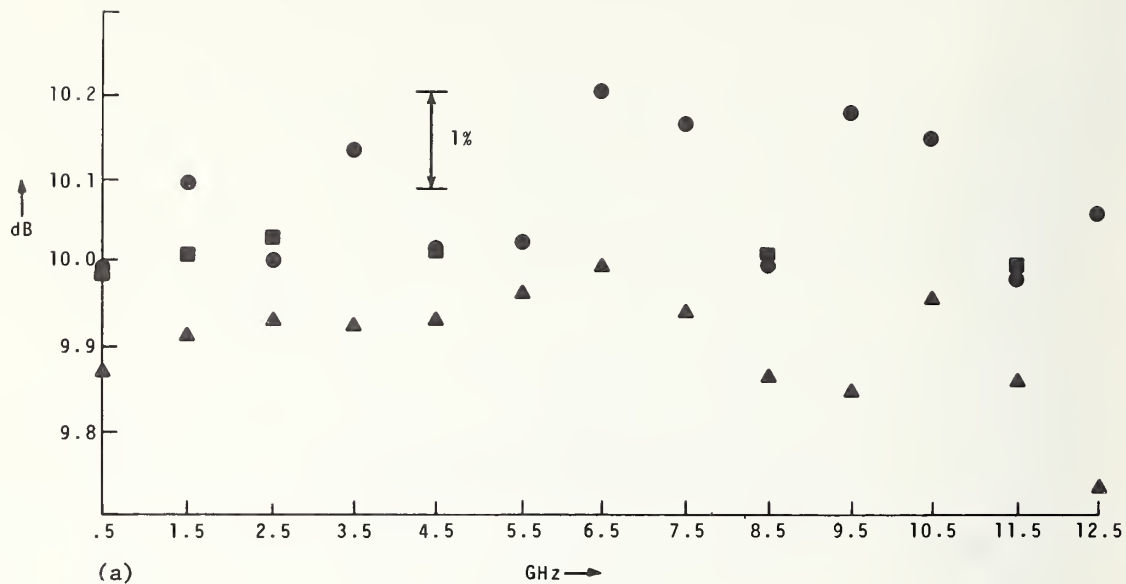


Figure 3-5. Comparison of NBS TDNA measurements Δ with commercial ANA (FDANA) O, and NBS fixed frequency tuned systems \square , for (a) 10 dB attenuator and (b) 40 dB attenuator.

d. Six-port Coupler

Recently, Hoer and Roe [146] have shown how an arbitrary six-port coupler may be used to measure complex ratios. They have calibrated a six-port coupler using a technique similar to that described by Allred and Manney [124], and have measured the magnitude and phase shift of an attenuator at frequencies from 8 to 12 GHz. A programmable calculator was used to control the measurements and process the data. The results were within 0.2 dB at 8 dB and within 1° at 35° of measurements made on the same attenuator using a commercially available automatic network analyzer.

This preliminary work demonstrates the validity of the techniques developed and provides a basis for further work that could lead to a different automatic system to measure the S-parameters of networks.

e. Ratio Measurements Without Standards

Techniques described by Allred and Manney [124] for measuring complex ratios without standards do employ a highly reproducible insertion device which need not be initially known, but is subsequently determined. In this respect, they resemble the independently developed technique of Somlo, Hollway, and Morgan [111]. However, the work of Allred and Manney is of potentially wider application, although not carried through to as great a degree of practical utility.

A number of so-called "self-calibrating" techniques have been developed, but have not been widely applied because of the awkward procedures and tedious calculations required. During the taking of the large amount of data required, errors could be large due to drifts and instabilities. In addition, data processing was a tedious and expensive task. Recently, the development of frequency agile sources, digitally controlled measuring equipment and computer control and data processing capabilities, has encouraged some metrologists to take another look at the "self-calibrating" techniques.

f. Calibration of Automatic Network Analyzers

Prior to 1973, the model for the error network at the insertion point was evaluated at each frequency by sending energy through the insertion point in turn in each direction with a straight through connection, then measuring the reflection coefficient with a short-circuit, an offset short, and a non-reflecting load terminating each port in turn. From six measurements of both magnitude and phase, it was possible to determine the six complex parameters of the error network and make the necessary corrections.

The non-reflecting load was simulated by using a sliding load, moving it successively to three positions, and then calculating the center of the reflection coefficient circle which corresponded to a perfectly non-reflecting load. As computer memories became less expensive, the software was modified to increase the number of positions of the sliding load beyond three (the absolute minimum to determine the center of the circle), so as to increase the accuracy of the calibration [125]. Additional software was developed by B. C. Yates* at NBS to use additional positions of the sliding load, and to account for erroneous phase shifts of other than 90° in the detector, in making more accurate calibrations.

*Private communication from W. E. Little. -93-

In 1974, Rehnmark [129] presented explicit formulas for computing the scattering parameters of a 2-port measured by an imperfect network analyzer. By using explicit formulas rather than an iterative technique, the computing time could be significantly reduced. As shown in figure 3-6, a switch may be used to reverse the direction of energy flow

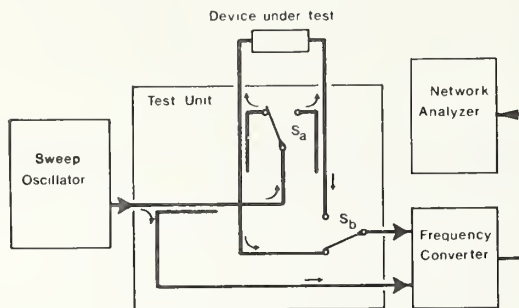


Figure 3-6. Switching arrangement in Automatic Network Analyzer. (Reprinted by permission: Stig Rehnmark, "On the Calibration Process of Automatic Network Analyzer Systems", IEEE Trans. on MTT, MTT-22, no. 4, April 1974, pp. 457-458.)

through the test item. If the switch is used, then the system model shown in figure 3-7

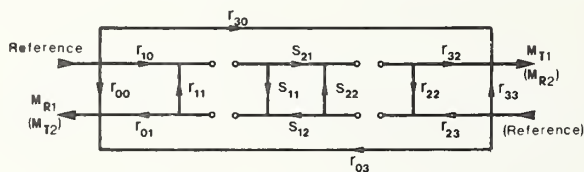


Figure 3-7. Signal flowgraph of system model (switch S_a included in test unit). (Reprinted by permission: Stig Rehnmark, "On the Calibration Process of Automatic Network Analyzer Systems", IEEE Trans. on MTT, MTT-22, no. 4, April 1974, pp. 457-458.)

is employed in the calibration and correction process. If the switch is not used, then the device under test must be manually turned to be measured from both directions. In this case, the system model shown in figure 3-8 is used. Rehnmark modified the error circuit based

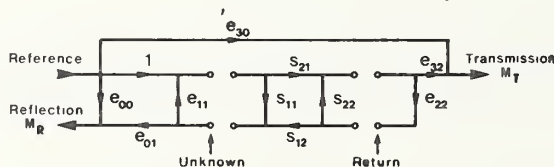


Figure 3-8. Signal flowgraph of system model (switch S_a not included in test unit). (Reprinted by permission: Stig Rehnmark, "On the Calibration Process of Automatic Network Analyzer Systems", IEEE Trans. on MTT, MTT-22, no. 4, April 1974, pp. 457-458.)

upon a switching arrangement (described by Hackborn [84] so as to include a leakage path. He obtained explicit solutions in this case also, and the result should not only reduce time but also improve accuracy. The latter result was similar to the explicit expression obtained by Davies et al [127], in 1973 for a slightly less complicated circuit model.

In 1974, Ridella [131] considered additional error sources in the calibration of A.N.A.'s for measurements of reflection coefficient. He considered errors due to non-repeatability, noise, calibration components errors, and instrumentation error (in particular the polar conversion). Working in the U. S. at NBS, Kasa [141] also considered the problem of A.N.A. calibration for the measurement of reflection coefficient. He derived expressions for the complex parameters a, b, and c in the equation

$$w = \frac{a \Gamma + b}{c \Gamma + 1}, \quad (37)$$

where Γ is the reflection coefficient of a termination and W is the A.N.A. uncorrected reflection coefficient measurement. The parameters a, b, and c were to be determined by connecting three standards in turn and measuring the corresponding W's. In one case, two fixed standards and one sliding load were used and in the other case one fixed standard and two sliding loads were connected. It was not required to know the reflection coefficients of the sliding loads, only their positions. Thus, in the second case, one required only one known standard, but a somewhat more lengthy calibration procedure was needed. Kasa did not solve the problem of obtaining Γ from W once a, b, and c were determined, since such a solution is straight-forward.

Later, Engen [143] addressed the above problem and his analysis was similar to that of Kasa, but with the difference that the sliding load positions did not need to be measured, and that the attenuation of the waveguide in which the loads were sliding was taken into account.

Engen also described a technique for obtaining the scattering coefficients of a reciprocal, linear 2-port from the calibration parameters a, b, and c of the A.N.A., plus a new set of calibration parameters a', b', and c'. The new set of parameters were obtained in the same way as the old set when the 2-port under test was connected to the A.N.A. output and the standard and sliding loads were then connected in turn to the output of the 2-port. A computer program was developed to handle the calculations. Increased accuracy can be obtained by substituting a different test set in which a pair of power meters measure the magnitude $|W|$ of the complex ratio. The phase is determined by the unmodified complex ratio detector of the A.N.A. This technique is particularly well suited for measuring efficiencies of low-loss 2-port devices.

g. Interface Systems

The increased development of programmable digital instruments by various manufacturers and their increased use in measurements of all kinds led to a general recognition of the need to standardize interface systems. The standard developed by one of the leading U.S.A. instrumentation companies for their own use was proposed for consideration as the basis for an international standard, and was widely supported. It has been adopted as an IEEE

(Institute of Electrical and Electronics Engineers) standard (No. 488-1975, SH04887) and is expected to become an IEC (International Electrotechnical Commission) standard after minor modifications.

The above standard defines physical details of an interface cable and connectors, the logic conventions, format, and timing of control and data signals plus protocol and procedures to be used in the interconnection of digital instruments, computers, and peripheral equipment. The complicated details are the subject of several articles, notably (Ricci and Nelson, 1974 [139], (Loughry 1974 [138]), and (Knoblock and Loughry, 1975 [149]).

In anticipation of general adoption of this standard, many companies are developing compatible instruments. Thus, the automation of all sorts of measurements is expected to become easier, less expensive, and more widespread.

h. Computer Operated Bridges

Both dc and ac bridges have been automated and computer-controlled (Hall, June 1974 [134]), (Coons, et al., June 1974 [133]). Different bridge configurations can be chosen by computer-controlled automatic switching, and the data can be presented in various optional forms. Accuracy is preserved and in some cases enhanced due to minimizing instability or drift effects. The ac bridge has a frequency range from 200 Hz to 30 MHz and a single point in a frequency run is obtained in 10 seconds. A wide range of immittances are measured with an optimum accuracy of better than 0.05% and 100 microradians, (0.006°).

i. Slotted Lines

At a small sacrifice in accuracy, direct readout of VSWR versus frequency has been automatically accomplished with a 7 mm slotted line system (Stauffer, et al., December 1974 [140]). Automatic slope correction can be made, but information on the phase of the unknown impedance is not obtained automatically. The system operates on a swept-frequency basis from 2-18 GHz.

3.4. Future Options

a. Introduction

It is felt to be valuable to look ahead to future developments. If we can judge which direction is the most profitable, and likely to be most successful, present efforts can be more efficiently channeled. It is recognized that such an approach is limited in value because some events turn out as predicted and others do not. Predictions based upon extrapolation are likely to have short range success, but may fail in the long run.

If one tries to avoid any predictions, but only attempts to list the options available to researchers, this approach is also likely to have success mainly in the short range. In the following, both the listing of options and prediction will be attempted.

b. Interface Developments

The advances in solid state integrated circuit technology will be further exploited. It has been stated (Grossman 1974 [136]) that almost any test or measuring instrument today is fair game for redesign around microprocessors. They are less expensive and slower than mini-computers, but can be incorporated almost invisibly into instruments of all kinds to automatically select ranges, store and process data, make logical decisions based upon incoming data, and assist fault diagnosis and self-testing (Falk 1974 [137]). The increased use of microprocessors will result in less traffic on the interface bus. While the job of the system

designer will become easier, that of the instrument designer will become more difficult. The designer of an instrument will need to be competent in hardware, software, and instrumentation technology. For applications in which high-speed data transfer is required, low-loss optical fibers may come into use as data bases. Advantages include 100 MHz bandwidths, immunity from ground currents and inductive pickup of interference, and independence from logic levels used at either end (Oliver, 1974 [135]).

In addition to a data bus consisting of a cable, data communication via radio may make remote control of measurements via laser beam, satellite, or deep-space probe feasible.

c. Automatic Tuning

It may come to pass that any measurement system that was previously manually controlled will be fully automated. Some manual functions such as adjustment of tuners, connection of standards and unknowns alternately to the measuring system, and fault detection and correction are difficult to perform automatically under computer control. Servo control of mechanical motion has been applied in the past, but it is slow and clumsy compared with electrical control of electronic devices. The calibration of present automatic systems is a slow process, requiring manual connection and adjustment of standards such as sliding shorts and sliding loads. One could conceivably speed this up by employing electronically variable phase shifters and fixed loads or short circuits. This is presently difficult, but when it becomes easier, one can also introduce electronically controlled tuning to reduce the need for calibration (Wang 1974 [144]).

It has long been recognized that higher accuracy can be obtained by comparing the unknown with a known standard whose value is close to that of the unknown. Thus, an automatic system might contain as stored data the responses to a number of standards. It would remain for the measuring system to measure only the differences between responses to a device under test and the stored response to the standard nearest in value to the unknown.

d. Performance Degradation Diagnosis

An automatic measuring system is very complex and subject to degradation of performance which may occur without warning and without complete breakdown of the system. One way to detect such degradation of performance is to routinely measure broadband, calculable 2-port standards (Beatty 1974 [145]). However, this does not pinpoint the difficulty or correct it. Some progress has been made in diagnostics, but more remains to be accomplished. Economics will force attention to this problem because it is expensive for an automatic system to be "down" or to be giving inaccurate results. Self-testing techniques will be extensively developed and internal standards will be employed. Perhaps even automatic fault correction will be developed.

e. Automatic Calibration

The elimination of calibration runs in automatic measurement is a future development which will save time and reduce operator errors. The operator does not always perform the calibration correctly, and the operating frequency is in general slightly different when testing than when calibrating. Systems which quickly compare the DUT with internal standards already exist and where higher accuracy is desired, the trend will be in this direction. Automatic tuning of the system, as previously mentioned should also reduce the need for system calibration.

f. Extended Range of Operation

The heterodyne or IF substitution technique has remained for many years the one yielding the greatest dynamic range along with excellent, proven linearity. Whether other detection methods, such as the Josephson junction, Fourier transformation of time domain data, frequency translation by sampling, or other techniques, will prove superior remains to be seen. Extension of the frequency range of present automatic measurement systems has been accomplished with "appliques" [123, 151], in which the frequency is translated upwards to the DUT and downwards to the automatic measurement system. It would appear that this technique will be extensively applied in the future. When using coaxial components, extension to frequencies higher than 18 GHz will require the development of components in smaller sizes of coaxial line. (Working in 1.5 mm line could extend the frequency range to 40 GHz.)

g. Reduction of Size and Cost

The great reductions in size and cost of solid state integrated circuit components has had its impact on computers, minicomputers, microprocessors, and electronic calculators. Oliver [135] has stated that the cost of a modern computer or calculator is almost entirely in its bulk memory and input-output (I/O) devices. In the future, not only the cathode ray tube graphic display will be miniaturized and reduced in cost, but the measurement hardware such as directional couplers, isolators, switches, etc., will undergo a corresponding reduction in size and cost.

The application of so-called "six-port" techniques (Hoer and Roe, May 1975 [146]) to automatic measurement systems could reduce the cost since only one signal source is required. Similarly, the time domain automatic network analyzer (Gans and Andrews, 1975 [150]) promises a more economical system.

h. Improved Resolution and Accuracy

It was mentioned in section 3.3c that improved accuracy and resolution can be achieved in principle by measuring only small differences between known standards and DUT's whose values are close to those of known standards. Unless the research on calculable standards is accelerated, the realization of this approach may be far off. In the meantime, the measurement of phase differences to $\pm 0.01^\circ$ appears to be approaching the limit dictated by mechanical instabilities of measurement systems. The measurement of magnitude ratios to ± 0.001 dB appears to be approaching the limits of connector non-repeatability, which is a critical, limiting factor in all electromagnetic measurements.

i. Unforeseen Developments

The extension to higher frequencies up into the optical range of the measurement of network parameters, and the automation of such measurements is presently unforeseen, but may occur in the future. The remote control of, and communication with distant measurement systems located perhaps on other planets, might be desirable and would not be impossible. Additional miniaturization of components and measurement systems is likely to occur. Advances in short pulse and electro-optical techniques may produce unforeseen capabilities with measurement applications, just as cryogenic techniques and the Josephson junction are remaining to be exploited. The unknown and the unforeseen await around some future corner to yield someday to the curiosity and ingenuity of the researcher.

4. References

a. Chronological List

- [1] Peterson, E., (June 1, 1926), U.S. Patent No. 1,586,533. Filed 27 April 1922.
- [2] Nyquist, H. and S. Brand (July 1930), Measurement of phase distortion, BSTJ 9, 522-549.
- [3] Turner, H. M. and F. T. McNamara (Oct. 1930), An electron tube wattmeter and voltmeter and a phase shifting bridge, Proc. IRE 13, No. 10, 1730-1747.
- [4] Best, F. H. (Jan. 1933), A recording transmission measuring system for telephone circuit testing, BSTJ 12, No. 1, 22-34.
- [5] Peterson, E., J. G. Kreer and L.A. Ware (Oct. 1934), Regeneration theory and experiment, BSTJ 13, 680-700.
- [6] Swift, G. (Feb. 1939), Amplifier testing by means of square waves, Communications 19, No. 2, 22-26, 52.
- [7] Koehler, G., H. J. Reich and L. B. Woodruff (1942), Ultra-high-frequency techniques, J. G. Brainerd, Ed., 43-47 (D. VanNostrand Co., New York, N.Y.).
- [8] Werthen H. and B. Nilsson (1947), An automatic impedance meter, Trans. Royal Inst. of Tech., Stockholm, Sweden, No. 8, 95 p.
- [9] Bauer, J. A. (Sept. 1947), Special applications of ultra-high-frequency wide-band sweep generators, RCA Rev. 8, No. 3, 564-575.
- [10] Purcell, E. M. (1947), Measurement of standing waves, Chap. 8, and Young, L. B. (1947), Impedance bridges, Chap. 9, Techniques of Microwave Measurements, 511-512, 537-560 (McGraw-Hill Book Co., New York, N.Y.).
- [11] Samuel, A. L. (Nov. 1947), An oscillographic method of presenting impedances on the reflection coefficient plane, Proc. IRE 35, No. 11, 1279-1283.
- [12] Libby, L. L. (June 1948), Frequency-scanning VHF impedance meter, Electronics 21, No. 6, 94-97.
- [13] Allen, P. J. (1948), An automatic standing-wave indicator, AIEE Trans. 67, 1299-1302.
- [14] Riblet, H. J. (Dec. 1948), A swept-frequency 3-centimeter impedance indicator, Proc. IRE 36, No. 12, 1493-1499.
- [15] Alsberg, D. A. and D. Leed (April 1949), A precise direct reading phase and transmission measuring system for video frequencies, BSTJ 28, No. 1, 221-238.
- [16] Meinke, H. H. (August 1949), Eine Messleitung mit Sichtanzeige, FTS 2, 233-241.
- [17] Musson-Genon, R. and P. Brissoneau (March 1950), Sur un mesurer d'impedances à couplage directif en hyperfréquence, Compt, Rend. Acad. Sci, 230, 1258-1259.
- [18] Whitehead, E. A. N. (Sept. 1951), A microwave swept-frequency impedance meter, The Elliott Journal, 57-58.
- [19] Alsberg, D. A., (Nov. 1951), A precise sweep-frequency method of vector impedance measurement, Proc. IRE 39, No. 11, 1393-1400.
- [20] Witten, A. L. and R. E. Henning (Nov. 1951), A recording broadband waveguide reflectometer, NEC Proc. 7, 173-180.
- [21] Meinke, H. H. (Sept. 1952), Ringförmige Messleitungen mit Sichtanzeige für Frequenzen von $10^8 \dots 3 \cdot 10^{10}$ Hz, ETZ 73, part A, No. 18, 583-584.
- [22] King, D. D. (1952), Measurements at centimeter wavelength, 242-245 (D. VanNostrand Co., New York, N. Y.).
- [23] Packard, D. S. (April 1953), Automatic Smith chart plotter, Tele-Tech, 65-67 and 181-183.
- [24] Grace, A. C. and J. A. Lane (May 1953), A direct-reading standing-wave indicator, J. Sci. Instr. 30, 168-169.
- [25] Rickert, H. H. and D. Dettinger (1954), An X-band rapid-sweep oscillator, IRE Con. Record 2, Part 10, 7-13.

- [26] Slonczewski, T. (April 1954), Precise measurement of repeater transmission, *Electrical Eng.* 73, No. 4, 346-347.
- [27] Gabriel, W. F. (Sept. 1954), An automatic impedance recorder for X-band, *Proc. IRE* 42, No. 9, 1410-1421.
- [28] Cohn, S. B. (Oct. 1954), Impedance measurement by means of a broadband circular-polarization coupler, *Proc. IRE* 42, No. 10, 1554-1558.
- [29] Hopfer, S. and H. A. Finke (Jan. 1955), Impedance measurements in the 50-1000 Mc/sec range with a new standing wave indicator, *PRD Reports* 3, No. 2, 1 and 3-7.
- [30] Bachman, H. L. (Jan. 1955), A waveguide impedance meter for the automatic display of complex reflection coefficient, *IRE Trans. on MTT* 3, No. 1, Jan. 1955, 22-30.
- [31] Hess, R. C. (1955), The diagraph, a direct reading instrument for graphic presentation of complex impedances and admittances, *IRE Con. Record* 3, Part 10, 23-25.
- [32] van der Hoogenband, J. C. and J. Stolck (May 1955), Reflection and impedance measurements by means of a long transmission line, *Philips Tech. Rev.* 16, No. 11, 309-320.
- [33] Egger, A. (May 1955), Widerstandsmessung mit der messverzweigung, *FTZ* 8, No. 5, 277-281.
- [34] Bachman, H. L. (March 1956), Automatic plotter for waveguide impedance, *Electronics* 29, 184-187.
- [35] Vinding, J. P. (1956), The Z-scope, an automatic impedance plotter, *IRE Con. Record* 4, Part 5, 178-183.
- [36] Watts, G. B., Jr. and A. Alford (1957), An automatic impedance plotter based on a hybrid-like network with a very wide frequency range, *IRE Con. Record* 5, 146-150.
- [37] Mittra, R. (Dec. 1957), An automatic phase-measuring circuit at microwaves, *IRE Trans. on Instrumentation* 6, No. 4, 238-240.
- [38] Kinnear, J. A. C. (May 1958), An automatic swept-frequency impedance meter, *British Comm. and Electronics* 5, No. 5, 359-361.
- [39] Cole, R. A. and W. N. Honeyman (July 1958), Two automatic impedance plotters, *Electronic Eng.* 30, No. 365, 442-446.
- [40] Tischer, F. W. (1958), *Microwellen-messtechnik*, Springer-Verlag/Berlin, Chaps: 4 and 6.
- [41] Dix, J. C. and M. Sherry (Jan. 1959), A microwave reflectometer display system, *Electronic Eng.* 31, No. 371, 24-29.
- [42] Hopfer, S. and L. Nadler (Jan. 1959), Waveguide rotary standing wave indicators, *PRD Reports* 6, No. 1, 1, 3-6.
- [43] Zykov, A. J. (March 1959), Impedance measurements by means of directional couplers, *Meas. Tech.* 3, No. 3, 211-215.
- [44] Laverick, E. and J. Welsh (April 1959), An automatic standing-wave indicator for the 3-cm waveband, *Jour. Brit. IRE* 19, No. 4, 253-262.
- [45] Kollanyi, M. and R. M. Verran (Nov. 1959), VSWR indicators with automatic read-out, *Electronic Eng.* 31, No. 381, 666-671.
- [46] Staff writer, (Nov. 1959), A versatile multi-frequency network analyzer, *Electronic Eng.* 31, No. 38, 683.
- [47] Engen, G. F. and R. W. Beatty (1960), Microwave attenuation measurements with accuracies from 0.001 to 0.06 decibel over a range of 0.01 to 50 decibels, *J. Res. NBS (USA)* 64C, April-June 1960, 139-145.
- [48] Schafer, G. E. (Sept. 1960), A modulated subcarrier technique of measuring microwave phase shift, *IRE Trans. on Inst.* 9, No. 2, 217-219.
- [49] Hunton, J. K. and E. Lorence (Dec. 1960), Improved sweep frequency techniques for broadband microwave testing, *HP Jour.* 12, No. 4, 1-6.
- [50] Cohn, S. B. and H. G. Oltman (March 1961), A precision microwave phase-measurement system with sweep presentation, *IRE Internat'l. Conv. Rec.*, Part 3, 147-150.

- [51] Lacy, P. (Aug. 1961), Analysis and measurement of phase characteristics in microwave systems, WESCON paper 23/3.
- [52] Elizarov, A. S. (Sept. 1961), Automatic waveguide measuring line, Meas. Tech., 54-56.
- [53] Leed, D. and O. Kummer (May 1961), A loss and phase set for measuring transistor parameters and two-port networks between 5 and 250 mc, BSTJ 40, No. 3, 841-884.
- [54] Cohn, S. B. (March 1962), Microwave automation, Microwave Journal 5, No. 3, 13, 16.
- [55] Chamberlain, J. K. and B. Easter (Jan. 1962), A direct reading waveguide impedance and reflection indicator, Elec. Eng. 34, No. 407, 14-20.
- [56] Brown, J. and S. A. A. Ahmed (May 1962), An automatic bridge for measurements on loss-free waveguide junctions, Proc. IEE (London) 109, Part B, Supplement No. 23, 713-717.
- [57] Chamberlain, J. K. and B. Easter (May 1962), A technique for the continuous indication of waveguide reflection coefficient, impedance, or admittance, Proc. IEE (London) 109, Part B, Supplement No. 23, 696-703.
- [58] Westcott, R. J. (May 1962), Equipment for the display of reflection coefficients over a 50 Mc/s band at 35 Gc/s, Proc. IEE (London) 109, Part B. Supplement No. 23, 693-695.
- [59] Chasek, M. B. (Nov. 1962), An accurate millimeter wave loss and delay measurement set, IRE Trans. on MTT 10, 521-527.
- [60] de Ronde, F. C. (Jan. 1963), An automatic swept-frequency Smith chart plotter, Program and Digest of Millimeter and Submillimeter Conf., Orlando, Florida.
- [61] Lacy, P. (March 1963), Automated measurement of the phase and transmission characteristics of microwave amplifiers, IEEE Internat'l. Conv. Rec., Part 3, 119-125.
- [62] Griffin, W. D. (April 1963), A precision phase measurement technique for pulsed signals, Microwave Journal 6, No. 4, 63-66.
- [63] Tsuchiya, S. (Nov. 1963), A Smith-diagram display unit of small reflection coefficients using the vibrating-dummy method, Proc. IEEE 51, No. 11, 1444-1454.
- [64] Cohn, S. B. and N. P. Weinhouse (Feb. 1964), An automatic microwave phase-measurement system, Microwave Journal 7, No. 2, 49-56.
- [65] Lacy, P. (July 1964), Measuring transmission delay distortion, MicroWaves 3, No. 7, 22-25.
- [66] Sanderson, A. E. (Jan. 1965), A slotted-line recorder system, Gen. Radio Exp. 39, No. 1, 3-10.
- [67] Ellerbruch, D. A. (Jan.-March 1965), Evaluation of a microwave phase measurement system, J. Res. NBS (USA) 69C, 55-65.
- [68] de Ronde, F. C. (July 1965), A precise and sensitive X-band reflectometer providing automatic full-band display of reflection coefficient, IEEE Trans. on MTT 13, No. 4, 435-440.
- [69] Zanboorie, M. H. (Sept. 1965), A semi-automatic technique for tuning a reflectometer, IEEE Trans. on MTT 13, No. 5, 709-710.
- [70] Leed, D. (March 1966), An insertion loss, phase and delay measuring set for characterizing transistors and two-port networks between 0.25 and 4.2 gc, BSTJ 45, No. 3, 397-440.
- [71] Stelzried, C. T., M. S. Reid and S. M. Petty (1966), A precision dc potentiometer microwave insertion loss test set, IEEE Trans. on I&M 15, No. 3, Sept. 1966, 98-104.
- [72] Mahle, C. and G. Epprecht (Oct. 1966), Reflection measurements with broadband frequency modulation using long transmission lines, IEEE Trans. on MTT 14, No. 10, 496-497.
- [73] Adam, S. F. (Dec. 1966), Swept-frequency VSWR measurements in coaxial systems, HP Journal 18, No. 4, 14-20.
- [74] Anderson, R. W. and O. T. Dennison (Feb. 1967), An advanced new network analyzer for sweep-measuring amplitude and phase from 0.1 to 12.4 GHz, HP Journal 18, No. 6, 2-9.
- [75] Ely, P. C., Jr. (Feb. 1967), The engineer, automated network analysis and the computer-signs of things to come, HP Journal 18, No. 6, 11-12.

- [76] Plice, W. A. (1967), An impedance meter for automatic test systems, IEEE Con. Record 15, Part 8, 72-78.
- [77] Hollway, D. L. (April 1967), The comparison reflectometer, IEEE Trans. on MTT 15, No. 4, 250-259.
- [78] Ellerbruch, D. A. (June 1967), UHF and microwave phase-shift measurements, Proc. IEEE 55, No. 6, 960-969.
- [79] Ely, P. C., Jr. (June 1967), Swept-frequency techniques, Proc. IEEE 55, No. 6, 991-1002.
- [80] Kerns, D. M. and R. W. Beatty, Basic theory of waveguide junctions and introductory microwave network analysis (Pergamon Press, New York, New York, 1967).
- [81] Chandra, K., R. Parshad and R. C. Kumar (Nov. 1967), Measurement of impedance at microwave frequencies using directional coupler and adjustable short-circuit, Proc. IEE (London) 114, No. 11, 1653-1655.
- [82] Goodman, D. M. (1968), Automatic sweep frequency ratio plotter and non-linear measurement systems, U. S. Patent No. 3,409,826, Nov. 5, 1968.
- [83] Evans, J. G. (April 1968), Linear two-port characterization independent of measuring set impedance imperfections, Proc. IEEE 56, No. 4, 754-755.
- [84] Hackborn, R. A. (May 1968), An automatic network analyzer system, Microwave Journal 11, No. 5, 45-52.
- [85] Adam, S. F. (Dec. 1968), A new precision automatic microwave measurement system, IEEE Trans. on I&M 17, No. 4, 308-313.
- [86] Nicolson, A. M. (1968), Broad-band microwave transmission characteristics from a single measurement of the transient response, IEEE Trans. on I&M 17, No. 4, 395-402.
- [87] Sorger, G. U. (Dec. 1968), Coaxial swept-frequency VSWR measurements using slotted lines, IEEE Trans. on I&M 17, No. 4, 408-412.
- [88] Ely, P. C., Jr. (May 1968), Cut-and-try vanquished by computerized microwave instruments, Microwave Journal 11, No. 5, 10.
- [89] MacKenzie, T. E., J. E. Gilmore and M. Khazam (March-April 1969), The new sweep-frequency reflectometer, Gen. Radio Exp. 43, No's. 3 and 4, 3-14.
- [90] Hollway, D. L. and P. I. Somlo (April 1969), A high-resolution swept-frequency reflectometer, IEEE Trans. on MTT 17, No. 4, 185-188.
- [91] Evans, J. G. (May-June 1969), Measuring frequency characteristics of linear two-port networks automatically, BSTJ 48, No. 5, 1313-1338.
- [92] Geldart, W. J., G. D. Haynie and R. G. Schleich (May-June 1969), A 50 Hz-250 MHz computer-operated transmission measuring set, BSTJ 48, No. 5, 1339-1381.
- [93] MacKenzie, T. E. (June 1969), Some recent advances in coaxial components for sweep-frequency instrumentation, Microwave Journal 12, No. 6, 69-77.
- [94] Jurkus, A. (Dec. 1969), A semi-automatic method for the precision measurement of microwave impedance, IEEE Trans. on I&M 18, No. 4, 283-289.
- [95] Weinschel, B. O. (Dec. 1969), Automatic transformation of curved to flat calibration lines by a normalizer, IEEE Trans. on I&M 18, No. 4, 307-316.
- [96] Hand, B. P. (Feb. 1970), Developing accuracy specifications for automatic network analyzer systems, HP Journal 21, No. 6, 16-19.
- [97] Shimba, M. and M. Kikushima (Feb. 1970), An accurate delay-time measuring equipment in the 50 GHz region, IEEE Trans. on I&M 19, No. 1, 9-14.
- [98] Tsuchiya, S. (May-June 1970), A broadband impedance display unit for millimeter waves, Rev. of the Electrical Comm. Lab. (Japan) 18, No's. 5-6, 307-324.
- [99] Beatty, R. W. (June 1970), An automatic method for obtaining data in the Weissfloch-Feenberg node-shift technique, Nat'l. Bureau of Standards (U.S.) Spec. Pub. 300, 4, 341-379. See also Proc. IEEE 53, No. 1, Jan. 1965.

- [100] Lamb, J. D. (1970), System frequency response using p-n binary waveforms, IEEE Trans. on Auto. Control 15, No. 4, August 1970, 478-480.
- [101] Last, J. D. and S. T. Smith (Oct. 1970), Offline correction of microwave-network-analyzer reflection-coefficient errors, Electronics Letters 6, No. 20, 641-642.
- [102] Krupps, W. and K. F. Sodomsky (Jan. 1971), An explicit solution for the scattering parameters of a linear two-port measured with an imperfect test set, IEEE Trans. on MTT 19 No. 1, 122-123.
- [103] Beatty, R. W. (1971), Short discussion of error reduction in network parameter measurement through computerized automation, Prog. in Radio Sci. 2, 1966-1969, URSI, Place Emile Damco 7, 1180 Brussels, Belgium, 237-248.
- [104] Nichols, S. T. and L. P. Dennis (1971), Estimating frequency response function using periodic signals and the F.F.T., Electronics Letters 7, No. 22, Nov. 4, 1971, 662-663.
- [105] Nicolson, A. M., C. L. Bennett, Jr., D. Lamensdorf and L. Susman (1972), Applications of time domain metrology to the automation of broad-band microwave measurements, IEEE Trans. on MTT 20, No. 1, 3-9.
- [106] Somlo, P. I. (Feb. 1972), The locating reflectometer, IEEE Trans. on MTT 20, No. 2, 105-112.
- [107] Davis, J. B., C. F. Hempstead, D. Leed and R. A. Ray (Feb. 1972), 3700-4200 MHz computer-operated measurement system for loss, phase, delay and reflection, IEEE Trans. on I&M 21, No. 1, 24-37.
- [108] Shaffer, W. H. (1972), Organizing the automatic spectrum analyzer system, HP Journal 23, No. 6, Feb. 1972, 7-9.
- [109] Hempstead, C. F. (1972), Applications of a broad capability computer-controlled measurement center in a communications development laboratory, CPEM Digest, 150-151.
- [110] Goodman, D. M. (1972), Automation with precision and prediction, 1972 CPEM Digest, IEEE Cat. No. 72 CHO 630-4-PREC, 178-179.
- [111] Somlo, P. I., D. L. Hollway and I. G. Morgan (1972), The absolute calibration of periodic microwave phase shifters without a standard phase shifter, IEEE Trans. on MTT 20, No. 8, 532-537.
- [112] Hoer, C. A. (1972), Theory and application of a 6-port coupler (unpublished report) August 1972.
- [113] Beatty, R. W. (1972), Invariance of the cross ratio applied to microwave network analysis, Nat'l. Bureau of Standards (U.S.) Technical Note 623, 26 p., issued Sept. 1972.
- [114] Wardrop, B. (1972), The measurement of group delay, Marconi Review 35, 4th quarter.
- [115] Nelson, G. E. and D. W. Ricci (1972), A practical interface system for electronic instruments, HP Journal 24, No. 2, October 1972, 2-7.
- [116] Loughry, D. C. (1972), A common digital interface for programmable instruments: the evolution of a system, HP Journal 24, No. 2, October 1972, 8-11.
- [117] Nelson, G. E., P. L. Thomas and R. L. Atchley (1972), Faster gain-phase measurements with new automatic 50 Hz-to-13 MHz network analyzers, HP Journal 24, No. 2, October 1972, 12-19.
- [118] Gorss, C. C. (Nov. 1972), A precision system for radio-frequency network analysis, IEEE Trans. on I&M 21, No. 4, 538-543.
- [119] Geldart, W. J. and G. W. Pentico (Nov. 1972), Accuracy verification and intercomparison of computer-operated transmission measuring sets, IEEE Trans. on I&M 21, No. 4, 528-532.
- [120] Oldfield, W. W. (1972), Present-day simplicity in broadband VSWR measurements, Wiltron Tech. Rev. 1, No. 1.
- [121] Beatty, R. W. (25 Jan 1973), 2-port $\lambda_g/4$ waveguide standard of voltage standing-wave ratio, Electronics Letters 9, 24-26.

- [122] Lacy, P. and W. Oldfield (April 1973), A precision swept reflectometer, Microwave Journal 16, No. 4, 31-34, 50.
- [123] Geldart, W. J. (1973), Automated measurements for transmission systems, Bell labs. Record 51, No. 6, June 1973, 174-180.
- [124] Allred, C. M. and C. H. Manney (1973), Self-calibration of complex ratio measuring systems, Acta Imeko 1, 157-166.
- [125] Fitzpatrick, J. K. (1973), A new direction for automatic network analyzer software, Microwave Journal 16, No. 9, Sept. 1973, 65-68.
- [126] Ridella, S. (1973), Computerized microwave measurements accuracy analysis, Proc. European Microwave Conf., Brussels, Belgium.
- [127] Davies, O. J., R. B. Doshi and B. Nagenthiram (1973), Correction of microwave network analyser measurements of 2-port devices, Electronics Letters, No. 23, Nov. 15, 1973, 543-544.
- [128] Larson, W. and E. Campbell (1974), Microwave attenuation measurement system (series substitution), Nat'l. Bureau of Standards (USA) Tech Note No. 647, Feb. 1974, 28 p.
- [129] Rehnmark, S. (1974), On the calibration process of automatic network analyzer systems, IEEE Trans. on MTT 22, No. 4, April 1974, 457-458.
- [130] Beatty, R. W. (May 1974), A frequently reinvented circuit, IEEE Trans. on MTT 22, No. 5, 583.
- [131] Ridella, S. (1974), Computerized reflection measurements, 1974 CPEM Digest, IEEE Cat. No. 74 CHO 770-81M, 51-53.
- [132] Beatty, R. W. (1974), 2-port standards for evaluating automatic network parameter measuring systems, CPEM Digest, 87-89.
- [133] Coons, R. W., O. Kummer, R. C. Strum and L. D. White (1974) A computer operated bridge for accurate immittance measurements from 200 Hz to 30 MHz, 1974 CPEM Digest, IEEE Cat. No. 74 CHO 770-81M, 274-276.
- [134] Hall, H. P. (1974), Techniques used in fast, computer-controlled dc bridge, CPEM Digest, 293-296.
- [135] Oliver, B. M. (Nov. 1974), Looking ahead, IEEE Spectrum 11, No. 11, 44-45.
- [136] Grossman, S. E. (1974), Instrumentation, Electronics 47, No. 21, 99-109.
- [137] Falk, H. (Nov. 1974), The microprocessor: jack of all trades, IEEE Spectrum 11, No. 11, 46-51.
- [138] Loughry, D. C. (1974), What makes a good interface?, IEEE Spectrum 11, No. 11, Nov. 1974, 52-57.
- [139] Ricci, D. W. and G. E. Nelson (1974), Standard instrument interface simplifies system design, Electronics, 47, No. 23, 95-106.
- [140] Stauffer, G. H. et. al. (1974), Direct reading swept frequency slotted-line system with slope correction, IEEE Trans. on I&M, No. 4, 394-398.
- [141] Kasa, I. (1974), Closed-form mathematical solutions to some network analyzer calibration equations, IEEE Trans. on I&M 23, No. 4, Dec. 1974, 399-402.
- [142] Cronson, H. M., A. M. Nicholson and P. G. Mitchell (1974), Extensions of time domain metrology above 10 GHz to materials measurement, IEEE Trans. on I&M 23, No. 4, Dec. 1974, 52-57.
- [143] Engen, G. F. (1974), Calibration technique for automated network analyzers with application to adapter evaluation, IEEE Trans. on MTT 22, No. 12, Dec. 1974, 1255-1260.
- [144] Wang, Y-C. (1974), Computerized reflection and transmission coefficient magnitude measurement using an electronically tuned reflectometer, Dept. of E.E., Howard Univ., Washington, D. C. (private communication).
- [145] Beatty, R. W. (1974), Calculated and measured S_{11} , S_{21} , and group delay for simple types of coaxial and rectangular waveguide 2-port standards, NBS Tech Note No. 657 issued Dec. 1974.

- [146] Hoer, C. A. and K. C. Roe (1975), Using an arbitrary six-port junction to measure complex voltage ratios, 1975 MTT-S Internat l. Symp. Digest, 98-99. Also see IEEE Trans. on MTT 23, No. 12, 978-984.
- [147] Gans, W. L. (1975), A time domain automatic network analyzer for microwave measurements, M.S. Thesis, Dept. of E.E., Univ. of Colorado.
- [148] Andrews, J. R. and W. L. Gans (1975), Time domain automatic network analyzer, Colloque International sur L'Electronique et la Mesure, May 1975, 259-267.
- [149] Knoblock, D. E. and D. C. Loughry (1975), Insight into interfacing, IEEE Spectrum 12, No. 5, May 1975, 50-57.
- [150] Gans, W. L. and J. R. Andrews (1975), Time domain automatic network analyzer for measurement of RF and microwave components, Nat'l. Bureau of Standards (USA) Tech. Note No. 672. Issued Sept. 1975.
- [151] Evans, J. G., F. W. Kerfott, and R. L. Nichols (1976), Automated network analyzers for the 0.9 - 12.4 GHz range, BSTJ, July-Aug. 1976.

U.S. DEPT. OF COMM. BIBLIOGRAPHIC DATA SHEET	1. PUBLICATION OR REPORT NO. NBS-MN-151	2. Gov't Accession No.	3. Recipient's Accession No.
4. TITLE AND SUBTITLE Automatic Measurement of Network Parameters - A Survey		5. Publication Date June 1976	
7. AUTHOR(S) R. W. Beatty		6. Performing Organization Code	
9. PERFORMING ORGANIZATION NAME AND ADDRESS NATIONAL BUREAU OF STANDARDS DEPARTMENT OF COMMERCE WASHINGTON, D.C. 20234		8. Performing Organ. Report No.	
12. Sponsoring Organization Name and Complete Address (Street, City, State, ZIP)		10. Project/Task/Work Unit No.	
15. SUPPLEMENTARY NOTES Library of Congress Catalog Card Number: 76-12432		11. Contract/Grant No.	
16. ABSTRACT (A 200-word or less factual summary of most significant information. If document includes a significant bibliography or literature survey, mention it here.) A survey is made of principles, methods, and systems developed for semi-automatic and automatic measurement of network parameters, such as the complex scattering coefficients, impedance, VSWR, return loss, attenuation, and group delay time. The period covered is from 1922 to 1975 and developments range from simple ideas such as a motor driven probe for a slotted line, to computer-controlled transmission and reflection measurement systems. The essential ideas and features of each development are briefly described and both similarities and differences between various schemes are pointed out. Trends in modern developments are noted and some of the options open for future work are mentioned. A bibliography of 151 references is included.		13. Type of Report & Period Covered Final	
14. Sponsoring Agency Code		15. SUPPLEMENTARY NOTES	
17. KEY WORDS (six to twelve entries; alphabetical order; capitalize only the first letter of the first key word unless a proper name; separated by semicolons) Automatic network analyzers; computer-controlled measurement; magic tee; microwave measurement methods; multiple probe devices; reflectometers; rotating probe devices; slotted lines; survey of automatic techniques; swept frequency measurements; Wheatstone Bridge.			
18. AVAILABILITY <input checked="" type="checkbox"/> Unlimited <input type="checkbox"/> For Official Distribution. Do Not Release to NTIS <input checked="" type="checkbox"/> Order From Sup. of Doc., U.S. Government Printing Office Washington, D.C. 20402, SD Cat. No. C13. 44:151 <input type="checkbox"/> Order From National Technical Information Service (NTIS) Springfield, Virginia 22151		19. SECURITY CLASS (THIS REPORT) UNCLASSIFIED	21. NO. OF PAGES 113
		20. SECURITY CLASS (THIS PAGE) UNCLASSIFIED	22. Price \$4.50





